Soil-Planter Interaction Force Distribution as Affected by Planting Depth Setting and Planter Configuration

by

Rees W. Bridges

A thesis submitted to the Graduate Faculty of
Auburn University
in partial fulfillment of the
requirements for the Degree of
Master of Science

Auburn, Alabama
May 7, 2016

Keywords: Precision Agriculture, Soil Dynamics, Planter Force Distribution, Gauge Wheel Loading

Approved by

Timothy McDonald, Chair, Professor of Biosystems Engineering
Jeremiah Davis, Associate Professor of Biosystems Engineering
Thomas Way, Agricultural Engineer United States Department of Agriculture National Soil Dynamics Laboratory
John Fulton, Associate Professor of Food, Agricultural, and Biological Engineering, The Ohio State University
George Flowers, Dean of the Graduate School and Professor of Mechanical Engineering

Abstract

Agricultural field planting operations encounter great spatial and temporal variability. Research has shown that seeding depth and soil loading, produced by planting equipment, affect early crop growth as well as crop yield. For these reasons, control system development for seeding depth, planter down force, and press wheel force provides an opportunity to maximize crop yield potential by achieving greater precision in planting depth and more uniform soil loading.

Effective feedback control of these systems requires an improved knowledge of soil-planter interaction forces and how the force distribution changes with planting depth. An experiment was conducted in an indoor soil bin at the United States Department of Agriculture National Soil Dynamics Laboratory in Auburn, Alabama to determine the force distribution due to soil-planter interaction forces on a John Deere MaxEmerge™ Plus agricultural field planter row unit. The experimental design included two factors, planter configuration and planting depth setting, and four replications, which were run in a uniformly prepared Norfolk Sandy Loam soil. Data were collected for four-bar link angle, gauge wheel arm angle, vertical force on the gauge wheels, planting furrow depth, gauge wheel rut depth, and press wheel rut depth, as well as draft and vertical forces acting on the toolbar.

An analysis of variance with mixed effect models was conducted on the response variables previously mentioned. A change in target planting depth from 2.54 cm to 7.62 cm produced a 112% decrease in the gauge wheel rut depth. The same change in planting depth setting produced an increase of 80% and 273% in press wheel rut depths referencing the undisturbed soil surface and gauge wheel rut depth respectively. Across planting depths, vertical force on the double disc opener was not significantly affected; however, a trend of increased force with increased depth was observed. Vertical force decreased on gauge wheels by 48% and

increased on press wheels by 55% as planting depth increased. While a significant change in the distribution of total vertical load supported by the planter was not observed for every component interacting with the soil, the percentage supported by the gauge wheels was significantly decreased.

Two linear regression models were produced to estimate planting furrow depth. The first model utilized rut depth measurements and included gauge wheel arm angle (GWAS), an indicator of planting depth setting, and press wheel rut depth referencing the undisturbed soil surface. The model resulted in an adjusted R^2=0.82. The second model used resultant forces on planter components interacting with the soil. Stepwise elimination of variables resulted in a model including only GWAS with an adjusted R^2=0.78. It is not expected that this model will accurately estimate planting furrow depth for soil conditions outside those present during the experimental data collection, and highly uniform conditions within the soil bin may have contributed to the elimination of variables that would be present in models predicting planting furrow depth for in-field operations.

The response of soil-planter interaction forces, soil rut depths, and planting furrow depth observed during this experiment clearly demonstrated that a redistribution of forces occurred as planting depth setting adjustments were made. The data also indicated that planting depth setting adjustments and actual planting furrow depth are not a one-to-one relationship. Changes to any planter setting adjustment or force input to the system affected not only the component adjusted but also the balance of forces acting on the remainder of the planter row unit components. Results from this experiment and those previously conducted indicate that actual planting furrow depth is a function of planting depth setting and the distribution of forces acting on the planter. For this reason, maximizing crop emergence and yield through improved seeding depth and soil conditions around the seed will likely require feedback control of all planter adjustment settings working in conjunction with as opposed to independently controlled systems.

Acknowledgments

I would like to thank the Auburn University Department of Biosystems Engineering for their support and funding of graduate research that provides value to our nation's agricultural industry. I would also like to thank the United States Department of Agriculture's National Soil Dynamics Laboratory, their faculty and staff, and agricultural engineer Dr. Thomas Way, whose support was invaluable to the research conducted and the evaluation of results. Dr. Clarence Johnson, emeritus faculty of the Auburn University Biosystems Engineering Department, provided support and a wealth of knowledge to the project; for this I am sincerely grateful.

I would like to thank Dr. Timothy McDonald for his guidance in my graduate course work and research. I am grateful to my graduate committee members; Drs. Timothy McDonald, Thomas Way, Jeremiah Davis, and John Fulton; for their time, knowledge, and guidance through this process. I would also like to thank Gregory Pate of the E.V. Smith Research Center, for providing the planter used during research; the faculty and staff of the Biosystems Engineering Department; and the graduate student body of the Biosystems Engineering Department for their support. I would like to specifically thank three students whose efforts made my research a success: Aurelie Poncet, Pengmin Pan, and Chennen "Kevin" Xue.

I would like to thank my family and friends for their support and my father, Dr. David Bridges, for his guidance through my graduate research. Finally, I would like to thank my wife, Lindsay, and my two children, Sims and Miller, for their dedication to me and for their sacrifice during this time.

Table of Contents

List of Figures

List of Tables

Chapter 1

INTRODUCTION

The anatomy of agricultural field planters has varied significantly with time, planting method, field conditions, crop, and most recently technology. The emergence of precision agriculture opened the door for variable rate, force monitoring, and control technologies that were unheard of prior to the adoption of GPS and GIS systems. Many agricultural field planters in operation today are configured similarly to the John Deere MaxEmerge™ Plus planter shown in figure 1.1.

The design function of agricultural field planters is to accurately meter seed, at a specified rate, and to place them in the soil at a desired seed spacing, depth, and soil compaction. For planters configured similarly to the one shown, a "V" shaped furrow is opened in the soil by the coulter (7) and double disc opener (8) assemblies as the planter is drawn through the soil by the toolbar (1) and four-bar linkage assembly (3). The depth of the furrow in relation to the soil surface, also known as planting or seeding depth, is controlled by the vertical position of the gauge wheels (9) relative to the double disc opener. This position can be set with the use of the planting depth setting adjustment (12). Once the furrow is created, a seed is released by the metering device (6), travels through a seed tube located between the two opening disc, and is placed at the bottom of the furrow. As the planter continues to move forward, the soil furrow is closed and consolidated by the press wheels (10) on the rear of the planter. The planter configuration and components utilized may vary depending on the crop and conditions experience during planting.

Coulter assemblies vary based on the soil conditions and type of residues present at the time of planting. Furrow openers may consist of fixed components, such as chisel and runner openers, or rotating assemblies like the double disc opener on the John Deere planter shown.

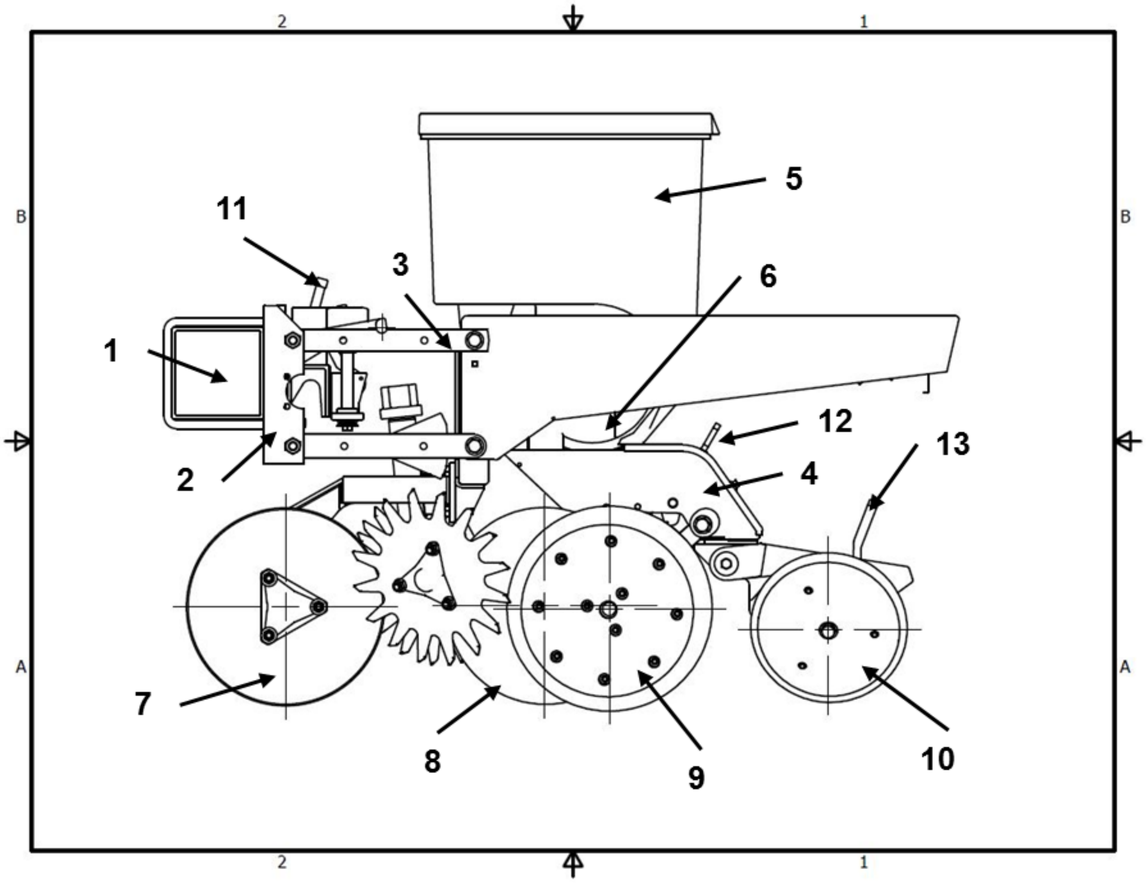

Figure 1.1: An illustration of the anatomy of a John Deere MaxEmerge™ Plus planter. (1)Toolbar, (2)Toolbar mount, (3)Four-bar link, (4)Row unit frame, (5)Seed hopper, (6)Metering device, (7)Coulter assembly with detrash wheels, (8)Double disc opener, (9)Gauge wheels, (10)Press wheels, (11)Spring down force system adjustment, (12)Planting depth adjustment, (13)Press wheel force adjustment.

Depth control devices vary greatly from depth bands fixed to the opening disc, to gauge wheels attached to the planter in several positions: on the toolbar, in front of or behind the opening device, or positioned on either side of the double disc opener. Closing/press wheels designed to close the planting furrow range in size, shape, and material. Finally, down force systems provide the force needed to achieve the desired planting depth when the weight of the planter row unit is not sufficient to do so. Down force systems transfer weight from the toolbar to individual row units by means ranging from simple, manually adjusted spring systems to computer controlled pneumatic and hydraulic systems. Setting and configuration changes of the planter's components alter distribution of soil-planter interaction forces, which affect planter performance, crop emergence, and ultimately crop yield potential.

Down force setting, planting depth setting, and press wheel force adjustments are currently used to control seeding at the desired depth. Because these settings are manually controlled on many agricultural planters, optimal seed depth and soil conditions may not be achieved for the highly variable environment encountered in the field. Optimal seeding depth and soil compaction around the seed require planter setting adjustments every time a change in field conditions is encountered. For this reason, real-time feedback control of planter adjustments provides a means of increased crop yield potential through improved planting depth precision and soil loading for the conditions present at the time of planting.

Control system development requires a greater knowledge of planter system dynamics as a result of interaction with the soil in which it is operating. A dynamic simulation capable of modeling soil-planter interaction would aid in this development to maximize crop yield potential through variable planting depth or improved planting depth precision for the highly variable conditions present during agricultural row crop planting operations. This research is the first step in the process and is designed to improve understanding of the distribution of forces on a planter and how they are affected by planter setting adjustments. Current systems provide the capability to monitor the force exerted on the gauge wheels during planting operations. Understanding how and why this force changes with planting depth setting adjustments is the focus of this research.

OBJECTIVES

The goals of this research are to characterize how force distribution on an agricultural field row planter, due to soil-planter interaction, is affected by planting depth setting adjustment and to understand how the soil surface profile is physically affected by these adjustments. The specific objectives of the research are:

1. How are gauge wheel and press wheel rut depths affected by planting depth setting?

2. Can gauge wheel rut depth be predicted from planter operating conditions?

3. Can planting furrow depth be predicted by planting depth setting and gauge wheel or press wheel rut depths?

4. How does soil-planter interaction force distribution change with planting depth setting?

5. Can actual planting furrow depth be predicted by planting depth setting and force distribution?

Chapter 2

REVIEW OF LITERATURE

Planting depth affects crop emergence and early crop growth. Thomason *et al.* (2008) concluded in a study on in-row subsoil tillage and planting depth that seeding depth produced variation in emergence and yield of corn. According to Knappenberger and Köller (2006) an increase in corn emergence of 2.4% to 5.4% could be achieved by adjusting seeding depth according to soil moisture content. Emergence increased with increased planting depths in sandy regions of the field. Later, Knappenberger and Köller (2011) stated that emergence was primarily a function of weather, but that the influence of spatial variation increased as weather conditions became less optimal. In these conditions emergence increased 1.5% to 4.4% for corn planted deeper than 80-90 mm in depth. In addition to planting depth, Erbach *et al.* (1991) found that corn yield increased when surface pressure produced by equipment was reduced from 110 to 20 kPa. Hanna *et al.* (2010) conducted a study on the soil loading effects of gauge wheels on corn emergence. He concluded that Emergence Rate Index (ERI), as described by Erbach (1982), was affected by gauge wheel down force pressure. Corn emerged more quickly with lighter pressure in moist soils and higher pressure in drier soils. Similarly, the Speed of Emergence Index (SEI), described by Siemens *et al.* (2007), was also significantly affected. Seedlings emerged more quickly in moist soils with reduced down force pressure.

Traditional agricultural row planters have two primary adjustment settings that control planting depth performance. The down force setting is customarily set prior to planting by adjusting the spring system until the load produced is just sufficient to maintain firm contact between the gauge wheels and the soil (Hanna *et al.* 2010). Hanna *et al.* (2010) stated that any force applied to the planter beyond what is required to insert the opening disc into the soil and maintain contact between the gauge wheels and soil surface could increase load transmitted to the soil and alter seedling emergence. Planting depth variations can also be produced by incorrect down force. Hanna *et al.* (2010) found that planting depths were 8 to 13 mm deeper for the same planting depth setting when higher down force on the gauge wheels was present.

Previous research findings highlight the potential for improved planter setting control. Knappenberger and Köller (2011) stated that optimal planting depth varies spatially in most heterogeneous fields. This is further complicated by the fact that down force required by the system is dependent upon the soil properties and crop residues encountered by the planter (Erbach *et al.* 1983). Morrison (1988b) stated that if planter settings are adjusted to produce desired planting depth in higher resistance conditions, then planting depths deeper than intended will be realized in areas of lower resistance. He suggested, "Ideal total vertical force on a furrow opener at any one time includes a force adequate to cut residue and open the furrow to the desired planting depth, a force to keep the depth controls in contact with the soil surfaces as they pass over surface undulations, and a force to effectively close the seeded furrow." Manually adjusted spring down force systems are a function of Hooke's Law and do not perform optimally to soil surface inputs (Morrison 1988a). For this reason several improved down force systems have been evaluated with a few making it to market.

Morrison (1988a and 1988b) conducted research evaluating the performance of two experimental pneumatic and hydraulic down force systems. The systems performed adequately over several years of research, but required manual adjustment for the range of down force values produced. Currently on the market, Precision Planting LLC© is offering pneumatic and hydraulic down force control systems, AirForce® and DeltaForce™ respectively (Precision Planting LLC; 2011 and 2014). Other systems include the ISOBUS Hydraulic Down Force system (Ag Leader, 2015) and Active Pneumatic Downforce (Deere, 2016). Force on the gauge wheel is monitored by the Precision Planting LLC© and John Deere© systems via load pins on the planting depth adjustment assembly.

It is evident that a single planter setting is not optimal for all conditions encountered in the field when press wheel force is also considered in the force distribution. Hanna *et al.* (2010) stated that, "seed placement and soil conditions created by planting equipment ideally should optimize soil conditions around the seed." Planter adjustments should be utilized to effect early crop growth by those seeking highest yield potential (Hanna *et al.* 2010).

Many of the independent component forces that affect the complete force distribution have been extensively researched. Tice and Hendrick (1991) conducted an experiment evaluating the performance of 12 mathematical coulter force models. Cochran *et al.* (1974), in a study of vertical forces on furrow openers and depth control devices, found that vertical force increased on both double disc openers with increasing planting depth and gauge wheels with increased depth (rut depth). Schaaf *et al.* (1981) stated that when operating depth of smooth coulters increased from 30 to 70 mm, draft and vertical force increased by 99% and 45% respectively. Johnson and Burt (1990) produced a model to predict total stress induced on soil loaded by a tire. The interaction of all the forces produced by planter contact with the soil is important to accurately predict force distribution and how the system will respond to setting and configuration changes.

Chapter 3

PRELIMINARY WORK

3.1 CAD Model Development

Prior to collecting data or designing an experiment a more complete understanding of the operational constraints and geometry of the John Deere MaxEmerge™ Plus planter was needed. It was critical to understand how planter adjustments affected the relationship of the planter's components to one another. This understanding guided our expectations of how the planter would interact with the soil at varying planting depths, enabled the selection of response variables for the experiment, and aided in the development of equations describing the planter's operational force distribution.

Increased knowledge of the planter row unit began with a general evaluation of the planter's system of operation and how its adjustment settings altered that operation. The row unit was completely disassembled. Components that could be separated were individually weighed on a lab scale (fig. 3.1). Weldments or components that could not be separated were weighed as an assembly. Individual components were then measured and reproduced in Autodesk's® 3D computer aided design package, Inventor (Inventor 2015). Weldment components were modeled separately and assembled within the CAD package (fig. 3.2). This enabled the models to be more representative of the OEM product and provided additional value for future research projects evaluating the components and performance of the planter. As the modeling of each component was completed, its material and mass properties were updated to match the data collected during disassembly.

Figure 3.1: Measurement of component part weights in the lab.

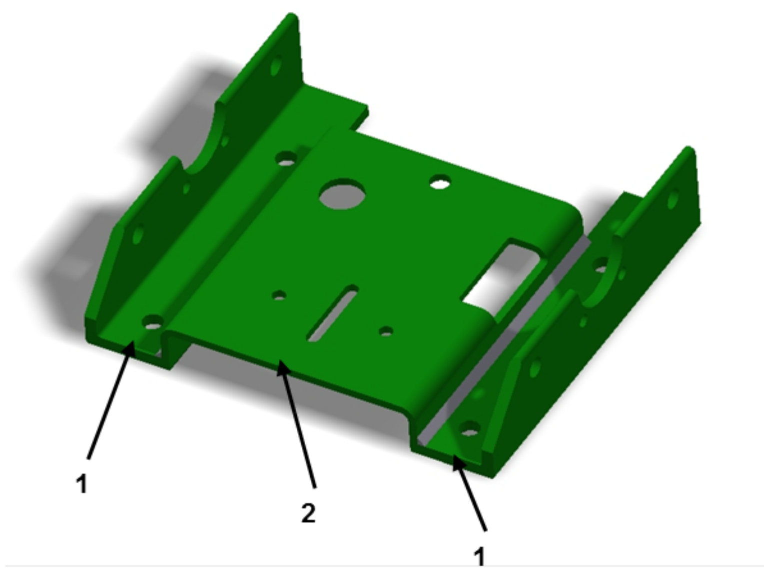

Figure 3.2: Weldment assembly produced in Autodesk® Inventor from individual component parts. (1)Angle iron components (2)Formed plate.

Several components required measurement beyond simple weight or dimensional layout. Two springs, critical to the operation of the planter and its force distribution on the soil, were the spring down force compression spring (two springs in the assembly) and press wheel force tension spring. No-load measurements were taken on both springs. An Instron® tension and compression testing machine was used to measure the spring constant of each of the springs, shown in figures 3.3 and 3.4. Plotting the force per displacement produced spring constants for the compression and tension springs of 43.16 and 13.9 N/mm respectively. The springs were then reassembled into the planter row unit to make note of any preload that was present in the system. The spring down force system produced a preload of 2.47 kN per spring, when no additional load from the four-bar link system was applied. Preload on the press wheel mechanism is dependent on the adjustment handle position.

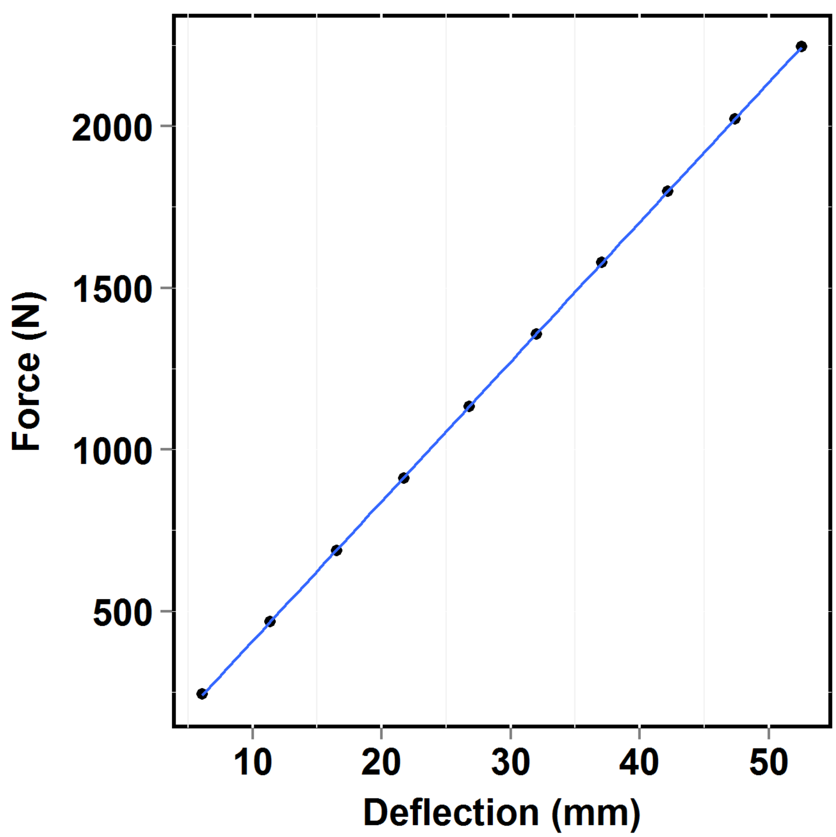

Figure 3.3: Down force system compression coil spring constant k_{comp} (N/mm) is calculated as force (N) per unit deflection (mm).

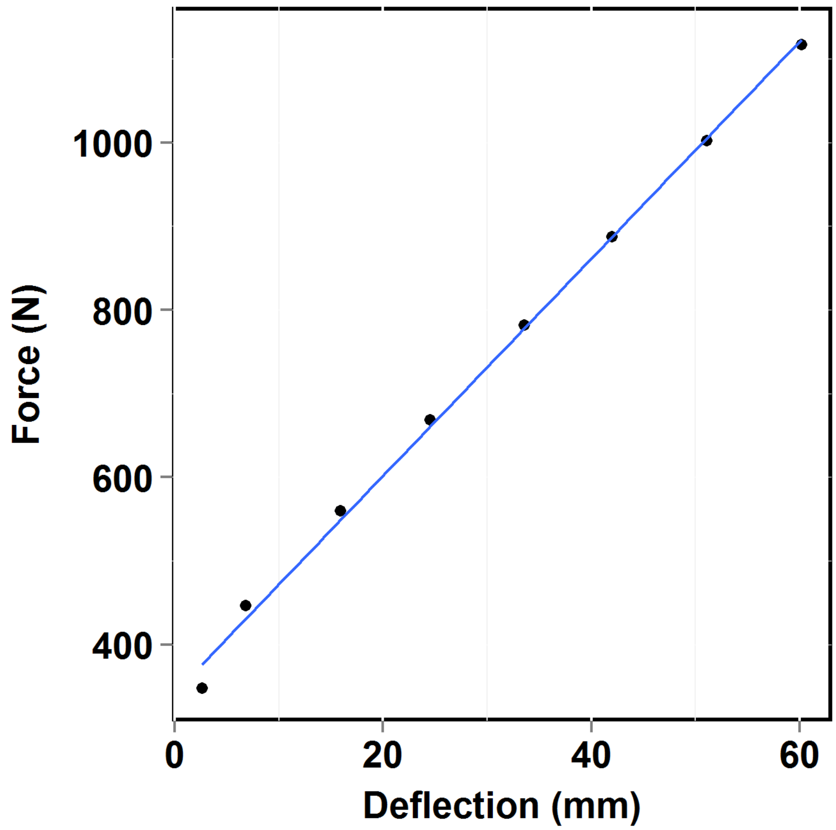

Figure 3.4: Press wheel force tension coil spring constant k_{tens} (N/mm) is calculated as force (N) per unit deflection (mm).

The structural frame of the row unit was particularly difficult to measure. It contained multiple stamped and machined components that were assembled into a weldment. Two spindles and a mounting boss, shown in figure 3.5, provide attachment points and rotation for the opening discs and the gauge wheel arm assemblies respectively. These components were not manufactured normal to any of the three primary reference planes of the planter row unit frame. For this reason, a 3D coordinate measuring machine (FaroArm) and 3D measurement software (CAM2) were used to accurately measure the critical areas of the frame (CAM2 2015). A global reference frame, XYZ, was established along the axis between the two upper four-bar link attachment holes and a plane along the lateral mid-point of the row unit frame.

Figures 3.6 and 3.7 detail the global reference frame (XYZ) and the components measured by the FaroArm.

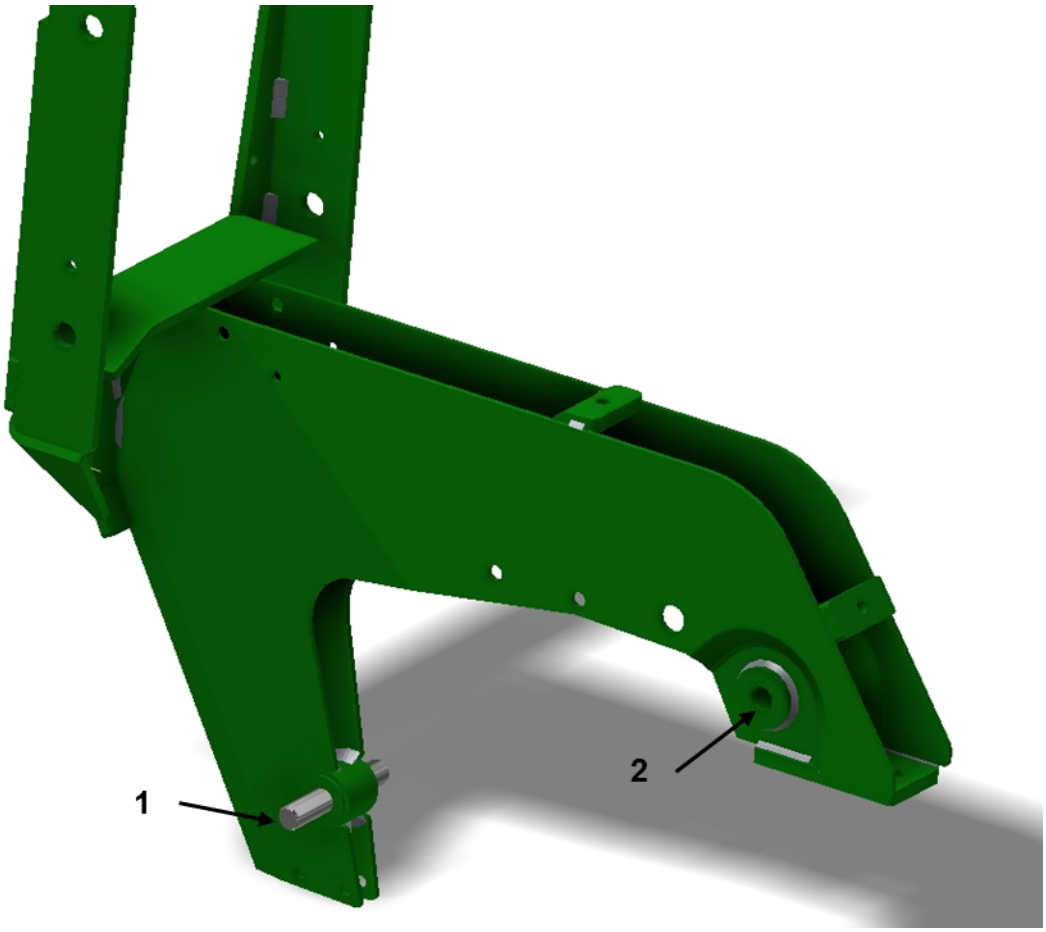

Figure 3.5: Mounting spindles and boss on the planter row unit frame which were measured with the FaroArm. (1) Double disc opener spindle (2) Gauge wheel arm mounting boss.

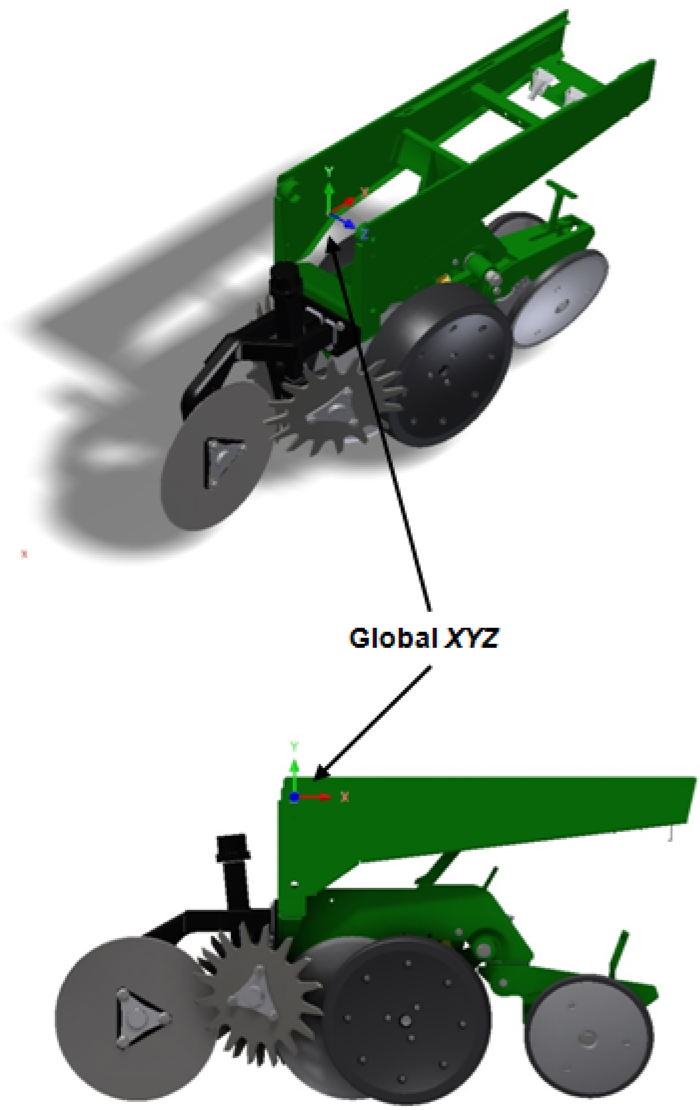

Figure 3.6: Position of the Global XYZ coordinate system for the planter row unit.

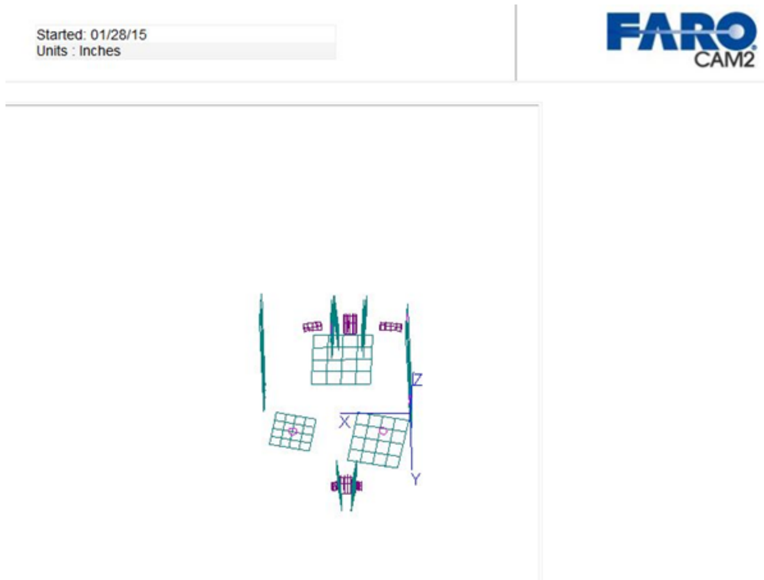

Figure 3.7: CAM2 software visualization of the spindle and mounting boss features measured with the FaroARM 3D coordinate measuring machine.

After every component was modeled, a planter row unit assembly was created. At this time several of the components were updated to improve alignment and fit. Assembly mechanisms were created on all moving components of the planter to verify functionality of the planter model matched that of the actual planter disassembled. The operation of the planter's adjustment settings and the geometry and force changes they caused were further evaluated.

3.2 Planter Row Unit Adjustment Mechanisms

Three adjustments can be made on a MaxEmerge™ Plus planter that will affect planting depth or force distribution: spring down force, planter depth setting, and press wheel force adjustments. The spring down force system, figure 3.8, consists of two coil springs, an adjustment handle, and a rotating force application arm. The adjustment handle acts as the connecting rod between the slide, capturing the lower end of the springs, and the adjustment lever on the force arm. Activation angle and spring compression rate of the system are controlled by the location of the adjustment handle attachment to the lever on the force arm. Four notch positions on the lever produce down force settings of: “No”, “Low”, “Medium”, and “High” down force by changing the travel of the adjustment handle and connected slide for any given rotation angle.

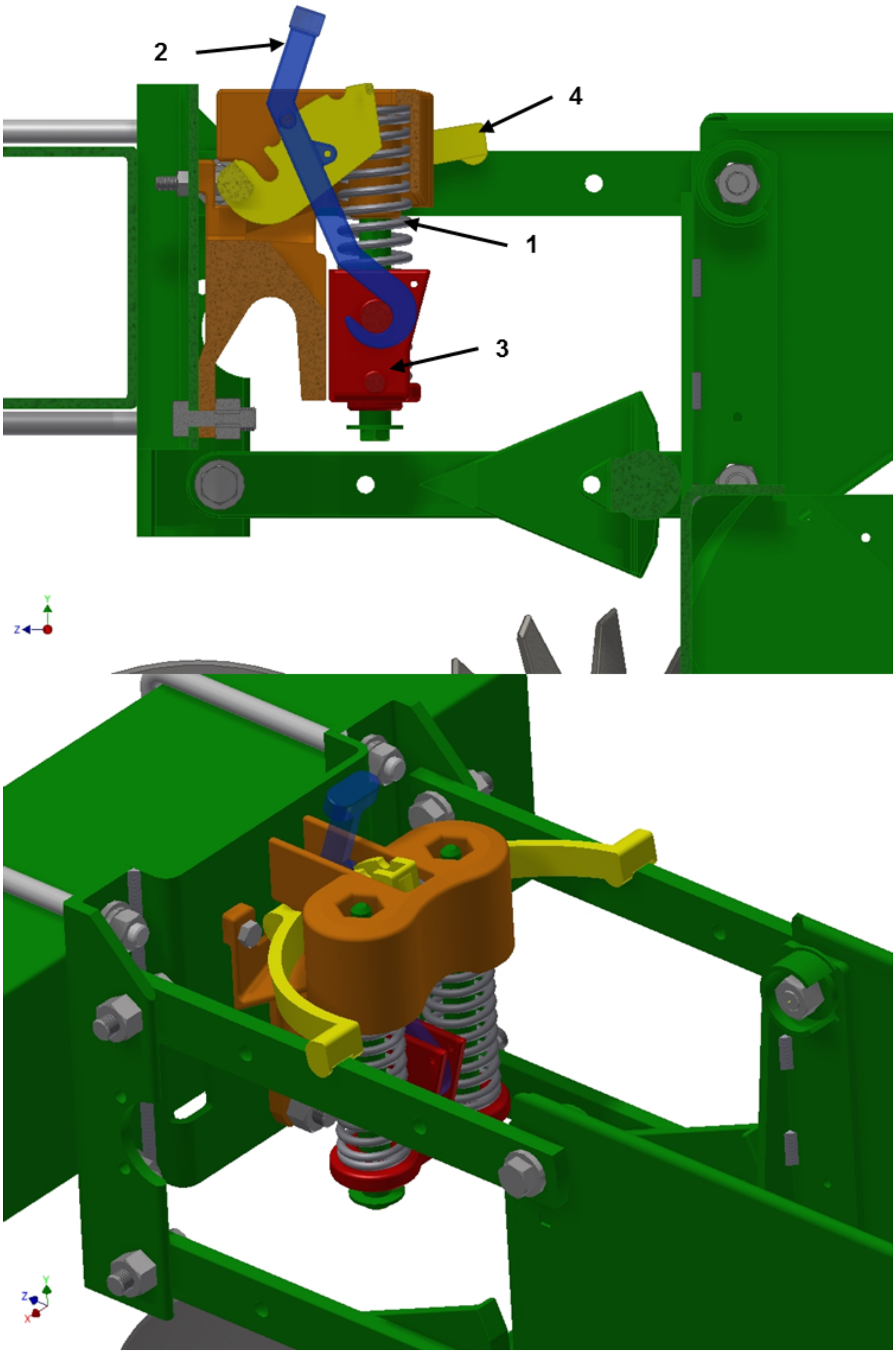

Figure 3.8: Spring down force mechanism. (1) Coil spring (2) Adjustment handle (3) Slide (4) Force arm.

The second adjustment mechanism on the planter row unit is the planting depth setting, shown in figure 3.9. A spring loaded adjustment handle can be positioned in a series of holes along the rear of the lower row unit frame. The adjustment handle assembly rotates about a revolute joint, normal to the XY plane, below the handle. The rocker, attached to the lower end of the adjustment assembly, provides an upper hard stop for both of the gauge wheel arms. The rocker rotates a few degrees in either direction allowing the gauge wheels to operate with limited independence from one another. As the adjustment handle is positioned further down the rear of the frame, the rocker moves in the negative X and positive Y directions. This movement allows the gauge wheel arms to rotate further before contacting the rocker, increasing the relative distance between the double disc opener and the gauge wheels and effectively increasing planting depth.

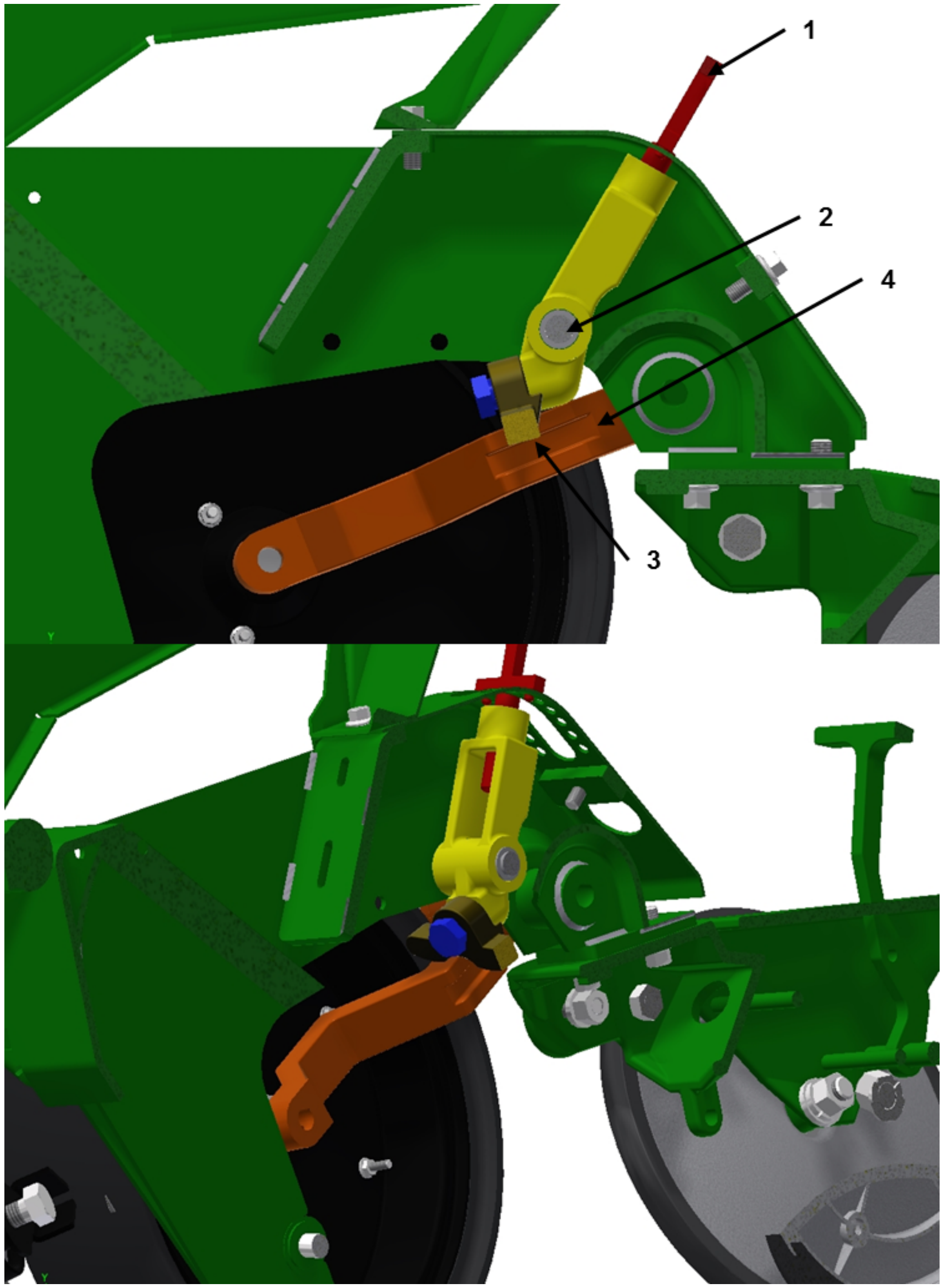

Figure 3.9: Planting depth adjustment mechanism. (1) Adjustment handle (2) Revolute joint (3) Rocker (4) Gauge wheel arm.

The final adjustment mechanism controls press wheel force (fig. 3.10). The press wheel assembly is attached to the lower, rear of the planter row unit frame by a revolute joint. A tension coil spring is attached, at the front, to a fixed position on the row unit frame and, at the rear, to the adjustment handle on the rotating press wheel assembly. The adjustment handle can be secured in five locations by rotating the handle about the revolute joint attaching it to the press wheel assembly. The distance between the fixed and adjustable spring attachment locations is increased as the handle is rotated in a clockwise direction, increasing the preload applied to the rotating press wheel assembly. The force that is generated on the soil and the planter by this assembly is a function of the handle adjustment position (preload) and the press wheels assembly's counter-clockwise rotation relative to the row unit frame.

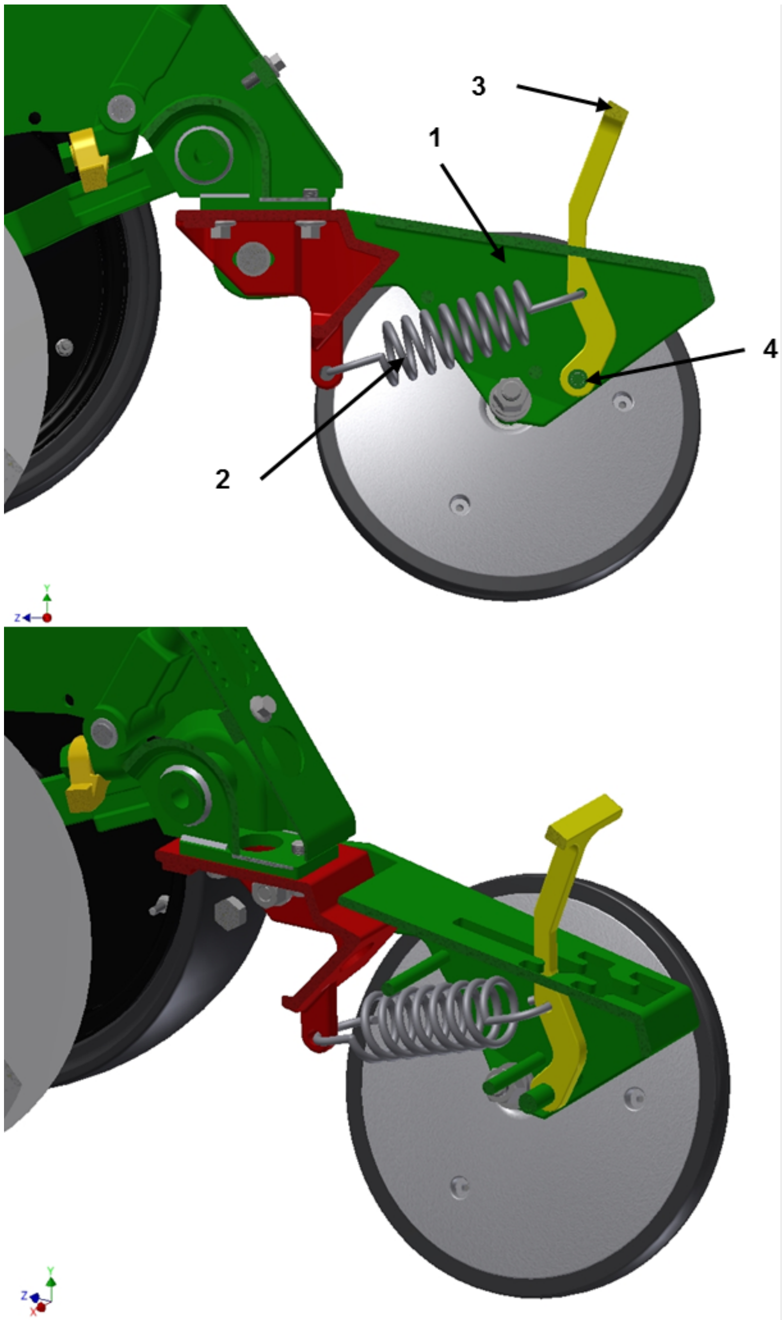

Figure 3.10: Press wheel force adjustment mechanism. (1) Press wheel assembly (2) Coil spring (3) Adjustment handle (4) Revolute joint.

3.3 Data Acquisition System

A planter data acquisition system (DAQ) was previously developed for experiments on in-field planting operations of the John Deere MaxEmerge™ Plus planter used during the course of this research (fig. 3.11). The system consists of a National Instruments© (NI) USB-6225 data acquisition module, four Analog Devices, Inc.© 5B38 load cell signal conditioners, one 12VDC voltage regulator, and one 5VDC voltage regulator. All of the components were assembled inside a weatherproof enclosure with power and I/O signals passed through via bulkhead Duetsch DT and DTM series connectors. Connectors and wiring were added to the enclosure for two additional analog I/O channels and one additional discrete I/O channel.

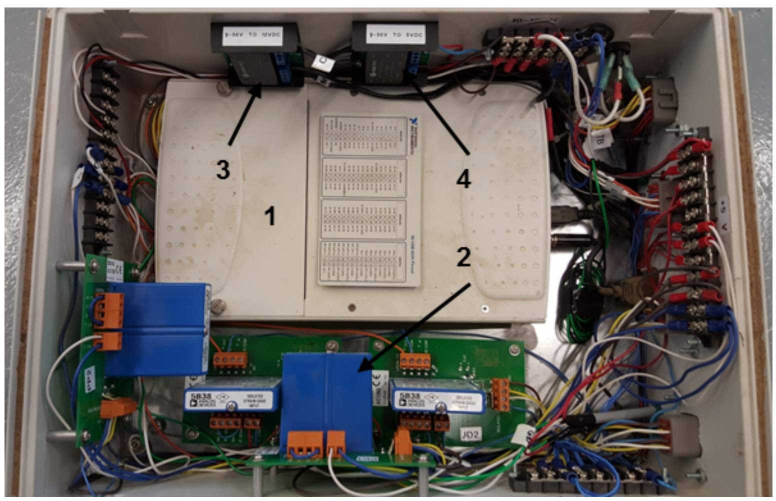

Figure 3.11: Planter data aquisition system. (1) NI USB-6225 data acquisition module (2) Analog Devices 5B38 signal conditioners (3) 12VDC voltage regulator (4) 5VDC voltage regulator.

A data collection program using National Instruments LabVIEW™ was developed to record data from the planter, display it real-time, and synchronize data collection with external systems (LabVIEW 2015). Four channels, three analog input and one discrete output, were run in a loop displaying their values on the front panel of the virtual instrument (VI). Data collection began with input from one of two momentary push button switches on the VI. Each button started a corresponding one-second or three-second count-down timer inside the loop. During count-down of the timer, the discrete output was low and data from the analog inputs was compiled into a multi-dimensional array. Data collection was verified on the front panel of the VI with a LED indicator. Once the timer count-down completed, the discrete output was once again high and the array, built during the data collection cycle, was converted to spreadsheet format and saved. The one- and three-second collection-time buttons were used during experimental data collection for baseline (bias) and operation data sets, respectively. The discrete output was used to control and synchronize data collection through a secondard DAQ. The front panel and block diagram for the experimental data collection program is included in Appendix B.1. This program was slightly modified to be used in the calibration data collection of the spring down force system and gauge wheel load pin. The modified program included an additional gauge on the VI front panel as well as an indexing value within the array that was logged. This value was used to identify and separate data sets during statistical analysis. The calibration program front panel and block diagram are included in Appendix B.2.

Chapter 4

MATERIALS and METHODS

4.1 Experimental Design

An experiment was conducted with the collaboration of the United States Department of Agriculture, Agricultural Research Service (USDA-ARS) National Soil Dynamics Laboratory, located in Auburn, Alabama, to meet the five primary objectives of the research. Experimental design was a completely randomized design with two factors: planter configuration and planting depth setting. There were four replications. Experiments were conducted in a soil bin containing Norfolk Sandy Loam soil. Norfolk Sandy Loam is poorly graded sandy loam soil that was excavated from the Auburn University Agricultural Engineering Farm in Marvyn, Alabama and installed in one of the two indoor soil bins at the National Soil Dynamics Laboratory (Batchelor 1984). A full description of the properties and composition of Norfolk Sandy Loam are included in Appendix C.1.

Due to the envelope of usable area inside the bin, the lateral spacing required between plots, and the longitudinal distance required for acceleration and deceleration, it was determined that 50 experimental unit plots could fit within the soil bin. Each plot was 45.7 cm (18 in.) wide and 9.144 m (30 ft) long arranged 10 plots per row with 5 rows covering the longitudinal length of the soil bin, as shown in figure 4.1. The unused area on the south end of the bin was occupied by the power cart that was used to pull the dyno cart along the bin during the test (fig. 4.2).

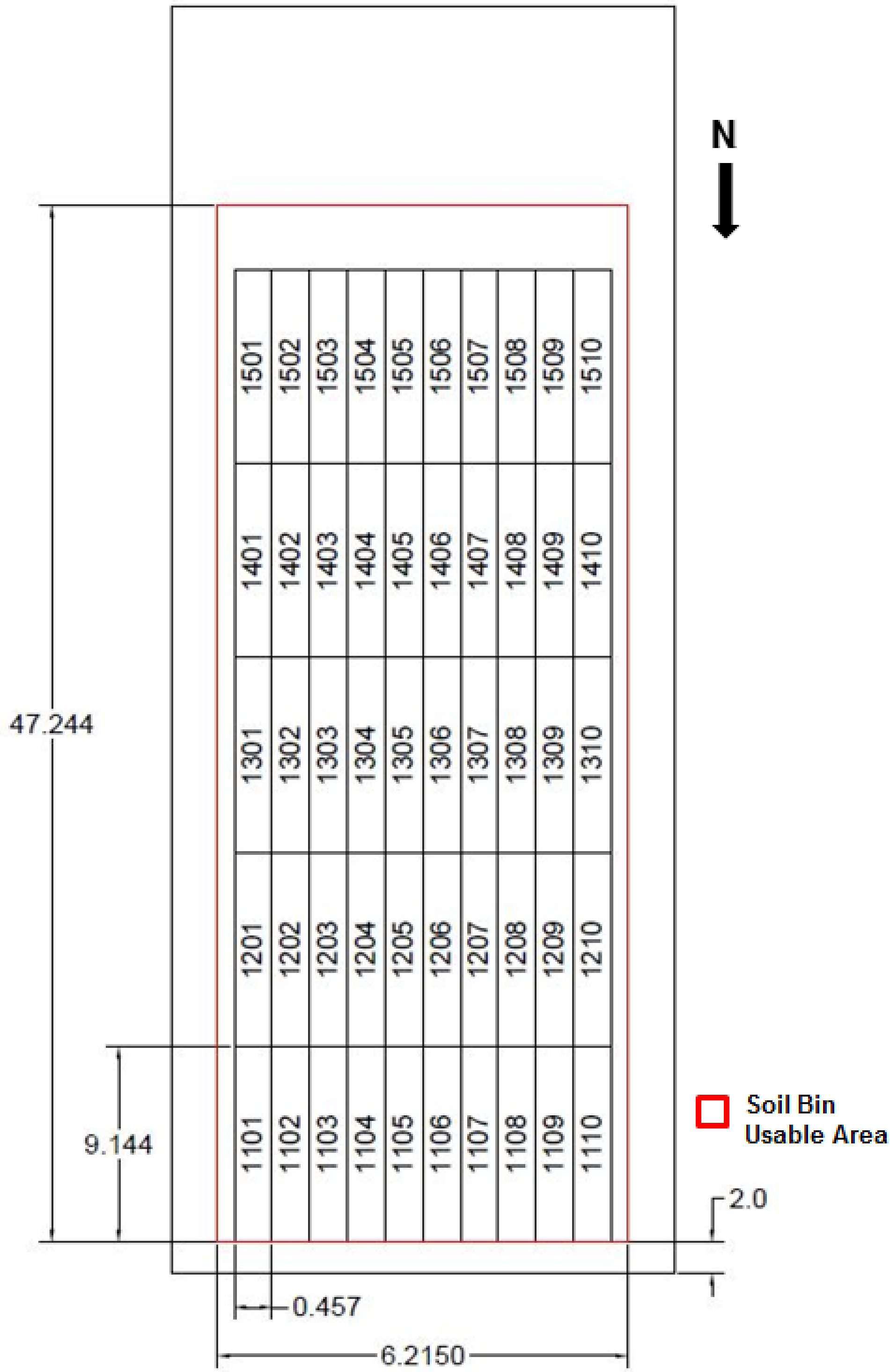

Figure 4.1: Plot number layout in soil bin 1 at the USDA National Soil Dynamics Laboratory. Experimental treatments were completely randomized within the soil bin.

Figure 4.2: Power and dyno carts positioned in the unused area at the south end of the soil bin.

With 50 total experimental units available for the experiment, it was determined that four planter configurations should be tested to improve understanding of individual component loadings. The configurations, shown in figure 4.3, were as follows:

1. An operational configuration consisting of a coulter assembly forward of the double disc opener including detrash wheels that were raised so as not to contact the soil during the experiment, double disc opener, gauge wheel assemblies, and a press wheel assembly.

2. An operational configuration consisting of the double disc opener, gauge wheel assemblies, and a press wheel assembly. The coulter assembly including detrash wheels remained on the planter to maintain the total planter weight and center of gravity as closely as possible, but the coulter disc was removed and placed on top of the planter row unit frame.

3. A non-operational configuration consisting of the double disc opener and gauge wheel assemblies. The coulter disc was removed and placed on top of the planter row unit

frame as in configuration 2. The press wheel force adjustment was positioned to remove spring tension from the assembly, and the press wheel assembly was tied to the planter row unit frame to ensure that it did not contact the soil.

4. A non-operational configuration consisting of only the double disc opener. The coulter disc and press wheel assemblies were removed from contacting the soil as described in configuration 3. Finally, both gauge wheel assemblies were removed and placed on top of the planter row unit frame above their operational position.

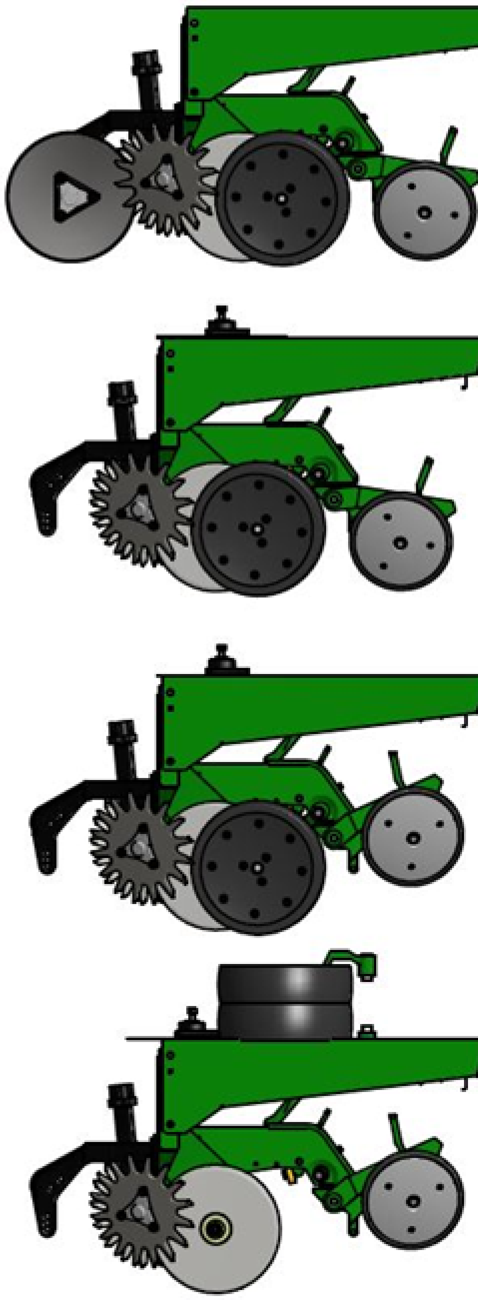

Figure 4.3: Planter configurations tested in the soil bin.

In addition to the four planter configurations, three planting depth settings were tested. Planter depth adjustment settings 4-4, 6-6, and 8-8 were selected, as experiment planting depth settings 1, 2, and 3 respectively, for their range of nominal planting depth as well laboratory planting depth calibrations (table 4.1 and fig. 4.4) that were previously conducted by the Auburn University Biosystems Engineering Department (Simerjeet Virk, Auburn University Biosystems Engineering Department, unpublished data, 2014). During previous in-field experiments using these settings, actual planting depths achieved were approximately 2.54, 5.08, and 7.62 cm respectively.

Table 4.1: Theoretical calibration for depth settings on a John Deere MaxEmerge™ Plus planter.

Position (L-R)[1]	**Planting Furrow Depth (cm)**
2-1	1.27
2-2	1.91
3-2	2.54
3-3	3.18
4-3	3.81
4-4	4.45
5-4	5.08
5-5	5.72
6-5	6.35
6-6	6.99
7-6	7.62
7-7	8.26
8-7	8.89
8-8	9.53
9-8	9.84
9-9	10.16

The planting furrow depths displayed represent theoretical values derived from a laboratory calibration. Actual planting depths achieved during in-field operation may vary.

[1]Left and right planter depth setting adjustment hole positions, located on the rear of the lower row unit frame.

Figure 4.4: Planter depth setting adjustment, shown in position 9-9.

Four replications were used to maximize the power of the experiment within the physical limitation of space in the soil bin. All of the treatments utilized a constant spring down force setting (medium), press wheel force setting, soil moisture, soil compaction, and planter velocity (approximately 0.85 m/s). Due to the fact that an indoor soil bin was used, seeds were not placed in the soil during the test and seeding rate was not considered. The 48 experimental units required by the design allowed for two empty plots in which an experimental unit could be reproduced if needed. Response variable data were collected using three systems. The first system was the planter DAQ described in section 3.3 (Fig. 4.5).

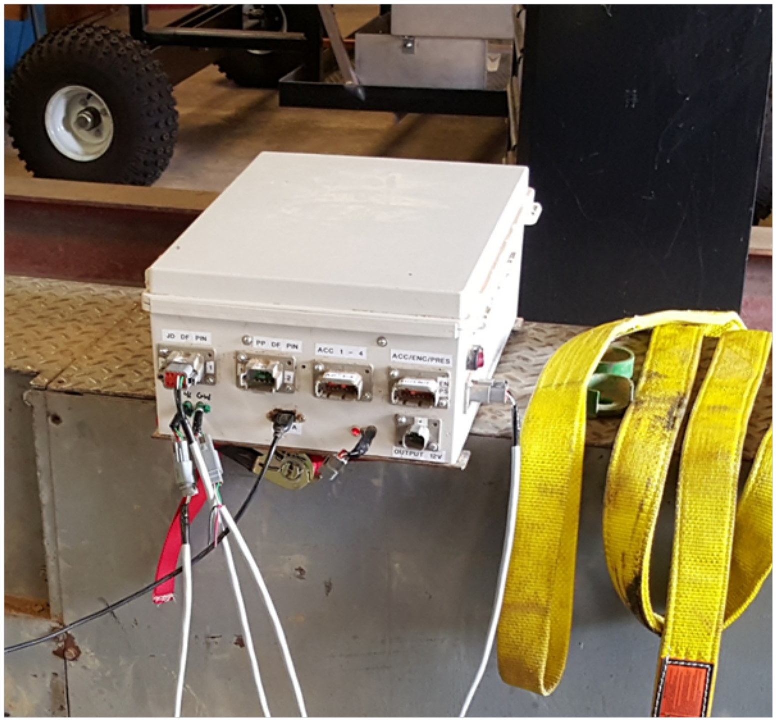

Figure 4.5: Planter data acquisition system enclosure.

The following data were collected at 100 Hz from the planter: four-bar link angle (FLAS) and gauge wheel arm angle (GWAS) using ASM magnetic angle encoders as well as vertical gauge wheel force (Fgw_Y) using a John Deere load cell pin (JD P/N: AA78166). Four-bar link angle was used to compute planter row unit position relative to the toolbar, apply four-bar link tension and compression loads correctly, and to estimate spring down force on the planter row unit. Gauge wheel arm angle was needed to compute gauge wheel position relative to the planter row unit frame and to provide a continuous variable describing planter depth setting. Finally, gauge wheel vertical force is needed to calculate the soil-planter interaction force distribution for each treatment. The planter DAQ also provided an output signal to synchronize data collection with the second system, the SoMat DAQ.

The SoMat DAQ system is an integral part of the National Soil Dynamics Laboratory's dyno cart and was used to collect data at 100 Hz from three 22.241 kN (5000 lbf) draft load cells, two 8.896 kN (2000 lbf) side load cells, one 8.896 kN (2000 lbf) vertical load cell, and one radar ground speed transducer. The six load cells on the dyno cart, shown in figure 4.6, enable the calculation of loads normal to the three orthogonal planes of the XYZ coordinate system as well as moments about the x, y, and z axes. All of these loads are critical in understanding the draft and vertical loads produced by the soil-planter interaction during operation. Details of each response variable monitored by the planter and SoMat DAQs are shown in table 4.2.

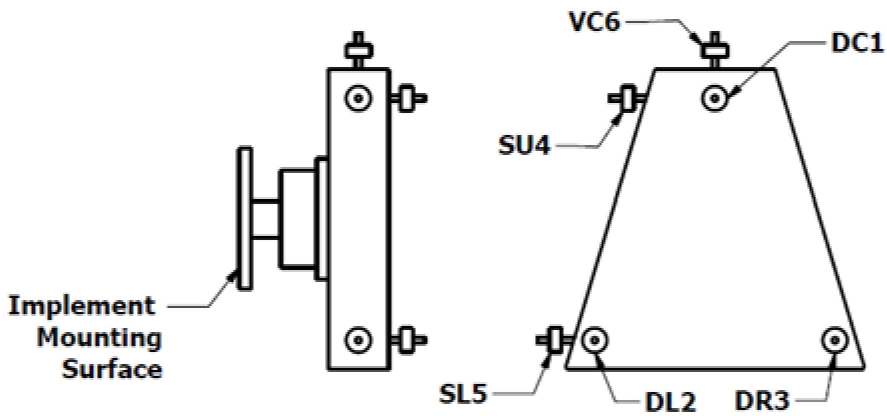

Figure 4.6: Configuration of the SoMat data acquisition system's load cells on the dyno cart at the USDA National Soil Dynamics Laboratory.

Table 4.2: Response variable descriptions for data collected by the planter and SoMat DAQs.

Name	Description	Units	Positive Convention
	Planter DAQ		
FLAS	Four-bar link internal angle	Degrees	CCW rotation
GWAS	Gauge wheel arm angle	Degrees	CW rotation
$\mathrm{Fgw_Y}$	Vertical force on the gauge wheels	kN	Positive global Y
	SoMat DAQ		
DC1	Toolbar draft force center	kN	Positive global X
DL2	Toolbar draft force left	kN	Positive global X
DR3	Toolbar draft force right	kN	Positive global X
SU4	Toolbar upper side force	kN	Positive global Z
SL5	Toolbar lower side force	kN	Positive global Z
VC6	Toolbar vertical force	kN	Negative global Y

Finally, data were collected manually on each treatment as well as randomly across the soil bin. Prior to beginning data collection volumetric water content (VWC) measurements were taken at the north end of each treatment plot, and ten bulk density (d_b) samples at 0-5 cm and 5-10 cm in depth were collected from the north end of treatments at random. During data collection toolbar height was measured at the beginning and end of each experimental unit. After all experimental units were run, the following soil measurements were taken within each plot referencing the undisturbed soil surface: five planting furrow depth measurements, five gauge wheel rut measurements, and five press wheel rut measurements. Finally, 13 cone penetrometer (CPT) readings were collected in undisturbed soil at random locations. Table 4.3 details the variables for initial condition data collected on the Norfolk Sandy Loam soil in the soil bin.

Table 4.3: Soil variable descriptions for data collected prior to conducting the experiment in the soil bin.

Name	Description	Units
VWC	Volumetric water content	%
d_{b_1}	Bulk density 0-5 cm depth	g cm^{-3}
d_{b_2}	Bulk density 5-10 cm depth	g cm^{-3}
CPT	Cone penetrometer test	kPa

4.2 Sensor Calibration

Prior to conducting the experiment in the soil bin the magnetic angle encoders were installed on the planter left-upper four-bar link and left gauge wheel arm. One hundred data points were collected for the four-bar link angle (FLAS) at three different angles of rotation. The internal angle from the rear surface of the toolbar mount to the bottom of the upper-left four-bar link was also measured for each rotation (fig. 4.7). The 100 data points for each rotation were then averaged and used with the manually collected internal angles to produce a linear regression calibration for four-bar link angle in degrees. The regression model, shown in equation 4.1, produced an adjusted R^2 and P-value of 1.0 and <0.05 respectively.

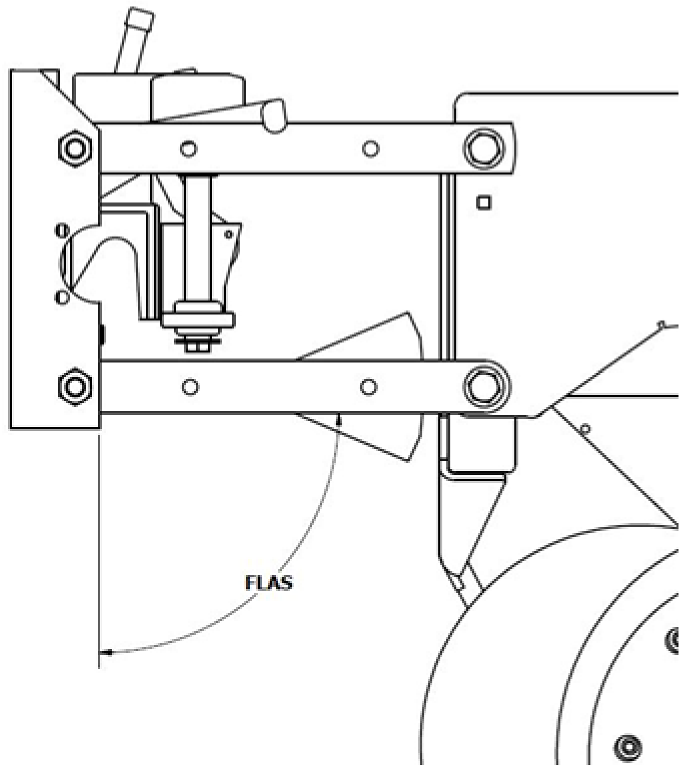

Figure 4.7: Manual measurement of internal angle FLAS, in degrees, between the rear surface of the toolbar mount and the lower surface of the four-bar link.

$$FLAS = 76.646x - 102.72 \tag{4.1}$$

Where x is the VDC output of the angle encoder.

The gauge wheel arm is offset and recessed into the backside of the gauge wheel during operation. For this reason, gauge wheel arm angle (GWAS) could not be manually measured while the gauge wheel was attached to the gauge wheel arm. Therefore, 100 data points were collected while the gauge wheel arm was contacting the upper hard stop, the planter depth setting rocker at the deepest setting; and the lower hard stop, the press wheel assembly frame. After data collection was complete, the gauge wheel was removed from the arm, and the arm was returned to the two hard stop positions. A manual internal angle measurement was made from the longitudinal axis of the gauge wheel arm to the upper horizontal surface of the lower planter row unit frame at each of the hard stop positions (fig. 4.8). The slope and intercept of the line intersecting the two points was calculated as the calibration for gauge wheel arm angle in degrees (eq. 4.2).

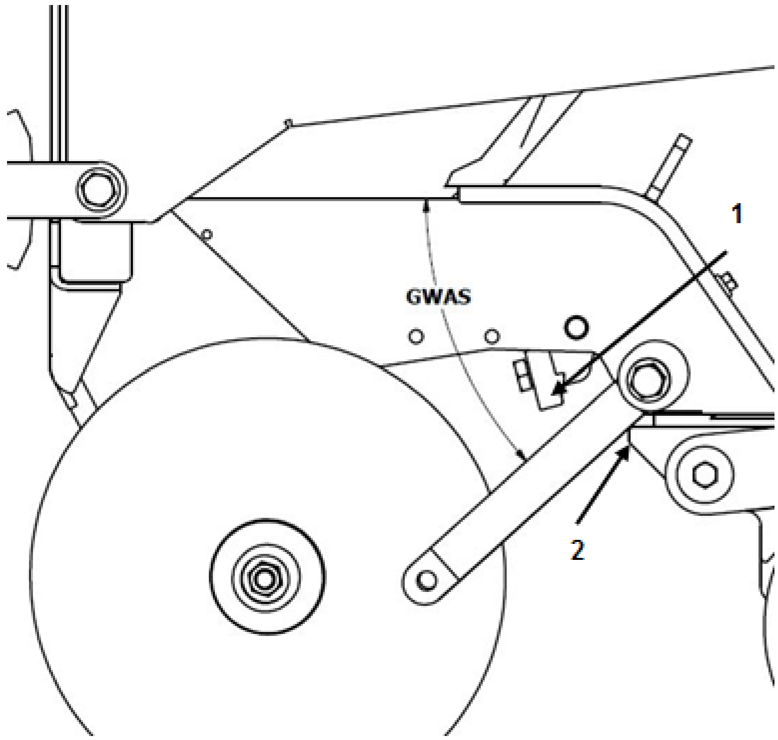

Figure 4.8: Manual measurement of internal angle GWAS, in degrees, between the horizontal surface on the lower frame and the gauge wheel arm.

$$GWAS = 82.106x - 170.31 \tag{4.2}$$

Where x is the VDC output of the angle encoder.

Due to the change in geometry of the gauge wheel arm assembly in relationship to the planter row unit frame and load cell pin used to record vertical gauge wheel force, a different load cell pin calibration was required for each planting depth setting used in the experiment. A scale was positioned under the planter with blocks under the gauge wheels to ensure that the entire weight of the planter row unit would rest on the gauge wheels and no other component (fig. 4.9). The planter depth setting was set to position 4-4, and the scale was zeroed. While being supported by the dyno cart, the toolbar was lowered until FLAS read 90°.

Figure 4.9: Calibration of the gauge wheel load pin for each planting depth setting.

Weights were then stacked onto and off of the planter frame. With each addition or removal of weight, data were collected from the load cell pin using the planter DAQ at 100 Hz for one second, and a scale reading was recorded. A total of 23 weight readings were collected for each replication, and three replications were conducted for each of the three planter depth settings used during the experiment. The 100 data points were averaged for each weight reading. The average sensor readings and recorded scale values were then used to produce a linear regression model calibration for Fgw_Y at each planting depth setting. The calibration models for Fgw_Y are presented below in table 4.4.

Table 4.4: Calibration of load cell pin for vertical force on the gauge wheels (Fgw_Y) per planting depth setting.

Depth Setting	Model	Adjusted $\mathbf{R}^2$	P-value
4-4	$Fgw_{\mathrm{Y}_{4-4}} = 0.7201x$	1.0	<0.001
6-6	$Fgw_{\mathrm{Y}_{6-6}} = 0.7193x$	0.99	<0.001
8-8	$Fgw_{\mathrm{Y}_{4-4}} = 0.7793x$	1.0	<0.001

Where Fgw_Y is in kN, and x is the VDC output of the load cell signal conditioner.

4.3 Spring Down Force System Calibration

The spring down force system was calibrated so that down force applied to the planter row unit frame by the system ($\mathrm{DF_Y}$) could be estimated for any FLAS. While supported by the dyno cart at the National Soil Dynamic Laboratory, a 10,000 lbf tension load cell was attached with an overhead hoist to the planter frame at the midpoint between the upper four-bar link attachment points on the planter row unit, as shown in figure 4.10. The planter DAQ was used to collect FLAS data as well as the output from the tension load cell for the calibration. The planter down force adjustment was set to medium down force (fig. 4.11), and the planter was lowered to a position just above the lower travel stop of the row unit. Static FLAS and load cell data were collected at 100 Hz for one second at this position. The planter row unit was then raised a couple of degrees FLAS with the overhead hoist and load cell and another set of static data points were collected. This process was continued, incrementally raising the planter to just below its upper travel stop and lowering it back to its starting position. Four replications of this process were completed. The 100 FLAS and load cell data points for each position were averaged to produce a total of 143 pairs. Once the averaged pairs were plotted, it was clear that spring down force was applied non-linearly (fig. 4.12). The data were divided into three independent data sets: constant, ramp, and spring. A linear regression was fit to the ramp and spring sections, while the data for the constant section were averaged to produce a single constant value, shown in table 4.5. The intersection points between the three sections of the calibration were then calculated using the constant and two regression equations. The final equation for estimating DF_Y for medium down force setting is shown in equation 4.3 below. Calibrations were also developed for down force settings low and high and are included in Appendix A.

Figure 4.10: Calibration of the spring down force system for four-bar link angle FLAS.

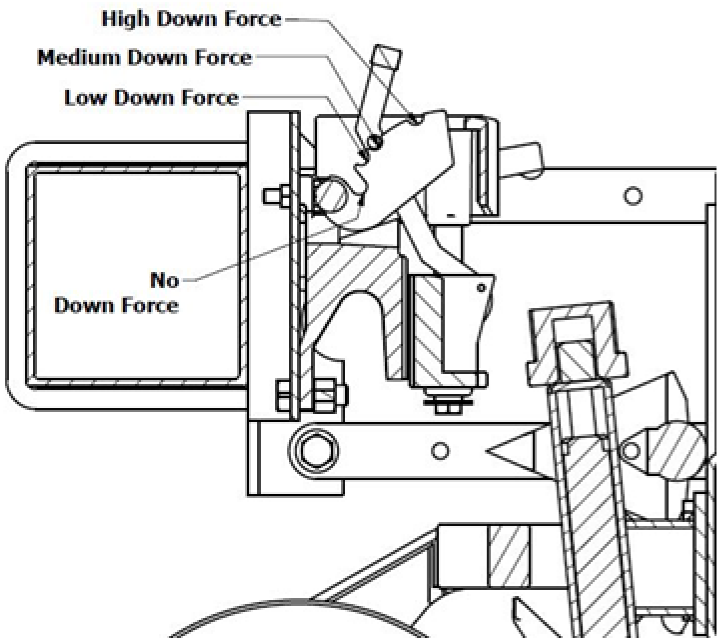

Figure 4.11: Down force settings for the John Deere MaxEmerge™ Plus planter.

Table 4.5: Linear regressions for spring down force system.

Section	**Model**	**Adjusted R^2**	**P-value**
Constant	$DF_{Y_{const}} = 0$	NA	NA
Ramp	$DF_{Y_{ramp}} = 0.3281x - 26.7851$	0.98	<0.001
Spring	$DF_{Y_{spring}} = 0.0205x - 0.8031$	1.0	<0.001

Where DF_Y is in kN, and x is the four-bar link angle, $FLAS$.

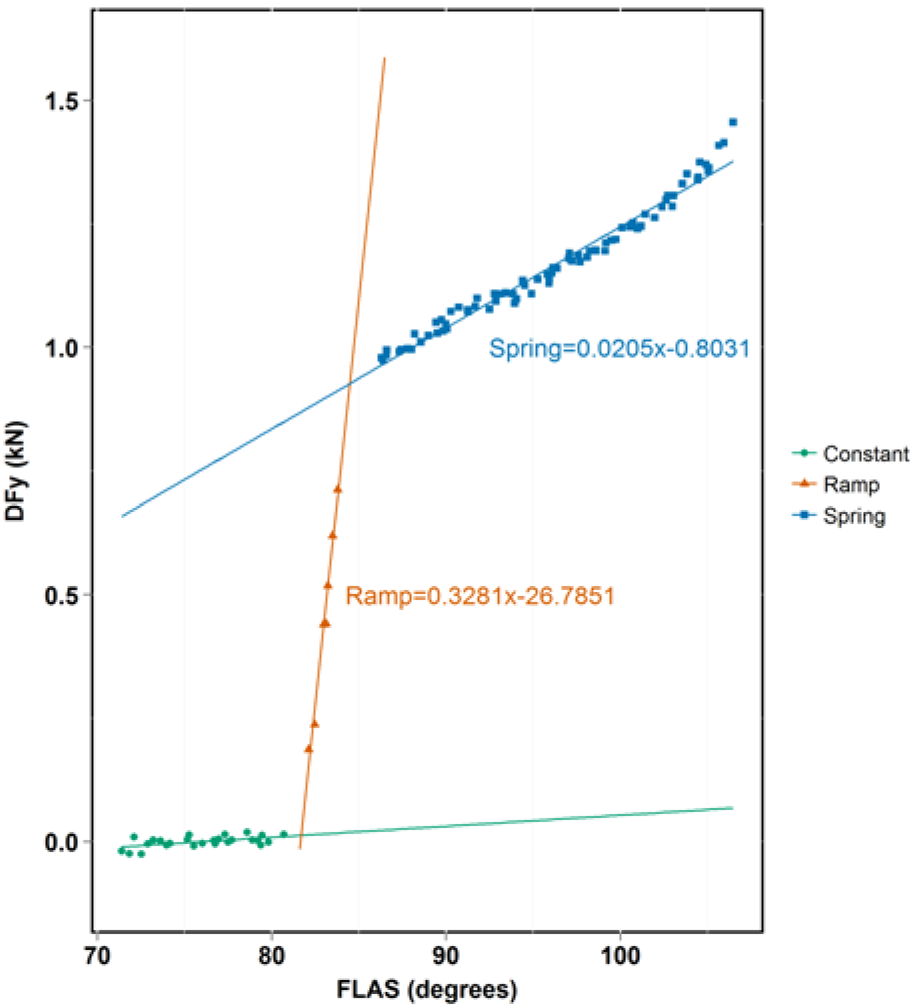

Figure 4.12: $\mathrm{DF_Y}$ calibration for medium spring down force setting.

$$
\begin{aligned}
FLAS \leq 81.65^\circ & \quad DF_Y = 0 \\
81.65^\circ < FLAS < 84.47^\circ & \quad DF_Y = 0.3281 * FLAS - 26.7851 \\
FLAS \geq 84.47^\circ & \quad DF_Y = 0.0205 * FLAS - 0.8031
\end{aligned}
\tag{4.3}
$$

4.4 Soil Bin Preparation

Preparing the soil bin so that planting conditions could be as uniform as possible and as described in the experimental design required multiple processes. First, water was applied to the soil bin using the water-grading cart (fig. 4.13). Two cycles of water application, consisting of one pass down the bin and one return pass, were conducted. The bin was allowed to sit undisturbed for at least four hours to allow the water to infiltrate the soil. Next, a rotary tiller cart, figure 4.14, was used to till the soil in three side-by-side passes to cover the bin width, to a depth of approximately 30-35 cm. The water and grading cart was then used again to grade the soil in the bin. Finally, the graded soil was compacted with one pass down the soil bin and one return pass of the roller cart (fig. 4.15). The bin preparation process produces a planting environment that is uniform in soil moisture, compaction, and surface profile (fig. 4.16). After preparation of the soil bin was complete, the plots were laid out and flagged. Special consideration was taken to not disturb the soil within each plot; walking across the bin only at the north and south ends of each plot.

Figure 4.13: Applying water to and grading the soil in the soil bin. (a) Water application (b) Grading.

(a)

(b)

Figure 4.14: Tilling the soil using three side-by-side passes across the width of the soil bin. (a) Tillage pass one along the left hand side of the bin. (b) Tillage pass three along the right hand side of the bin.

Figure 4.15: Compacting the soil in the soil bin with the roller cart.

Figure 4.16: Prepared soil bin at the USDA National Soil Dynamics Laboratory.

4.5 Planter and SoMat DAQs Experimental Data Collection

Prior to running the planter, volumetric water content (VWC) readings were taken approximately one meter south of the north end of each plot along the longitudinal centerline of the plot. The readings were taken with a FieldScout TDR-300 moisture meter per the manufacturer's specifications (Spectrum 2011) and logged within the meter (fig. 4.17). Bulk density (d_b) samples were taken at 0-5 cm and 5-10 cm in depth from the north end of ten plots selected randomly within the soil bin (fig. 4.18). The samples were taken using soil cores of known volume and analyzed using the oven dry method and procedures specified in the *USDA Soil Survey Field and Laboratory Methods Manual* (Soil Survey Staff 2014). Soil compaction (CPT) measurements were taken with a Rimik CP-20 cone penetrometer, using a 30° cone with base diameter of 12.7 mm. Data were collected in undisturbed soil at 13 locations randomly selected within the bin at depth increments of 15 mm to a maximum depth of approximately 390 mm. The files for each measurement were stored in the meter and downloaded at a later date. Figure 4.19 shows the plot layout of the bin as well as locations where the bulk density samples and soil compaction measurements were taken.

Figure 4.17: Volumetric soil water content data collected with a FieldScout TDR-300 meter.

(a)

(b)

Figure 4.18: Bulk density samples collected from ten locations within the soil bin.

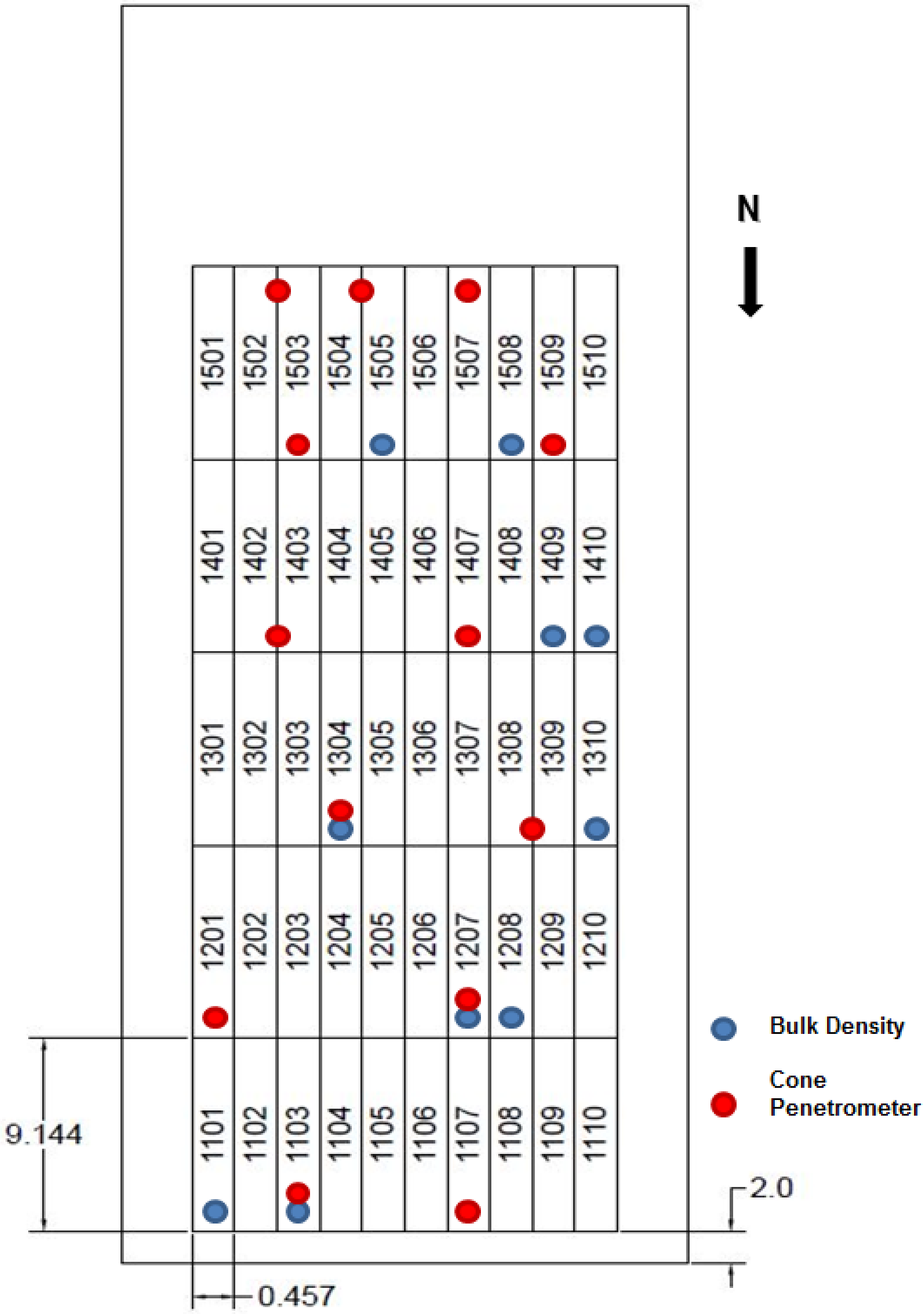

Figure 4.19: Locations within the soil bin where bulk density samples and cone penetrometer data were collected.

Prior to running the first treatment the planter was assembled in configuration 1, with spring down force in the medium setting, and the press wheel adjustment was positioned as shown in figure 4.20. The spring down force and press wheel force adjustments were left in these positions for the duration of the experiment. Before running the configuration 1 treatments, the planter was lowered onto a wooden block positioned under the double disc opener. The toolbar was lowered until the four-bar links were determined to be parallel with the concrete pad that was supporting the planter. A level positioned on the upper four-bar link was used to verify the parallel condition (fig. 4.21). With the planter row unit weight resting on the wooden block, the six SoMat DAQ load cells were zeroed (fig. 4.22).

Figure 4.20: Press wheel force adjustment position used for the duration of the soil bin experiment.

Figure 4.21: Four-bar links positioned level to the concrete surface prior to zeroing the load cells.

Figure 4.22: Planter in configuration 1 while SoMat load cells were zeroed.

After the load cell zero procedure was complete, the planter was moved to plot 1410 and the depth setting adjustment was moved to position 8-8, depth setting 3. While the planter was suspended in the air by the dyno cart, baseline data were collected by the SoMat DAQ from the six load cells on the dyno cart at 100 Hz for one second. This data set was later used to determine the bias present in any of the load cells. Next, the planter was lowered onto the soil at the north end of the plot. The toolbar was lowered until the four-bar links were determined to be parallel with the planting surface and verified as before with a level. A toolbar height measurement was recorded from the soil surface to the bottom edge of the planter toolbar mount, as shown in figure 4.23. The dyno cart with planter was then pulled toward the south end of the plot by the power cart. Once desired planter velocity was achieved, data were collected by the planter DAQ and SoMat DAQ at 100 Hz for three seconds. The power cart, dyno cart, and planter were then decelerated prior to reaching the south end of the plot. A second toolbar height measurement was then recorded in the manner previously detailed. Finally, the planter was lifted, via the dyno cart, vertically out of the soil. The planter was then moved to the next closest configuration 1 plot and the planting depth setting was adjusted as dictated by the treatment layout. The process from collection of baseline data to removing the planter from the soil at the end of the plot was repeated for all 12 configuration 1 experimental units.

Figure 4.23: Toolbar height measured from the soil surface to the bottom of the toolbar mount.

After all configuration 1 experimental units were run, the planter was moved back to the concrete pad adjacent to the soil bin. The coulter disc was removed and secured on top of the planter row unit frame to prepare the planter for configuration 2 experimental units as described in experimental design section 4.1. Once again the planter was lowered until the row unit's weight was supported by the wooden block under the double disc opener. The four-bar links were leveled, and the SoMat DAQ load cells were again zeroed. The configuration 2 experimental units were then run in the same manner as was described for the configuration 1 experimental units above. The entire process from configuration setup, load cell zeroing, and data collection was repeated for configuration 3 experimental units.

The planter was once again moved to the concrete pad adjacent to the soil bin. The GWAS magnetic angle encoder was removed to allow removal of the left gauge wheel assembly. Both gauge wheel assemblies were removed at the bosses on the row unit frame and secured on top of the frame above their operational position (fig. 4.24).

Figure 4.24: Planter in configuration 4 while SoMat load cells were zeroed.

The SoMat DAQ load cells were once again zeroed as was done for configurations 1 through 3. The planter was moved to the first configuration 4 plot and baseline data were again taken while the planter was suspended in the air. Unlike previous configuration treatments, the planter was then lowered until the double disc opener barely contacted the soil surface. Without gauge wheels providing planting furrow depth control, the dyno cart toolbar height was used to regulate furrow depth in place of planter depth setting and gauge wheels. A measurement was taken from the soil surface to the bottom surface of the planter toolbar mount. The dyno cart toolbar was then lowered from this position 2.54 cm for depth setting one, 5.08 cm for depth setting two, and 7.62 cm for depth setting three treatments. The planter weight, with the exception of the force produced by the interaction between the double disc opener and soil, was supported by the dyno cart through the four-bar links (fig. 5.13). The height from the soil surface to the bottom of the toolbar mount after setting the planting depth was then recorded. Data were collected in the same manor as was done for configurations 1-3. At the end of the run, height from the soil surface to the bottom of the toolbar mount was again measured and recorded.

Figure 4.25: Configuration 4 data collection.

4.6 Manual DAQ Experimental Data Collection

After the planter was setup and run for all 48 experimental units, the planter, dyno cart, and power cart were removed from the soil bin. Planting furrow depth (PD_{ref}), gauge wheel rut depth (GRD), and press wheel rut depth (PRD_{ref}) all referencing the undisturbed soil surface were then manually measured and recorded. The soil surface profile print, shown in figure 4.26, details the reference surface for each rut and furrow depth dimension.

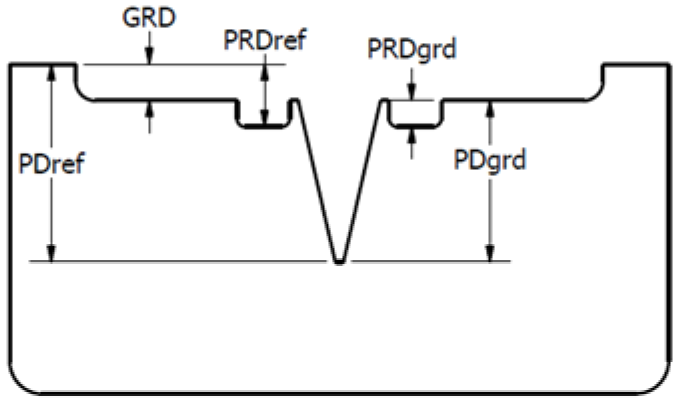

Figure 4.26: Variable descriptions and reference surfaces for planting furrow and rut depth data collected manually.

Where:

GRD: Gauge wheel rut depth measured from the undisturbed soil surface to the bottom of the gauge wheel rut in cm.

$\mathbf{PRD_{ref}}$: Press wheel rut depth measured from the undisturbed soil surface to the bottom of the press wheel rut in cm.

$\mathbf{PRD_{grd}}$: Press wheel rut depth measured from the bottom of the gauge wheel rut to the bottom of the press wheel rut in cm.

$\mathbf{PD_{ref}}$: Planting furrow depth measured from the undisturbed soil surface to the bottom of the planting furrow in cm.

$\mathbf{PD_{grd}}$: Planting furrow depth measured from the bottom of the gauge wheel rut to the bottom of the planting furrow in cm.

Starting with plots in row 1 and moving southward across the soil bin, a small cable was suspended above the soil surface from the cart rails along either side of the soil bin. The cable was randomly positioned laterally across the soil bin above the plots in row 1 and tensioned. For each plot, a reference measurement was made from the cable to the undisturbed soil surface just outside the outermost rut or furrow disturbance (fig. 4.27). The reference measurement was recorded to be used with rut and furrow measurements taken at this position within the given plot. Measurements were recorded from the cable to the bottom center of the gauge wheel rut (GRD), press wheel rut (PRD_{ref}), and planting furrow (PD_{ref}) (fig. 4.28). If press wheels or gauge wheels were not included for the treatment in any given plot, an "NA" was recorded for the corresponding value. If press wheels were included for the treatment in the plot being measured, a planting furrow depth measurement could only be made at the end of the plot where the planter was lifted out of the soil. Therefore, planting furrow depth measurements were only taken at these random positions within the plot for configurations 3 and 4. Once reference, rut depths, and furrow depth measurements were made across all plots for the current cable position, the cable assembly was moved southward across the plot and tensioned for another set of measurements. Reference, rut depth, and furrow depth measurements were taken as allowed by the configuration of the treatment in each plot for five random positions. For plots that contained a treatment that would not allow for furrow depth measurements, configurations 1 and 2, a reference and furrow depth measurement were taken from three positions at the end of the plot where the planter was lifted from the soil and the furrow had not been closed by the press wheel assembly (fig. 4.29).

Figure 4.27: Reference measurement used to calculate planting furrow and rut depth values.

(a)

(b)

Figure 4.28: Rut measurements for (a) gauge wheels and (b) press wheels.

Figure 4.29: Planting furrow depth measurement method for configurations 1 and 2 treatments.

4.7 Data Formatting and Manipulation

Data recorded by all three systems were imported into *R* for formatting, computation, statistical analysis, and graphical representation (R 2015). All *R* code is included in Appendix D. Data collected by the planter and manual DAQs were recorded individually and associated with their unique experimental unit plot number. The SoMat DAQ files, however, were a grouping of data sets consisting of all data collected from the time the SoMat system was started until it was reinitialized, usually when a configuration change or other lengthy break occurred during data collection. For this reason, code was written to analyze the time stamp on each data point within the set and separate the data into individual files when a gap in time stamp of 0.03 seconds or greater was observed. The individual files consisted of a treatment baseline file of approximately 100 data points followed by a treatment run file of approximately 300 data points. The sequence in which the data were collected was used to separate and assign file names to the individual data sets. Each experimental unit baseline data set was averaged to produce a single value per variable, and the averaged baseline values were compiled into a single data set by experimental unit baseline number. The baseline data set included the following variables: plot, Base_DC1, Base_DL2, Base_DR3, Base_SU4, Base_SL5, Base_VC6, Base_Total_DR, Base_Total_Side, and Base_Calc_MPH.

Next, each planter DAQ experimental unit file, consisting of approximately 300 data points per variable, was modified to include an index variable, providing each row of data points a unique number. All of the planter DAQ experimental units were merged by plot number and index number to maintain the order in which the data points were collected. This was done to ensure proper merging of the synchronous planter DAQ and SoMat DAQ data sets. The SoMat DAQ files were modified and merged in the same manner as the planter DAQ files. Finally, the two consolidated data sets were merged by plot and index number into a single complete sensor data set. The following variables were included in the sensor data set: plot, ID, config, plant_depth, rep, FLAS, GWAS, JD, time, DC1, DL2, DR3, SU4, SL5, VC6, Total_DR, Total_Side, and Calc_MPH.

The manually collected data were averaged to produce a single value per variable for each experimental unit, consisting of the following: plot, config, plant_depth, rep, PD_{ref}, GRD, and PRD_{ref}. Values for planting furrow depth referencing the gauge wheel rut (PD_{grd}) and press wheel rut depth referencing the gauge wheel rut (PRD_{grd}) were also calculated and included. This data set was utilized when calculating the component position and forces included in the sensor data set.

4.8 Four-Bar Linkage Forces

The first step in computing the force distribution on the planter was to determine how the loads recorded by the SoMat DAQ load cells were translated to the planter row unit through the four-bar linkages. This was accomplished by solving the toolbar free body diagram, which included the load cells and toolbar mount shown in figure 4.30.

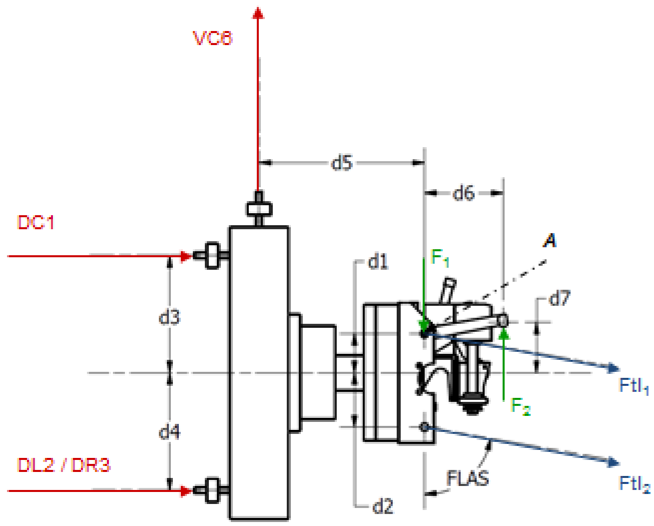

Figure 4.30: Dyno load cell free body diagram to solve for four-bar link forces.

First DF_Y was estimated using calibration equation 4.3 and populated for each datum point in the sensor data. A free body diagram of the upper four-link (fig. 4.31) and DF_Y produced the resultant force at the spring down force system arm (F_2) and the resultant force at the attachment point between the toolbar mount and the upper four-bar linkages (F_1) using the sum of moments about point A (eq. 4.4) and a sum of forces in the global Y (eq. 4.5). The computational values for DC1, DL2, DR3, and VC6 were calculated using the average baseline for the given treatment minus the running value, and positive sign convention for load cell values, shown in figure 4.30, was selected to match the sign convention previously established in the SoMat DAQ system. Positive sign convention for upper and lower four-bar link forces, Ftl_1 and Ftl_2 respectively, was selected to be in the positive global X direction. Positive sign convention for forces F_1 and F_2 was selected to be in the direction of application as determined by the four-bar link free body diagram (fig. 4.31). Ftl_2 was computed by a sum of moments about point A, eq. 4.6, with a clockwise rotation positive sign convention. Ftl_1 was then computed by a sum of the forces in the global X direction (eq. 4.7). F_1, F_2, Ftl_1, and Ftl_2 were recorded in the sensor data for each datum point collected.

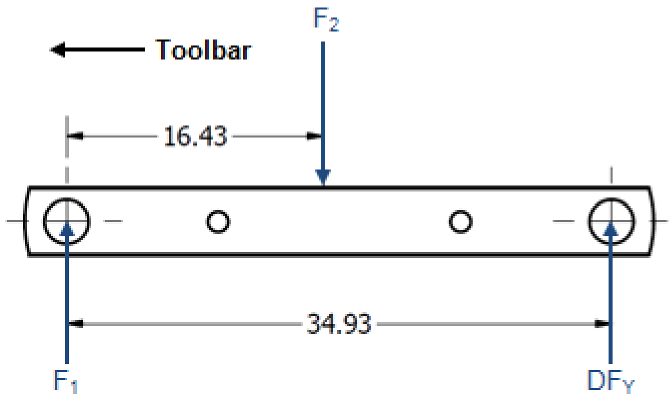

Figure 4.31: Four-bar link free body diagram.

$$F_2 = \frac{DF_Y(34.93 \sin FLAS)}{16.43} \tag{4.4}$$

$$F_1 = F_2 - DF_Y \tag{4.5}$$

$$Ftl_2 = \frac{(-DC1(d_3 - d_1) + (DL2 + DR3)(d_4 + d_1) - VC6(d_5) + F_2(d_6))}{(d_1 + d_2) \sin FLAS} \tag{4.6}$$

$$Ftl_1 = \frac{(-DC1 + (DL2 + DR3) - Ftl_2 \sin FLAS)}{\sin FLAS} \tag{4.7}$$

4.9 Gauge Wheel and Press Wheel Position and Force

Gauge wheel position is a function of the planting depth adjustment setting. The planting depth adjustment handle controls the position of the rocker (upper hard stop) which the gauge wheel arm contacts (fig. 3.9). However, GWAS was a better indicator of gauge wheel position and enabled the position to be calculated even when the gauge wheel arm was not in contact with the rocker. The gauge wheel arm rotated about a spindle that was not normal to any global reference plane, requiring two rotational transformations to calculate the gauge wheel hub position in the global XYZ reference frame. Two local reference frames were created on the gauge wheel arm spindle of the planter row unit frame with their origins aligned. The first reference frame, xyz, was aligned with the global reference frame XYZ. The second reference frame, $x'y'z'$, was rotated so that the z' axis was aligned axially with the boss. An Euler angle rotation ($\mathrm{R_z}$) was used with a vector describing the gauge wheel arm (BC) to calculate the position of the gauge wheel hub in the $x'y'z'$ reference frame for any rotation GWAS (eq. 4.8) (Marghitu 2011). A rotation transformation matrix ($\mathrm{R_{glb}}$) was then used to translate the gauge wheel hub position referencing $x'y'z'$ to local reference frame xyz (eq. 4.9) (Marghitu & Dupac 2011). $\mathrm{R_{glb}}$ was determined using two sets of three orthogonal unit vectors describing the x, y, and z axes of the global and local reference frames. The gauge wheel hub position in the global XYZ (eq. 4.10) was then given by the vector describing the position of the local reference frame xyz (AB), the transpose of Rglb, and the position calculated in equation 4.8 (Marghitu & Dupac 2011). Force on the gauge wheels in the global Y ($\mathrm{Fgw_Y}$) was estimated using the planting depth specific calibrations from table 4.4.

$$GWhub_{x'y'z'} = \begin{bmatrix} \cos\gamma_{z'} & \sin\gamma_{z'} & 0 \\ -\sin\gamma_{z'} & \cos\gamma_{z'} & 0 \\ 0 & 0 & 1 \end{bmatrix} \begin{bmatrix} BC \end{bmatrix} \tag{4.8}$$

$$R_{glb} = \begin{bmatrix} a_{x'x} & a_{x'y} & a_{x'z} \\ a_{y'x} & a_{y'y} & a_{y'z} \\ a_{z'x} & a_{z'y} & a_{z'z} \end{bmatrix} \tag{4.9}$$

$$GWhub_{XYZ} = \begin{bmatrix} AB \end{bmatrix} + \begin{bmatrix} R_{glb} \end{bmatrix}^T \begin{bmatrix} GWhub_{x'y'z'} \end{bmatrix} \tag{4.10}$$

Press wheel position in the global X and Y (eq. 4.12 and eq. 4.13) was calculated from the gauge wheel position at the time the datum point was recorded and the average press wheel rut measured from within the experimental unit plot, as detailed in figure 4.32. The resultant force produced on the press wheels is a function of the tension spring length in the assembly. The geometry of the system is shown in figure 4.33. The angle between the fixed and adjustable spring attachment points through the press wheel assembly hinge axis (γ_{PWSpg}) was calculated with equations 4.11 and 4.14. The tensioned spring length (D_9) was calculated using the law of cosines equation 4.15. The angle between the press wheel assembly hinge axis and the adjustable spring attachment point through the fixed spring attachment point (γ_3) was calculated using the law of cosines equation 4.16. The angle between the tension spring axis and the global XZ plane (γ_4) was then computed using γ_1 and γ_3 (eq. 4.17). Finally, the press wheel assembly free body diagram shown in figure 4.34 was produced including the press wheel spring force (Fpws), which was estimated using the spring length and the spring calibration (fig. 3.4), and resultant forces: press wheel in the global Y ($\mathrm{Fpw_Y}$), press wheel hinge in the global X ($\mathrm{FpwH_X}$), and press wheel hinge in the global Y ($\mathrm{FpwH_Y}$). $\mathrm{Fpw_Y}$ was calculated by a sum of the moments about the press wheel assembly hinge axis A (eq. 4.18) and recorded for each datum point within the sensor data set. Positive sign convention for the moment about A was selected to be clockwise rotation. For each of the forces included in the press wheel free body diagram positive sign convention was selected for their expected direction of application.

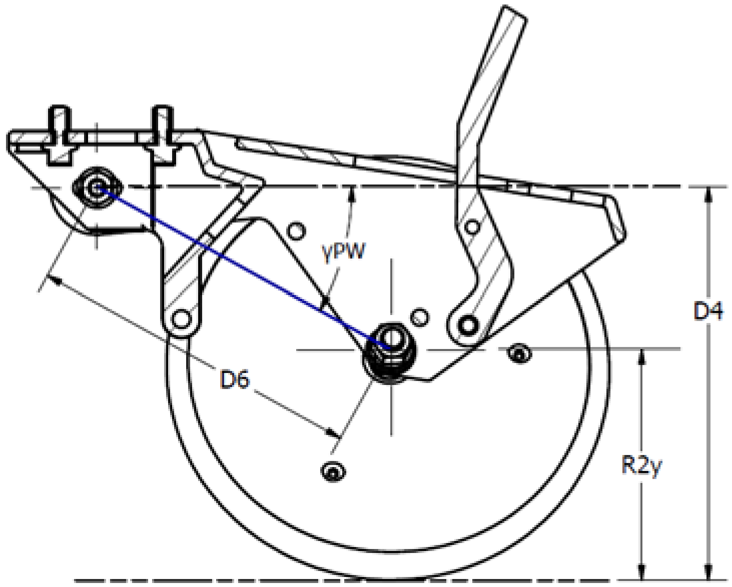

Figure 4.32: Position of press wheel hub axis in global XYZ.

$$\gamma_{PW} = \sin^{-1}\left(\frac{D_4 - R2_Y}{D_6}\right) \tag{4.11}$$

$$PW_X = D_5 + D_6 \cos\gamma_{PW} \tag{4.12}$$

Where D_5 is the horizontal distance along global X from the origin to the axis of the press wheel assembly hinge.

$$PW_Y = GW_Y - R1_Y - PRD_{grd} + R2_Y \tag{4.13}$$

Where $R1_Y$ is the vertical component, in the global Y, of the gauge wheel radius.

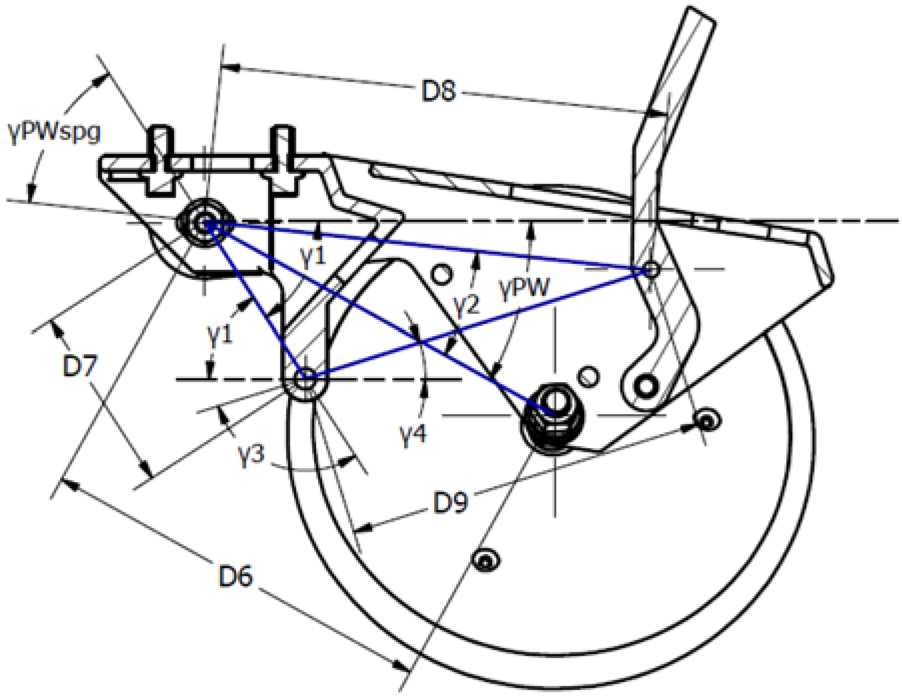

Figure 4.33: Press wheel assembly geometry.

$$\gamma_{PWSpg} = \gamma_1 - (\gamma_{PW} - \gamma_2) \tag{4.14}$$

$$D_9 = \sqrt{D_8^2 + D_7^2 - 2(D_8)(D_7)\cos\gamma_{PWSpg}} \tag{4.15}$$

$$\gamma_3 = \cos^{-1}\left(\frac{-D_8^2 + D_7^2 + D_9^2}{2(D_7)(D_9)}\right) \tag{4.16}$$

$$\gamma_4 = 180^\circ - \gamma_1 - \gamma_3 \tag{4.17}$$

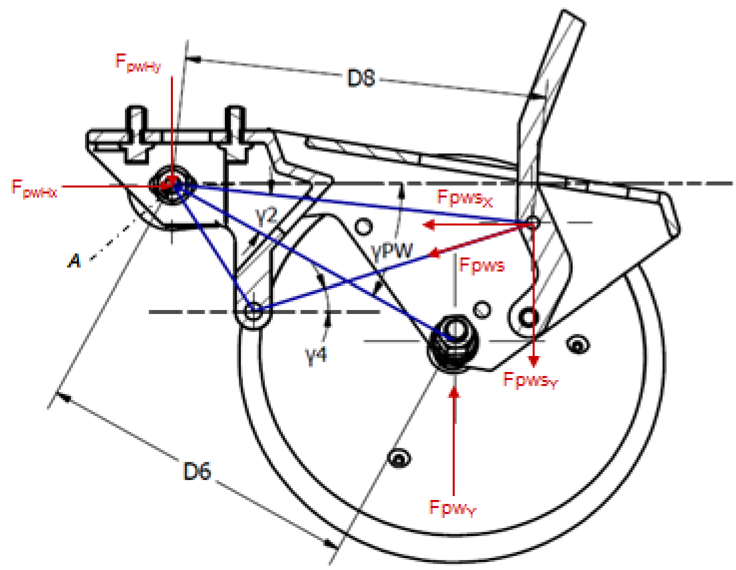

Figure 4.34: Press wheel assembly free body diagram.

$$Fpws_X = Fpws\cos\gamma_4$$

$$Fpws_Y = Fpws\sin\gamma_4$$

$$Fpw_Y = \frac{-Fpws_Y(D_8\cos\gamma_{PW} - \gamma_2) - Fpws_X(D_8\sin\gamma_{PW} - \gamma_2)}{-D_6\cos\gamma_{PW}} \tag{4.18}$$

4.10 Planter Force Distribution

The center of gravity for each planter configuration was determined using the CAD models produced prior to conducting the experiment at the National Soil Dynamics Laboratory. The planter weight (Wt) applied at the center of gravity (CG) was measured during the gauge wheel down force pin calibration. This information along with the forces and positions computed in the previous sections provided everything needed to determine the force distribution on the planter row unit due to its interaction with the soil. The positive sign conventions shown in table 4.6 were applied to all four planter configuration free body diagrams.

Table 4.6: Variable descriptions for forces acting on the planter in free body diagrams.

Name	Description	Units	Positive Convention
Fct_Y	Force on the coulter in the global Y	kN	Pos. global Y
Fdd_Y	Force on the double disc opener in the global Y	kN	Pos. global Y
Fgw_Y	Force on the gauge wheels in the global Y	kN	Pos. global Y
Fpw_Y	Force on the press wheel assembly in the global Y	kN	Pos. global Y
F_d	Total draft force in the global X	kN	Pos. global X
Wt	Weight of the planter row unit	kN	Neg. global Y
DF_Y	Applied down force acting in the global Y	kN	Neg. global Y
Ftl_1	Upper four-bar link comp./tens. force	kN	Neg. global X / Pos. global Y
Ftl_2	Lower four-bar link comp./tens. force	kN	Neg. global X / Pos. global Y

4.10.1 Configuration 4

For the most simplified configuration, configuration 4, only the double disc opener was contacting the soil. Therefore, any force generated in the global X or Y directions was a result of the double disc opener's interaction with the soil. The free body diagram for configuration 4 (fig. 4.35) details the forces acting on the planter row unit. Forces on the double disc opener in the global Y direction (Fdd_Y) and the global X direction (Fdd_X) are simply the difference in baseline and running values for VC6 and Total_DR, as shown in equations 4.19 and 4.20.

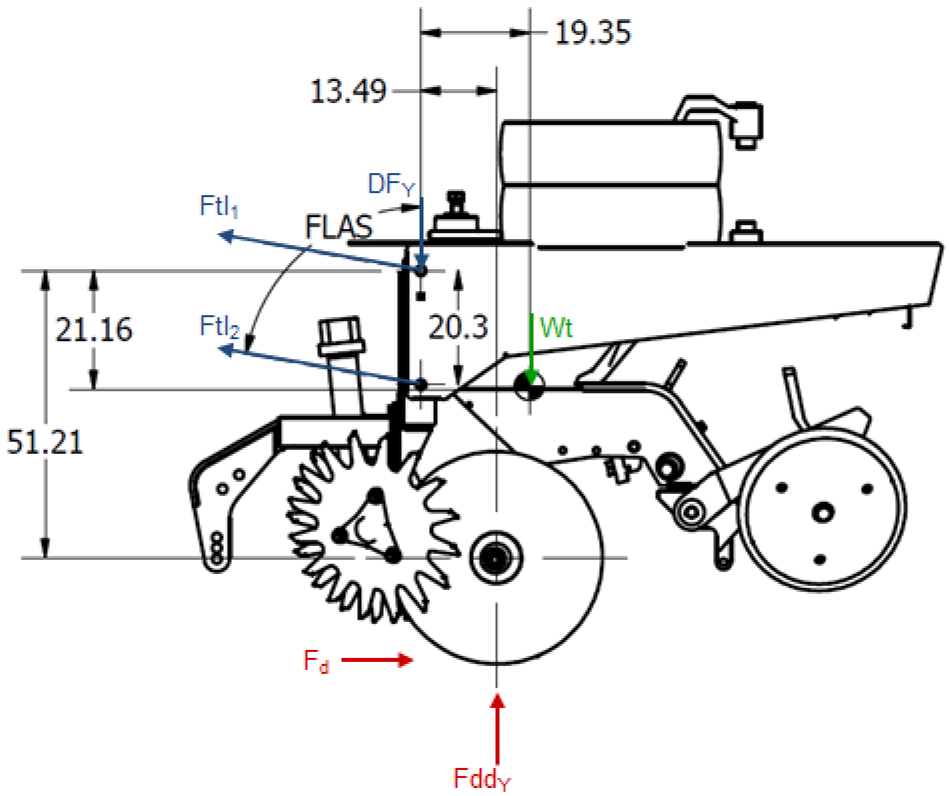

Figure 4.35: Configuration 4 free body diagram.

$$Fdd_{Y_{Config4}} = Base\_VC6 - VC6 \tag{4.19}$$

$$F_{d_{Config4}} = Fdd_{X_{Config4}} = Base\_Total\_DR - Total\_DR \tag{4.20}$$

4.10.2 Configuration 3

Unlike configuration 4, the four-bar linkage was run parallel to the ground in configuration 3. This requires the weight of the planter, applied at the CG, as well as any additional down force generated by the spring down force system to be supported by the components of the planter row unit interacting with the soil, as shown in the configuration 3 free body diagram (fig. 4.36). Since Fgw$_Y$ was estimated from the output of the load cell pin, Fdd$_Y$

can be computed by solving the sum of the forces acting on the planter row unit in the global Y direction (eq. 4.21). Total draft force (F_d) was calculated as the baseline minus the running Total_DR (eq. 4.22).

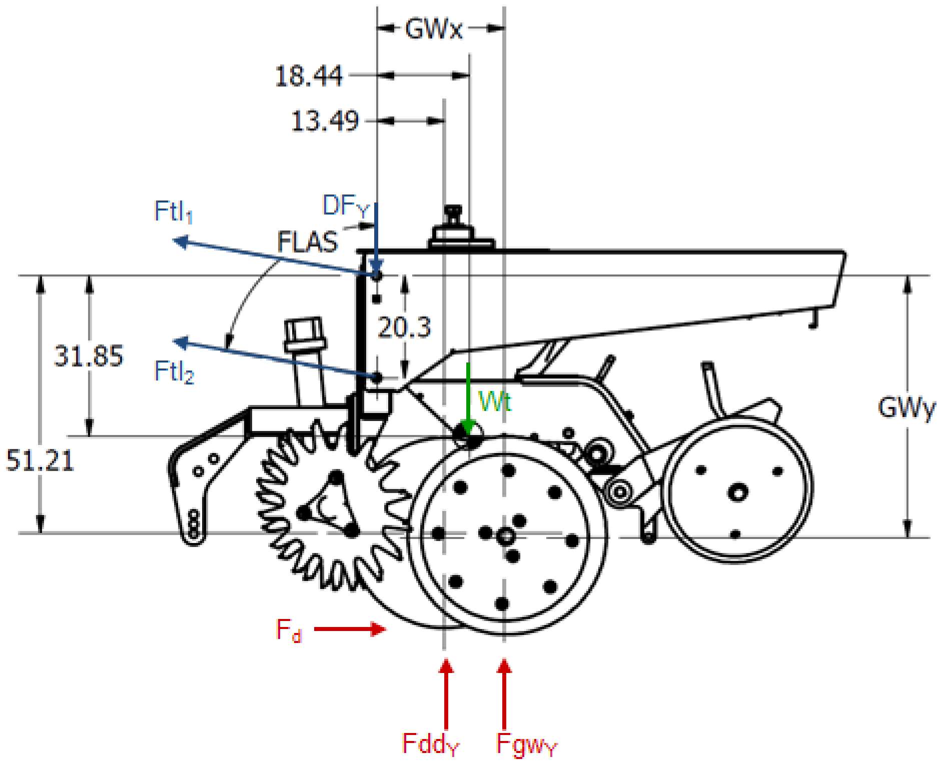

Figure 4.36: Configuration 3 free body diagram.

$$Fdd_{Y_{Config3}} = -Ftl_1 \cos FLAS - Ftl_2 \cos FLAS + DF_Y + Wt - Fgw_Y \tag{4.21}$$

$$F_{d_{Config3}} = Base\_Total\_DR - Total\_DR \tag{4.22}$$

4.10.3 Configuration 2

Similar to configuration 3 all of the forces acting on the planter row unit were already determined with the exception of $\mathrm{Fdd_Y}$. The forces and their positions were detailed in the configuration 2 free body diagram, shown in fig. 4.37. $\mathrm{Fgw_Y}$ and $\mathrm{Fpw_Y}$ were previously determined, and $\mathrm{F_d}$ was calculated in the same manner as in configuration 3 (eq. 4.22). $\mathrm{Fdd_Y}$ was once again solved using the sum of forces acting on the planter row unit in the global Y direction (eq. 4.23).

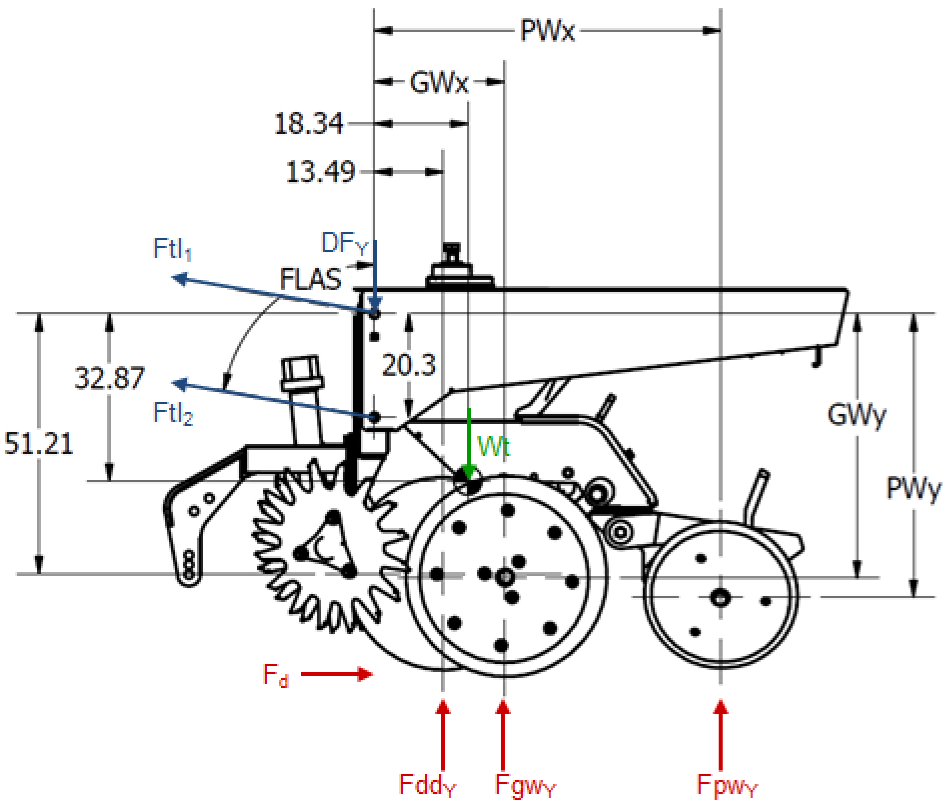

Figure 4.37: Configuration 2 free body diagram.

$$Fdd_{Y_{Config2}} = -Ftl_1 \cos FLAS - Ftl_2 \cos FLAS + DF_Y + Wt - Fgw_Y - Fpw_Y \tag{4.23}$$

4.10.4 Configuration 1

Configuration 1 is the most complex configuration and therefore required more computation to solve for all of the forces acting on the planter row unit frame. F_d, Fgw_Y, and Fpw_Y were calculated in the same manner as configuration 3. Using the free body diagram for configuration 1 (fig. 4.38), Fdd_Y was calculated by summing the moments acting on the planter row unit about the hub axis of the coulter disc (eq. 4.24). Fct_Y was then solved using a sum of the forces in the global Y (eq. 4.25). Fdd_Y and Fct_Y for configuration 1 were not included in the statistical analysis. Due to a geometry specific bias that was present in the baseline draft loads, the values produced by the moment calculation used to solve for Fdd_Y and ultimately Fct_Y were incorrect.

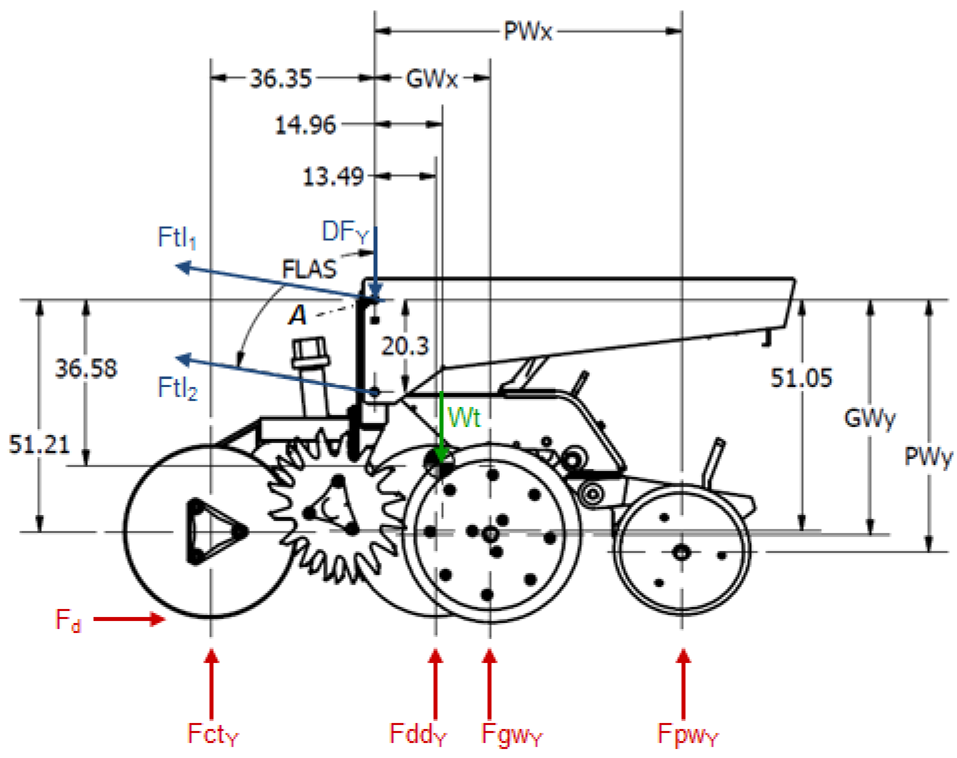

Figure 4.38: Configuration 1 free body diagram.

$$Fdd_{Y_{Config1}} = \frac{\begin{pmatrix} Flt_1(51.21 \sin FLAS + 36.35 \cos FLAS) \\ + Ftl_2(30.89 \sin FLAS + 36.35 \cos FLAS) \\ - 36.35 DF_Y - 51.31 Wt + Fgw_Y(36.35 + GW_X) \\ + Fpw_Y(36.35 + PW_X) + F_d((-GW_Y + R1_Y) - 51.21) \end{pmatrix}}{-49.83} \tag{4.24}$$

$$\begin{aligned} Fct_{Y_{Config1}} = & - Ftl_1 \cos FLAS - Ftl_2 \cos FLAS + DF_Y + Wt \\ & - Fdd_Y - Fgw_Y - Fpw_Y \end{aligned} \tag{4.25}$$

4.11 Data Analysis

Statistical analysis for all the experimental data was conducted using the open source statistical and graphical software package *R*. The function *aggregate* was used to compute the mean and standard deviation summary statistics for each variable per treatment. The data sets created by the *aggregate* function for the sensor data and manually collected data were combined to produce a data set with one mean value for each variable within an experimental unit. This data set was used to perform an analysis of variance with mixed effect models and to produce linear regression models.

Chapter 5

RESULTS and DISCUSSION

5.1 Soil Bin Uniformity

Summary statistics were calculated for the initial conditions of the Norfolk Sandy Loam soil in the soil bin including: bulk density (d_b), volumetric water content (VWC), and cone penetrometer values (CPT) to a depth of 105 mm. The results are displayed in table 5.1. Soil properties within the bin were considered to be uniform to a depth below the maximum measured planting furrow depth.

Table 5.1: Initial conditions of prepared Norfolk Sandy Loam soil in the soil bin.

Statistic	**VWC**[1] **(%)**	**Bulk Density (g cm^{-3})**		**Cone Penetrometer**[2] **(kPa) (mm)**						
		0-5 cm	5-10 cm	15	30	45	60	75	90	105
min	10.9	1.50	1.55	88	247	505	687	846	786	702
max	19.2	1.71	1.76	164	551	1346	1748	1779	1597	1468
mean	14.5	1.6	1.65	110	360	808	1067	1122	1085	1010
Std. Dev.	2.0	0.07	0.06	23	89	212	264	251	222	206
CV	0.14	0.042	0.036	0.2	0.2	0.3	0.2	0.2	0.2	0.2

[1] Volumetric Water Content collected with a Field Scout™ TDR 300 soil moisture meter.

[2] Cone Penetrometer Test data collected at 15 mm depth increments with a Rimik CP20 cone penetrometer.

5.2 Planting Furrow Depth

Planting/seeding depth is conventionally defined as a ”soil over seed” measurement (SOS). For this experiment seed was not placed in the soil, therefore the dynamics of placing the seed within the furrow and the consolidation of soil over the seed between planting and germination could not be considered. Planting furrow depth to the undisturbed soil surface (PD_{ref}) was recorded and used as a related measure of the soil over seed planting depth. While a definitive relationship between PD_{ref} and SOS is not known for the conditions present during the experiment, it is believed that the trends produced by changes in planter configuration, depth setting, and force distribution were accurately described by the PD_{ref} measure. As was expected a significant difference in planting furrow depth was observed across all planting depth settings for PD_{ref} (fig. 5.1) and PD_{grd} (fig. 5.2).

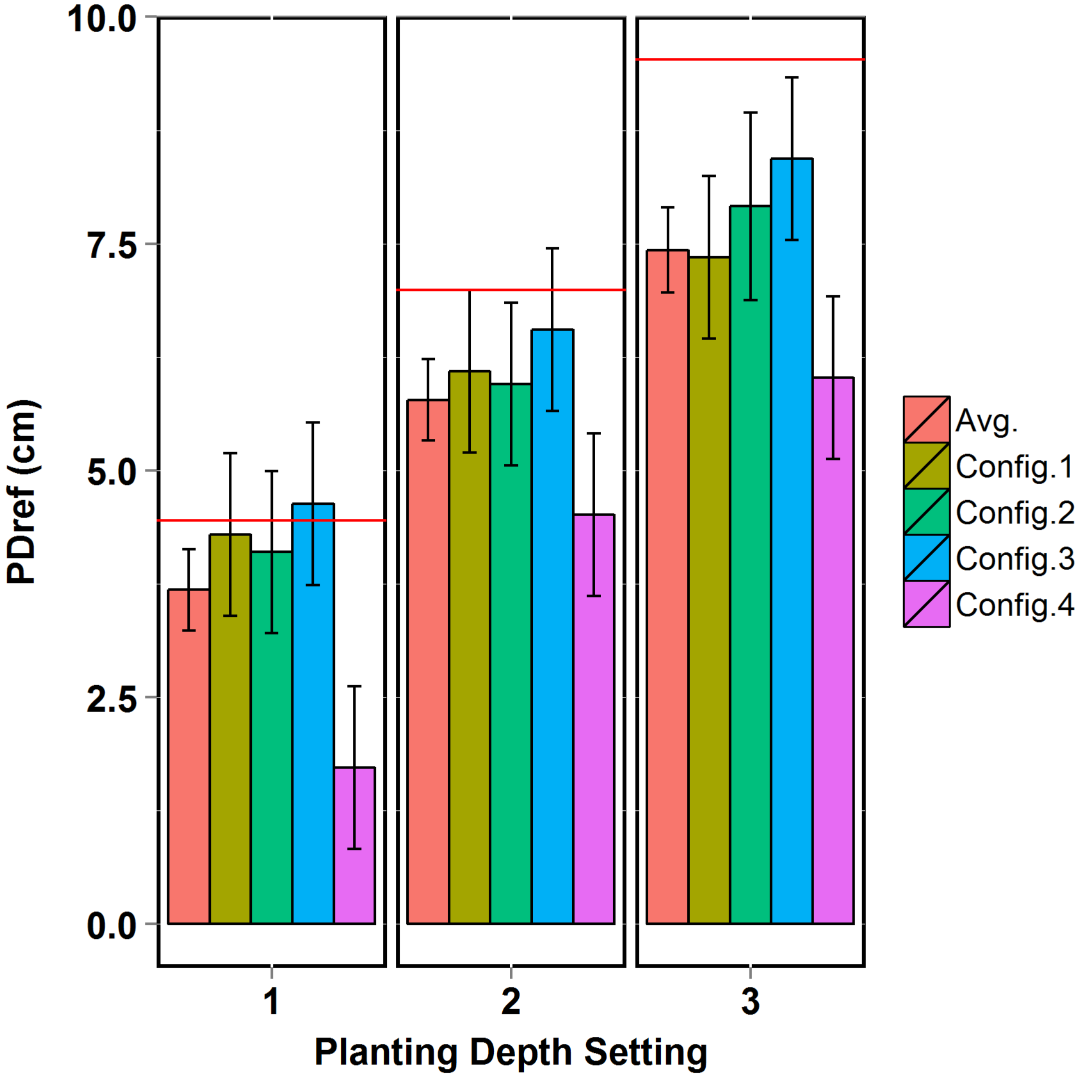

Figure 5.1: Planting furrow depth measured to the undisturbed soil surface.

Error bars represent 95% confidence intervals.

Horizontal red lines represent theoretical planting depth for each planting depth setting.

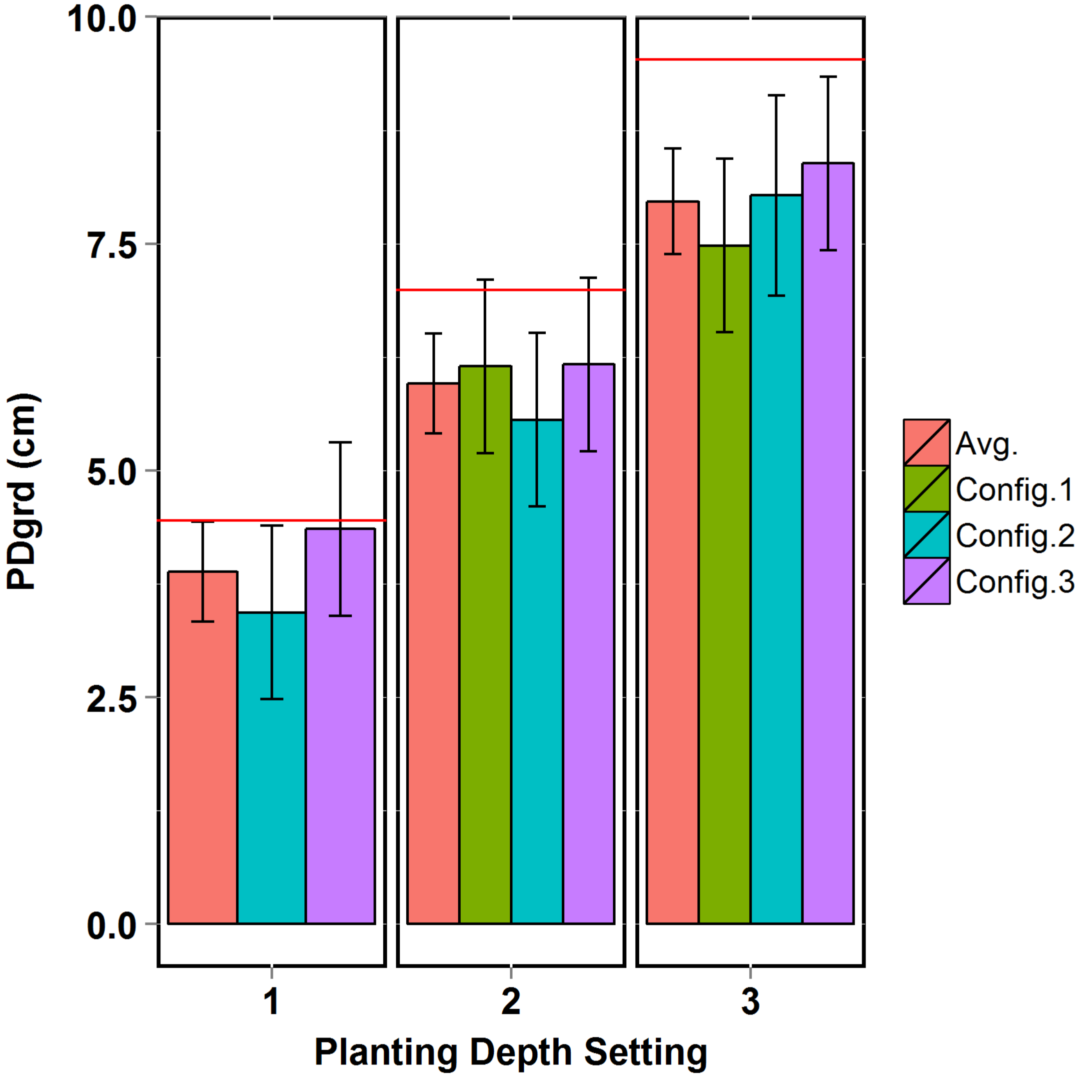

Figure 5.2: Planting furrow depth measured to the gauge wheel rut.

Error bars represent 95% confidence intervals.

Horizontal red lines represent theoretical planting depth for each planting depth setting.

As discussed in section 4.1 experimental planting depth settings 1, 2 and 3 equate to planter depth adjustment settings 4-4, 6-6, and 8-8 respectively. PD_{ref} of depth setting 1 closely matches the theoretical planting depth from table 4.1, shown in figures 5.1 and 5.2 by horizontal red lines ; however increasing planting furrow depth due to depth setting changes produces diminishing returns resulting in depth setting 3 falling far short of the theoretical depth of 9.53 cm. This indicates that planting depth setting and achieved planting furrow depth are not a one-to-one correlation, and additional factors should be considered when planting depth setting adjustments as made. The diminishing response to depth setting changes can partially be explained by the negative trend in gauge wheel rut depth to increased planting depth that will be presented in section 5.3.1. It is also affected by the increasing total contact area between the planter and soil as planting depth is increased. For any given down force setting and four-bar link angle, a finite amount of down force is available for the planter to achieve the desired planting depth. As planting depth increases, this force is ultimately balanced with the force generated by the components operating within the soil, and no additional force is carried by the those components rolling along the soil surface. At this point, increased down force on the planter is required to increase planting depth.

5.3 Physical Effects of Planter Depth Setting Adjustments on Soil Surface Profile and the Planting Furrow

The goal was to determine the physical effects of an agricultural planter row unit on the soil surface profile and planting furrow depth. Data collected from each experimental unit were evaluated to answer the following objectives:

1. How are gauge wheel and press wheel rut depths affected by planting depth setting?
2. Can gauge wheel rut depth be predicted from planter operating conditions?
3. Can planting furrow depth be predicted by planting depth setting and gauge wheel or press wheel rut depths?

5.3.1 Rut Depths

An analysis of variance using mixed effects models was conducted on the planting furrow and rut depth data collected during the experiment. Multiple comparisons were conducted using Fishers Least Significant Difference (LSD) (Piepho *et al.* 2003). Standard deviations were not different for PD_{ref}, GRD, and PRD_{ref} across planting depths or planter configurations. Therefore, changes in planting depth setting or configuration did not have an effect on variation in the previously mentioned variables.

Planter gauge wheels are designed to regulate the vertical position of the planter frame and double disc opener in relation to the soil surface that is being traversed. Therefore, if actual planting furrow depth referencing the undisturbed soil surface is desired, gauge wheel rut depth must be detectable or predictable. GRD, as shown in figure 5.3, trended down with increasing planting depth setting. A decrease of 112% in GRD was observed between planting depth setting 1 and depth setting 3. Also, mean gauge wheel rut depths were negative for configurations 1 and 2 at planting depth setting 3. This indicates that for the soil type and conditions present during the experiment, there was not enough load carried by the gauge wheels to re-consolidate the soil that was displaced by the double disc openers. A negative GRD condition may not be optimal for planting depth precision, because the gauge wheels are operating on a raised soil bed displaced by the double disc openers. A more ideal condition would likely be when the gauge wheels have consolidated the soil back to its original position, but not created a rut, and the load supported by the gauge wheels is distributed over a larger area.

Additionally, mean rut depth was negative for configurtion 1 and positive for configurations 2 and 3 for data collected in depth setting 2 treatments. This can be explained by the distribution of forces acting on the planter which will be discussed in section 5.4. As planter components were removed from contacting the soil in configurations 2 and 3, the load that was previously carried by those components was partially transfered to the gauge wheels, increasing the soil consolidation beneath them .

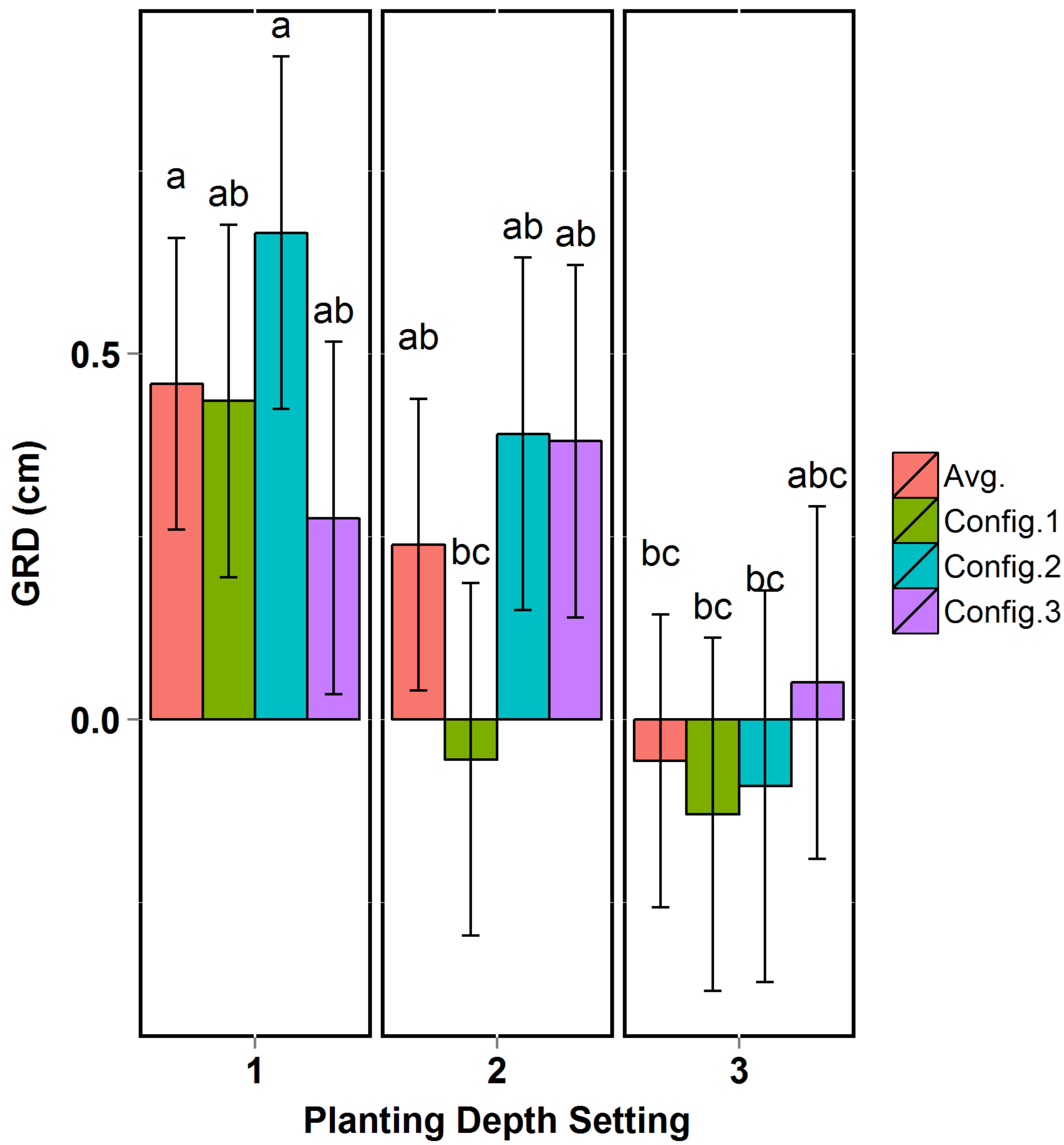

Figure 5.3: Gauge wheel rut depth measured to the undisturbed soil surface.

Error bars represent 95% confidence intervals. Standard deviations denoted by the same letter are not significantly different, based on 95% confidence intervals.

A significant difference was observed for values of PRD_{ref} between planting depth settings 1 and 3 and between depth settings 2 and 3 (fig. 5.4). PRD_{grd} was found to be different across all planting depth pairings (fig. 5.5). An increase in planting depth from depth setting 1 to 3 produced increases in mean PRD_{ref} and PRD_{grd} of 80% and 237% respectively. Press wheel rut depth is determined by the bearing capacity of the soil to support the force that is exerted on it by the press wheel assembly. Because press wheel force is directly a function of the press wheel force setting adjustment and the press wheel's vertical position relative to the planter row unit frame, rut depth increasing with planting depth was expected. Mean PRD_{ref} was more consistent across configurations for planting depth setting 1 than depth settings 2 or 3. This is likely due to the increased soil consolidation by the gauge wheels (GRD) and the reduced force produced by the press wheel assembly present in depth setting 1 experimental units.

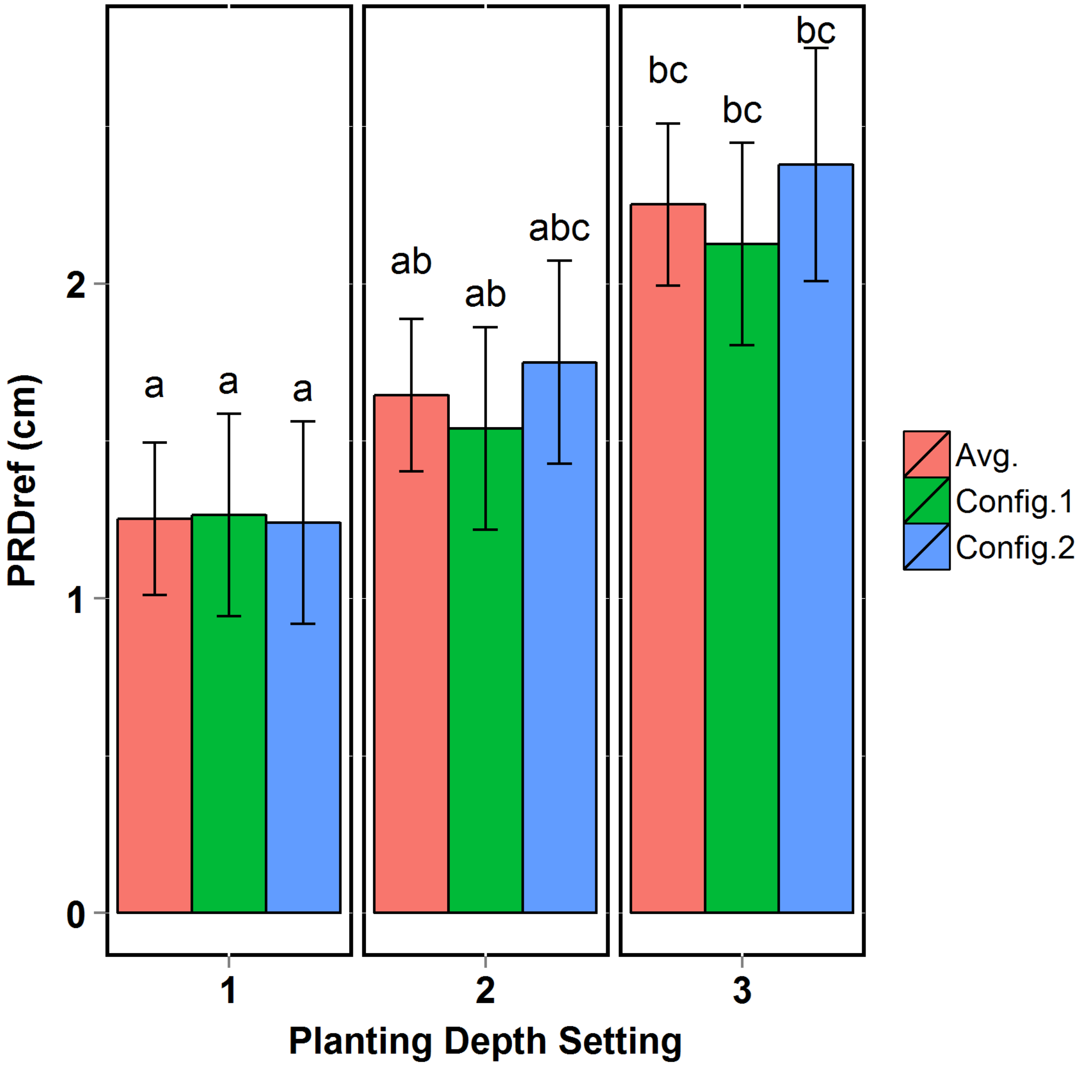

Figure 5.4: Press wheel rut depth measured to the undisturbed soil surface.

Error bars represent 95% confidence intervals. Standard deviations denoted by the same letter are not significantly different, based on 95% confidence intervals.

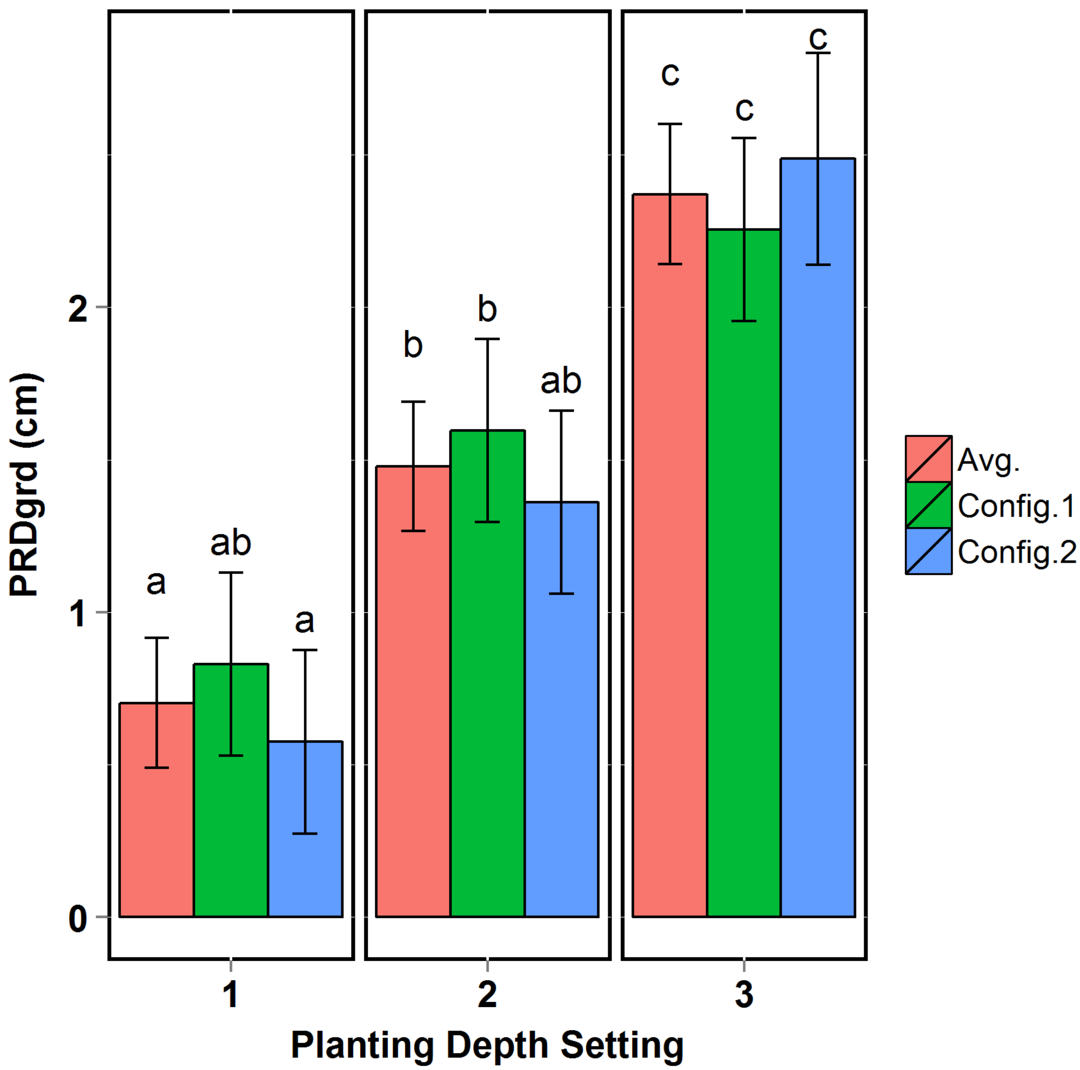

Figure 5.5: Press wheel rut depth measured to the horizontal surface of the gauge wheel rut.

Error bars represent 95% confidence intervals. Standard deviations denoted by the same letter are not significantly different, based on 95% confidence intervals.

5.3.2 Gauge Wheel Rut Depth

Real-time measurement of gauge wheel rut depth during in-field planting operations is difficult and will likely require an additional set of mechanisms to measure the position of the gauge wheel relative to the soil surface. A predictive model based on planter row unit setup and sensed loads would reduce complexity and potentially aid in planting depth controller performance. A linear regression model was produced to estimate gauge wheel rut depth from the independent variables: planting depth setting, configuration, FLAS, DF_Y, GWAS, and Fgw_Y. The best model resulted in an adjusted R^2 and P-value of 0.64 and <0.001 respectively. The model included only gauge wheel arm angle, which is a continuous variable describing planting depth setting, and vertical force on the gauge wheels. (eq. 5.1) Since this model was produced in uniform soil conditions on Norfolk Sandy Loam soil, an operational field model for gauge wheel rut depth will most likely require a calibration for the field conditions present at the time of planting.

$$GRD = 0.03 * GWAS + 0.40 * Fgw_Y - 0.75 \tag{5.1}$$

5.3.3 Planting Furrow Depth Prediction

For the purpose of this research, planting furrow depth is the primary means of evaluating planting depth performance. As would be expected, PD_{ref} and PD_{grd} were significantly different for each planting depth setting. Linear regression models were applied to estimate planting furrow depth from the variables that have been discussed in this section. The first model, shown in equation 5.2, uses planter depth setting and press wheel rut depth. This model resulted in an adjusted R^2 and P-value of 0.81 and <0.001 respectively.

$$PD_{ref} = 1.06 * X_{PD_2} + 1.50 * X_{PD_3} + 1.94 * PRD_{ref} + 1.77 \tag{5.2}$$

Where X_{PD_2} and X_{PD_3} are dummy variables representing planting depth settings 2 and 3 respectively.

While this model describes much of the variability in the model, planter depth setting is not a continuous variable and is not capable of describing the position of the gauge wheel in an operating condition where the gauge wheel arm is not contacting the planting depth setting rocker. A more reliable and better fit model, equation 5.3, produced an adjusted R^2 and P-value of 0.82 and <0.001 respectively using GWAS in place of planter depth setting and PRD_{ref}.

$$PD_{ref} = -0.13 * GWAS + 1.83 * PRD_{ref} + 5.37 \tag{5.3}$$

Due to the uniform soil conditions in the soil bin and the linear application of force produced by the press wheel assembly tension spring, PRD_{ref} was a good indicator of planter frame position in the soil relative to the press wheel assembly. This explains the significance of PRD_{ref} in the planting furrow depth prediction models. However, press wheel rut depth would not be as reliable a predictor for in-field operations, where soil conditions are more variable.

5.4 Effect of Planter Depth Setting on Soil-Planter Interaction Force Distribution

The goal was to determine the effect of soil-planter interaction force distribution as a result of planting depth setting. A static system analysis was conducted on the planter using data collected in each experimental unit as well as known geometric and force relationships of the planter to answer the objectives below:

1. How does soil-planter interaction force distribution change with planting depth setting?
2. Can actual planting furrow depth be predicted by planting depth setting and force distribution?

5.4.1 Planter Component Forces Results

Changing planting depth setting alters the geometry of the planter row unit. As planting depth setting is increased, the gauge wheels move in the negative X and positive Y directions relative to the planter row unit frame, as seen in figure 3.9. Similarly, due to the change in soil surface relative to the planter frame, the press wheels move in the positive X and Y directions as planting depth setting increases (assuming zero rut depth).

These position changes affect the moment arms that the forces applied to the gauge and press wheels act through. In addition to the varying geometry of the planter row unit during planting depth setting adjustments, it was expected that the change in contacting surface area of the components operating in the soil would directly affect the force produced on those components. The combination of these factors, as well as soil conditions, produce varying force distributions on the planter row unit during operation.

CAD model evaluation as well as knowledge gained during operation of the planter in the soil bin enabled the development of a planter force distribution general solution shown in figure 5.6. For this solution the following variables should be directly measured or calculated from related, measured variables: upper and lower four-bar link forces ($\mathrm{Ftl_1}$ and $\mathrm{Ftl_2}$), four-bar link angle (FLAS), down force applied to the planter row unit at the four-bar link attachment point ($\mathrm{DF_Y}$), vertical force on the gauge wheels ($\mathrm{Fgw_Y}$), vertical force on the press wheels ($\mathrm{Fpw_Y}$), gauge wheel position in the global XYZ ($\mathrm{GW_X}$ and $\mathrm{GW_Y}$), and press wheel position in the global XYZ ($\mathrm{PW_X}$ and $\mathrm{PW_Y}$).

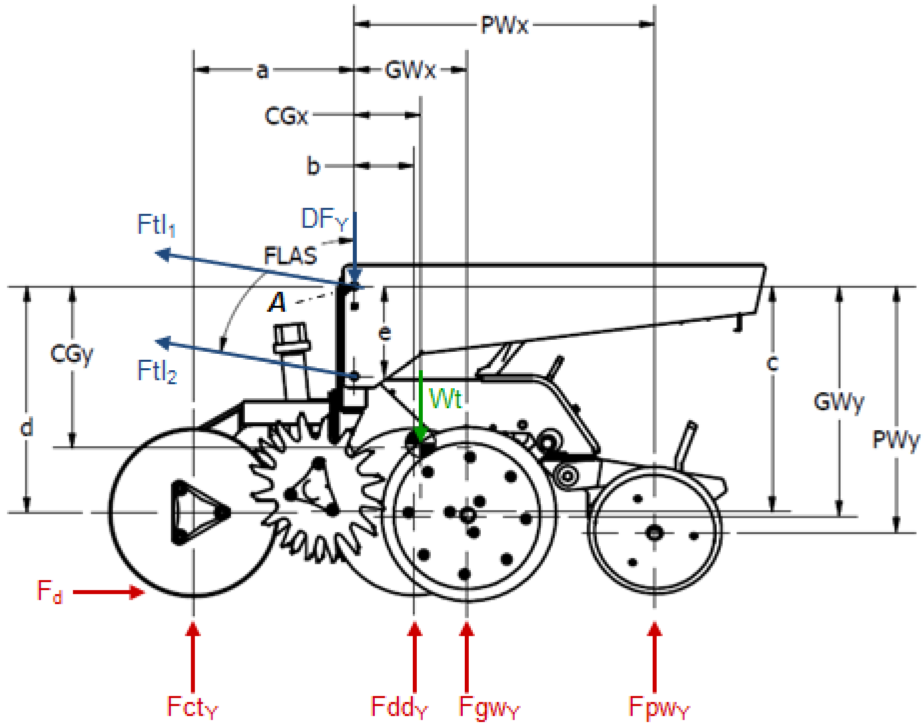

Figure 5.6: Free body diagram for the general solution of the planter force distribution.

The solutions for unknown soil-planter interaction forces, vertical force on the coulter (Fct_Y) and vertical force on the double disc opener (Fdd_Y), are given by a sum of the moments about the hub axis of the coulter disc (eq. 5.4) and a sum of the forces in the global Y (eq. 5.5).

$$Fdd_{Y_{Config1}} = \frac{\begin{pmatrix} Flt_1((d)\sin FLAS + (a)\cos FLAS) \\ + Ftl_2((d-e)\sin FLAS + (a)\cos FLAS) \\ -(a)DF_Y - (a+CG_X)Wt + Fgw_Y(a+GW_X) \\ + Fpw_Y(a+PW_X) + F_d((-GW_Y + R1_Y) - d) \end{pmatrix}}{(a+b)} \tag{5.4}$$

$$
\begin{aligned}
Fct_{Y_{Config1}} = & - Ftl_1 \cos FLAS - Ftl_2 \cos FLAS + DF_Y + Wt \\
& - Fdd_Y - Fgw_Y - Fpw_Y
\end{aligned}
\tag{5.5}
$$

An analysis of variance using mixed effect models was conducted on treatment mean and standard deviation values of the following forces: $\mathrm{Fdd_Y}$, $\mathrm{Fgw_Y}$, $\mathrm{Fpw_Y}$, and also $\mathrm{F_d}$. Multiple comparisons were conducted using Fishers Least Significant Difference (Piepho *et al.* 2003). While no significant difference in $\mathrm{Fdd_Y}$ mean force values were observed between any of the planting depth settings or planter configurations, a trend of increasing mean force with increased planting depth setting is apparent (fig. 5.7). Additionally, double disc opener force standard deviation was significantly reduced in configuration 4 treatments as compared to configurations 2 and 3. Double disc opener force standard deviation also showed a significant decrease from planting depth setting 1 to planting depth setting 3 (fig. 5.8).

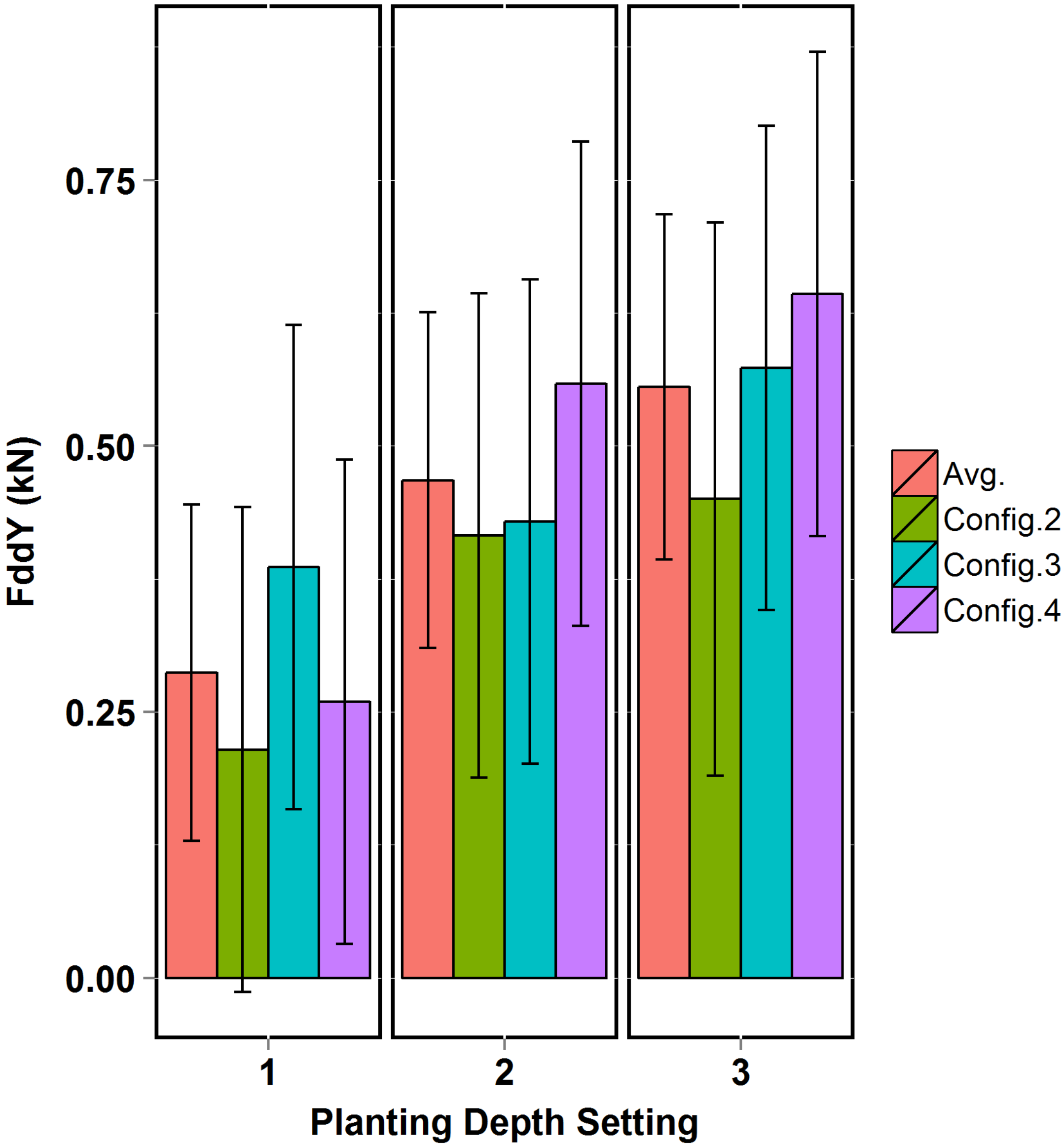

Figure 5.7: Vertical force measured on the double disc opener by planting depth setting.

Error bars represent 95% confidence intervals.

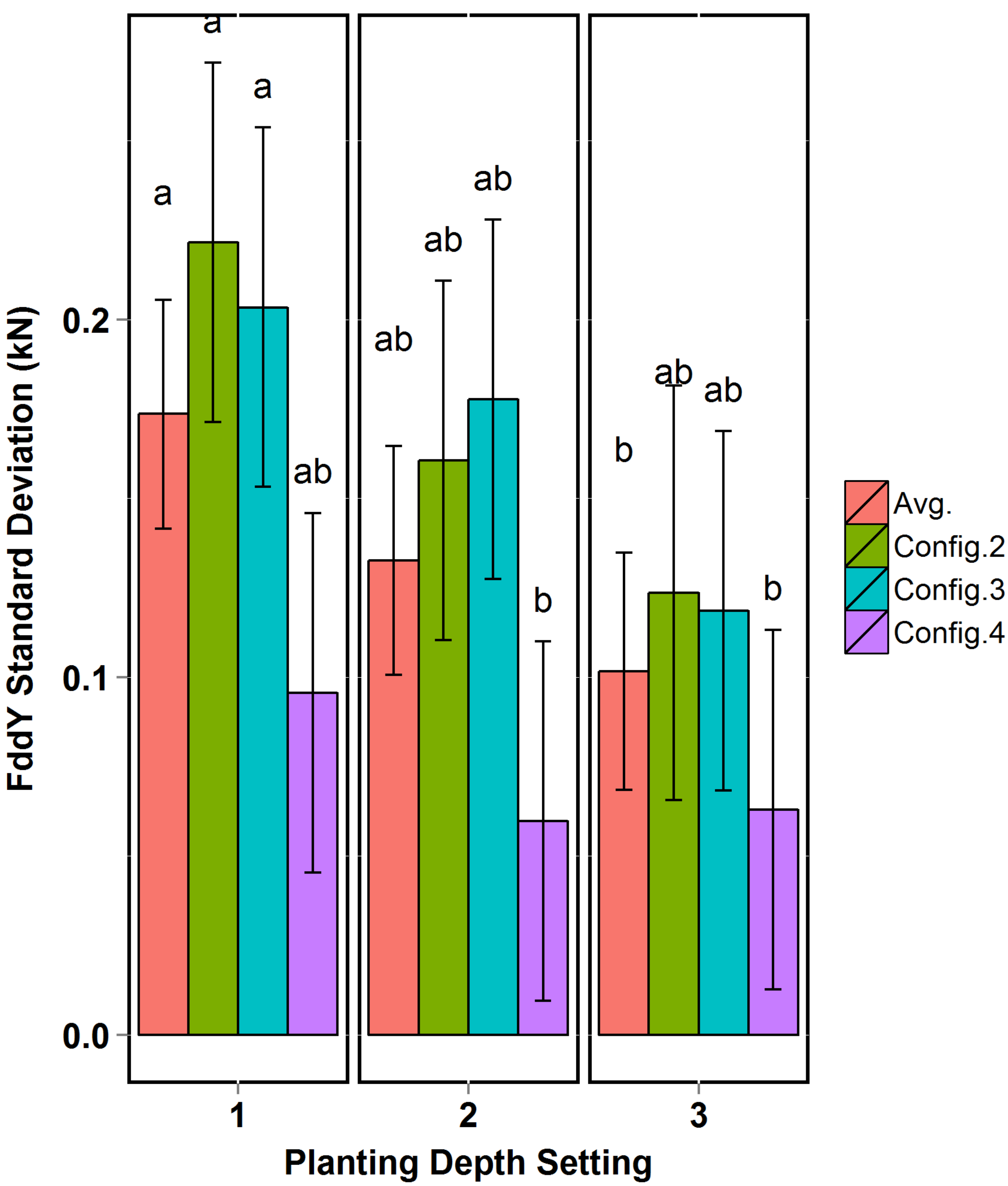

Figure 5.8: Standard Deviation of vertical force on the double disc opener by planting depth setting.

Error bars represent 95% confidence intervals. Standard deviations denoted by the same letter are not significantly different, based on 95% confidence intervals.

Standard deviation of Fgw_Y showed no significant change across planting depth or planter configuration; however a trend of decreasing standard deviation with increasing planting depth setting, similar to that of the double disc opener, was observed again (fig. 5.9).

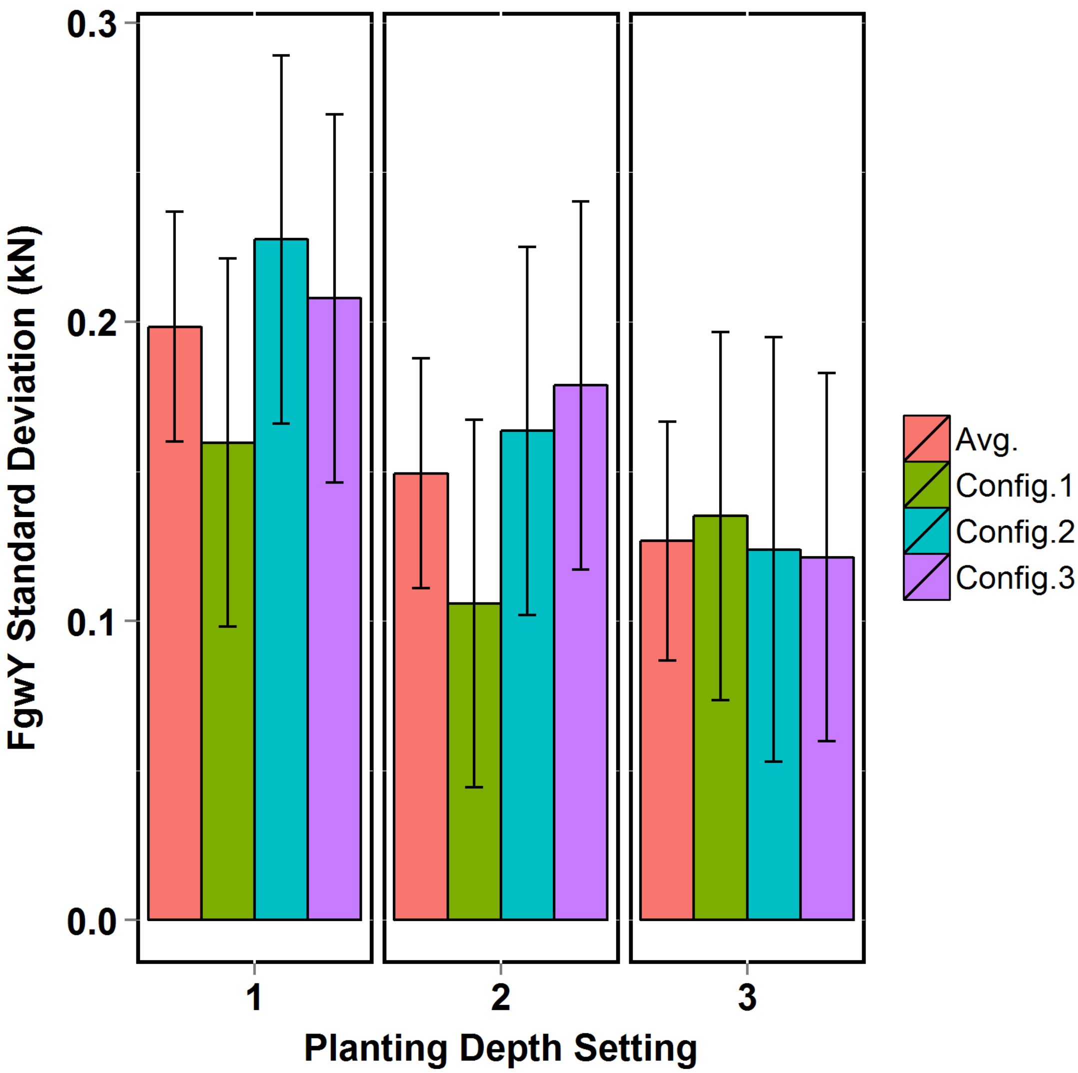

Figure 5.9: Standard Deviation of vertical force measured on the gauge wheels by planting depth setting.

Error bars represent 95% confidence intervals.

Fgw_Y produced a clear trend and a 48% decrease in force with increasing planting depth setting, as seen in figure 5.10. Significant changes in mean Fgw_Y were observed between planting depth settings 1 and 3 as well as depth settings 2 and 3.

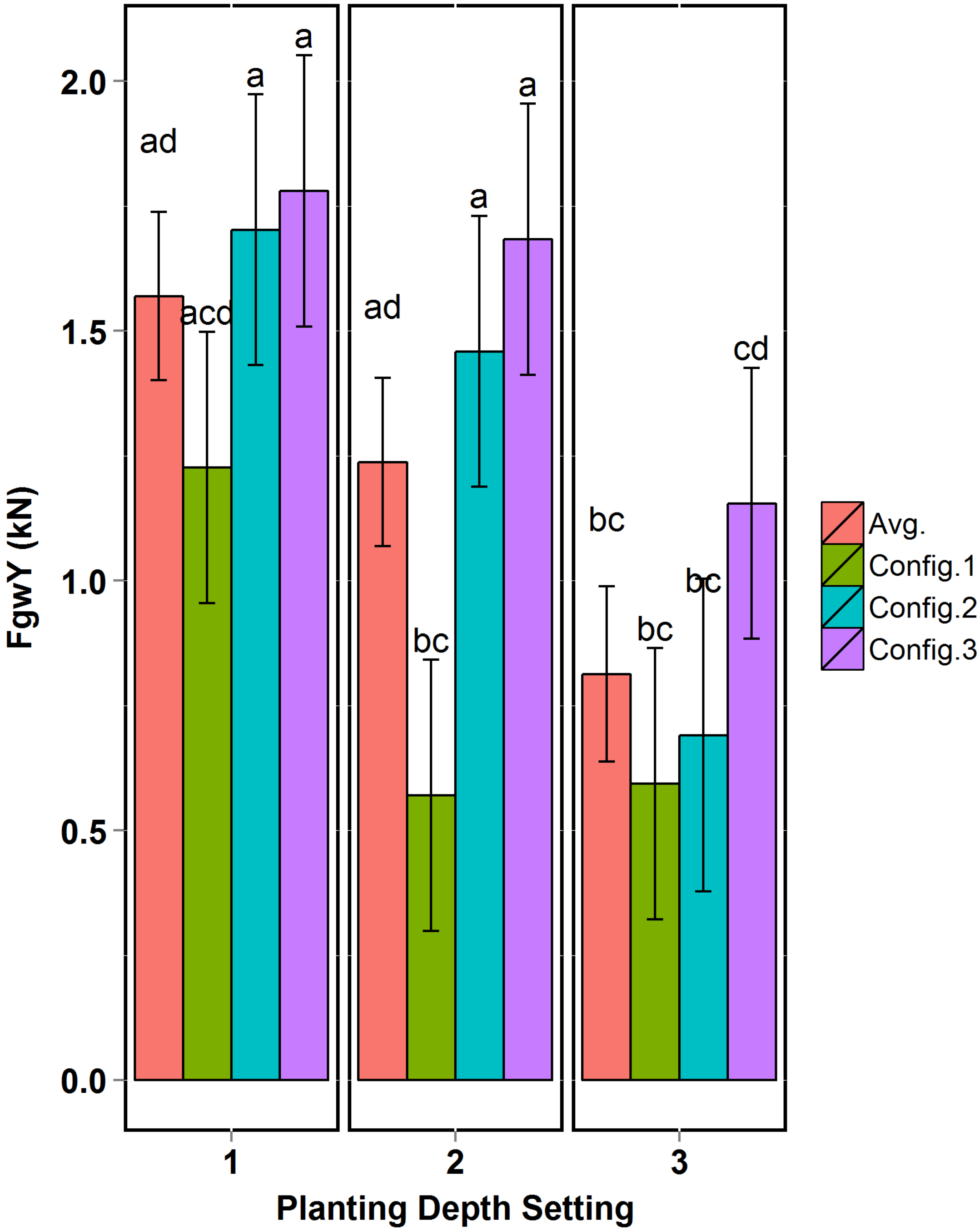

Figure 5.10: Vertical force measured on the gauge wheels by planting depth setting.

Error bars represent 95% confidence intervals. Standard deviations denoted by the same letter are not significantly different, based on 95% confidence intervals.

Standard deviation of Fpw_Y showed no change across planting depth settings or configurations. However, Fpw_Y changed significantly between planting depth setting 1 and 3 producing an increase of 55% (fig. 5.11).

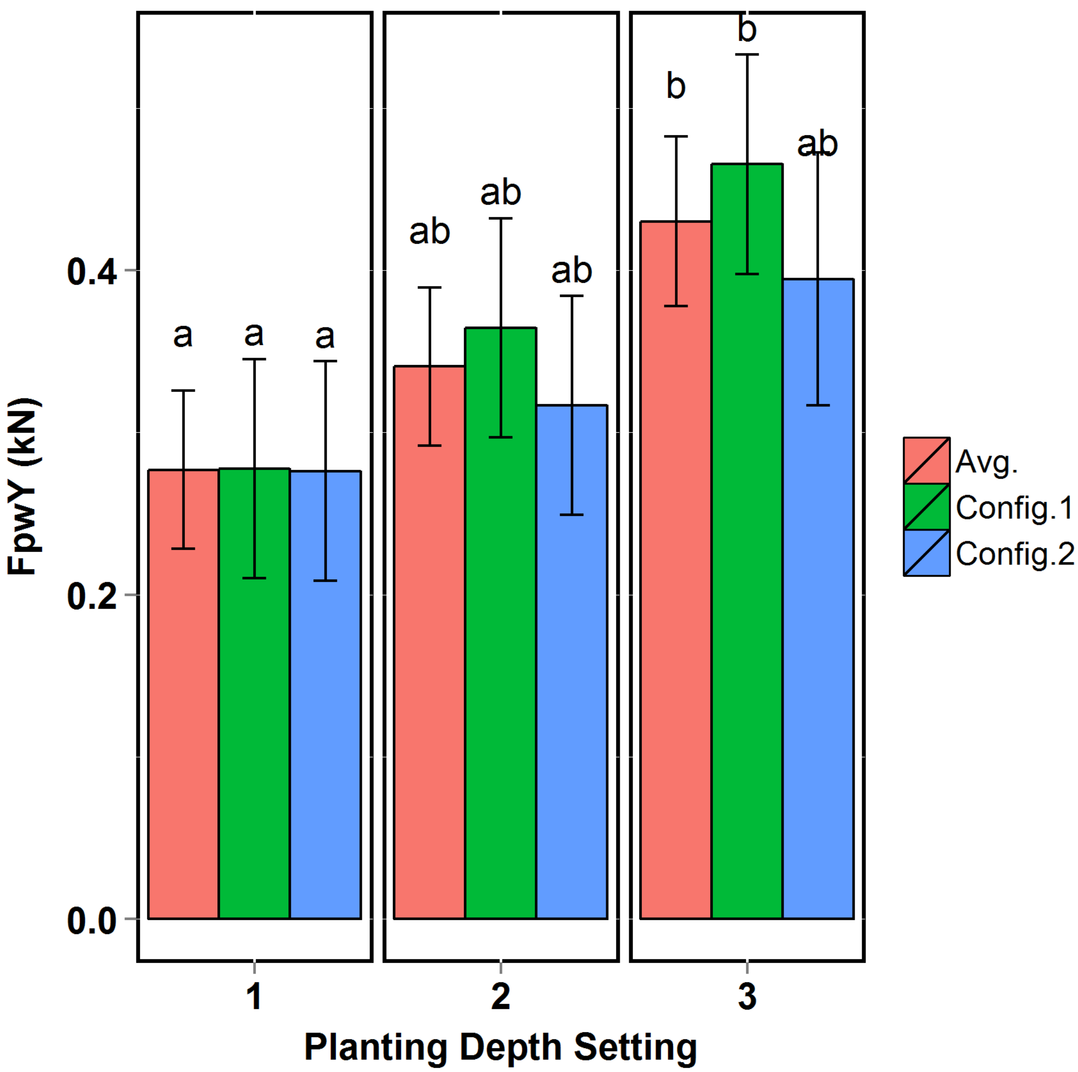

Figure 5.11: Vertical force on the press wheels by planting depth setting.

Error bars represent 95% confidence intervals. Standard deviations denoted by the same letter are not significantly different, based on 95% confidence intervals.

Standard deviation of total draft force (F_d) changed with planting depth setting and configuration, however it was non-linear. This indicates that the change in F_d variation was affected by some other, non-measured, variable to the system. An increase of 64% in F_d was observed when planting depth was increased from planting depth setting 1 to 3. Significant differences in Fd were observed between all three configuration pairings that included configuration 4, as seen in figure 5.12.

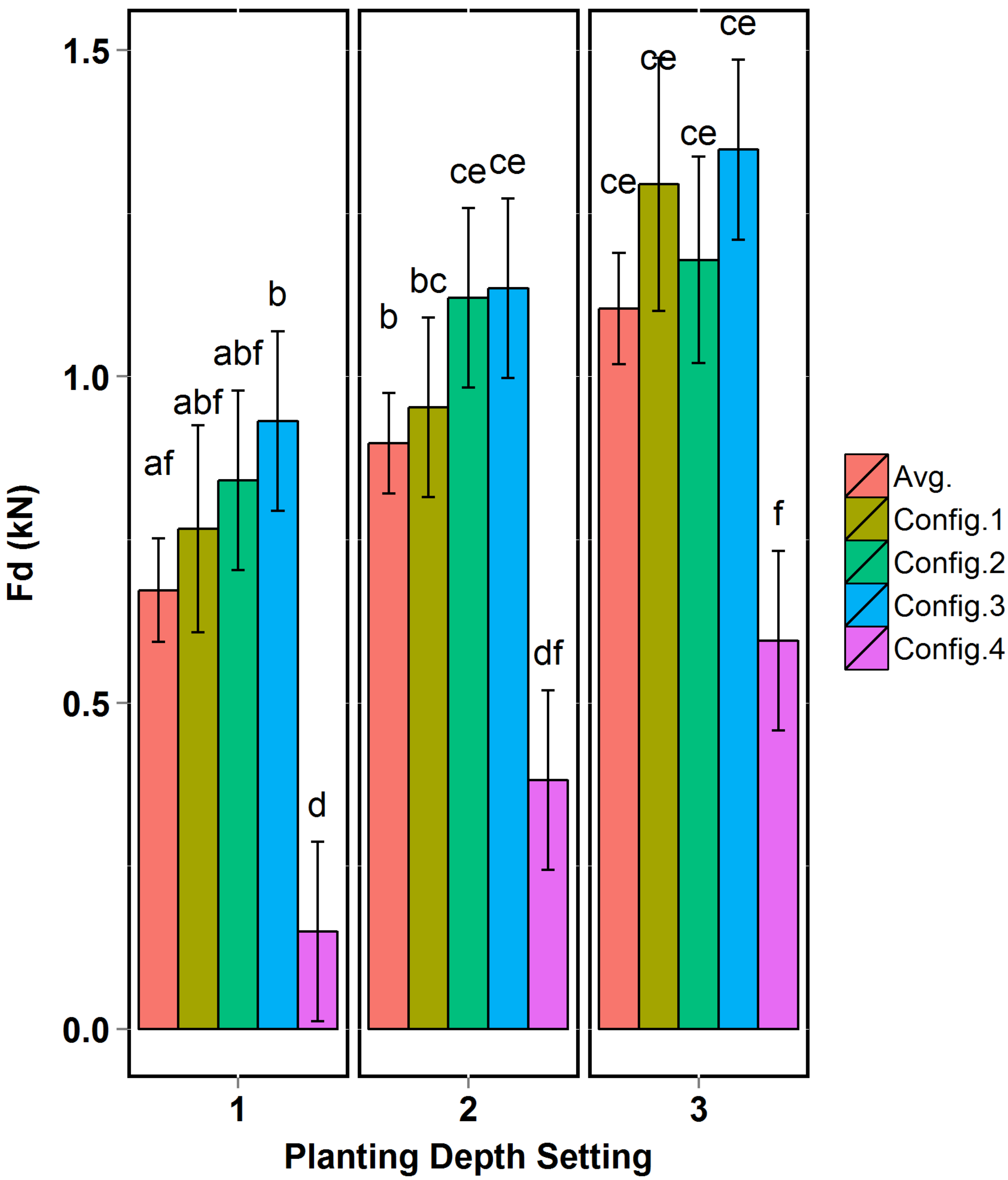

Figure 5.12: Total draft force on the planter row unit by planting depth setting.

Error bars represent 95% confidence intervals. Standard deviations denoted by the same letter are not significantly different, based on 95% confidence intervals.

5.4.2 Planter Component Forces Discussion

The reduced Fdd_Y variation present in the configuration 4 treatments can likely be attributed to two factors. First, configuration 4 data was collected without the use of planter gauge wheels, reducing the soil surface profile disturbance that is input to the system under normal operating conditions. As shown in figure 5.13, the planter's weight, with the exception of the force produced on the double disc opener, was supported by the dyno cart. Second, due to the angle of the four-bar links, no additional down force (DF_Y) was applied by the spring down force system during configuration 4 treatments. While no difference was observed in Fdd_Y, the increasing trend was supported by results from the experiments conducted by Cochran *et al.* (1974) and Schaaf *et al.* (1981).

The significant change in Fgw_Y was expected and indicated that the planter weight and spring down force supported by the gauge wheels at planting depth setting 1 was being redistributed to other planter components as planting depth setting increased (fig. 5.10). Total contact area of the coulter disc and double disc openers with the soil increased with planting depth, thereby increasing the vertical force that was produced on them. This further explains the decreasing gauge wheel rut depth with increasing planting depth setting that was discussed in section 5.3.1. Redistribution of forces acting on components in contact with the soil is also seen in the increase of Fgw_Y as planter configuration is changed from 1 to 3 within any planting depth setting. As planter components were removed, vertical force that was carried by the components was transfered in part to the gauge wheels.

Figure 5.13: Configuration 4 data collection.

As previously discussed, Fpw_Y is a function of press wheel assembly position relative to the planter row unit frame. This position is controlled by the planting depth setting, press wheel force setting, and the bearing capacity of the soil. While a significant difference in mean Fpw_Y is only seen between planting depth settings 1 and 3, the force trends as expected. A decrease in mean Fpw_Y was observed when planter configuration was changed from configuration 1 to 2 for depth settings 2 and 3 but not depth setting 1. This decrease may have resulted from the moment that was created about the gauge wheels by the coulter disc. While planter row unit rotation is limited by the four-bar link assembly, the bushing to pin (bolt) fit of the system allows for a small degree of freedom. The coulter assembly produced a clockwise moment about the gauge wheels, which increased with planting depth. Within the degree of freedom provided by the bushing to pin fit, the press wheel assembly was the only component generating a counterclockwise moment. When the coulter disc was removed from the system, Fpw_Y was reduced.

Total draft force (F_d) increased, as expected, with increased planting depth setting and surprisingly also as planter configuration increased from configuration 1 to 3. This increase in total F_d indicates that Fgw_Y contributes to total draft more so than Fdd_Y and Fpw_Y. As components were removed from the planter in configurations 2 and 3 the forces previously supported by the coulter and press wheels were transferred in part to the gauge wheels. This increased force produced the higher total draft forces observed. A linear regression model was produced to estimate total draft from planter forces, configuration, planting depth settings, component angles, as well as soil surface profile and planting furrow effects. The best fit model, equation 5.6 shown below, produced an adjusted R^2 and P-value of 0.86 and <0.001 respectively. The model confirms that vertical gauge wheel force plays a significant role in total draft force. While the change in mean F_d from configuration 1 to 2 is relatively small for a single row unit, the decision to operate without coulters could have a significant affect on required draft force for large multi-row planters.

$$F_d = -0.05 * GWAS + 0.24 * Fgw_Y + 1.74 \tag{5.6}$$

5.4.3 Force Distribution

An analysis of variance with mixed model effects was run on the distribution of forces produced on the planter components interacting with the soil for planter configurations 2 and 3 as well as all three planting depth settings. Multiple comparisons were conducted using Fishers Least Significant Difference (Piepho *et al.* 2003). The force distribution, shown in figure 5.14, was calculated for each component as a percentage of the total vertical force produced on the planter by soil interaction. The double disc openers and press wheels clearly supported an increased percentage of the total vertical force as planting depth setting increased. However, the change in percentage for these two components was not significant over the range of data collected in this experiment. Conversely, the percentage of total vertical force supported by the gauge wheels decreased with increased planting depth setting and produced a significant decrease between planting depth settings 1 and 3.

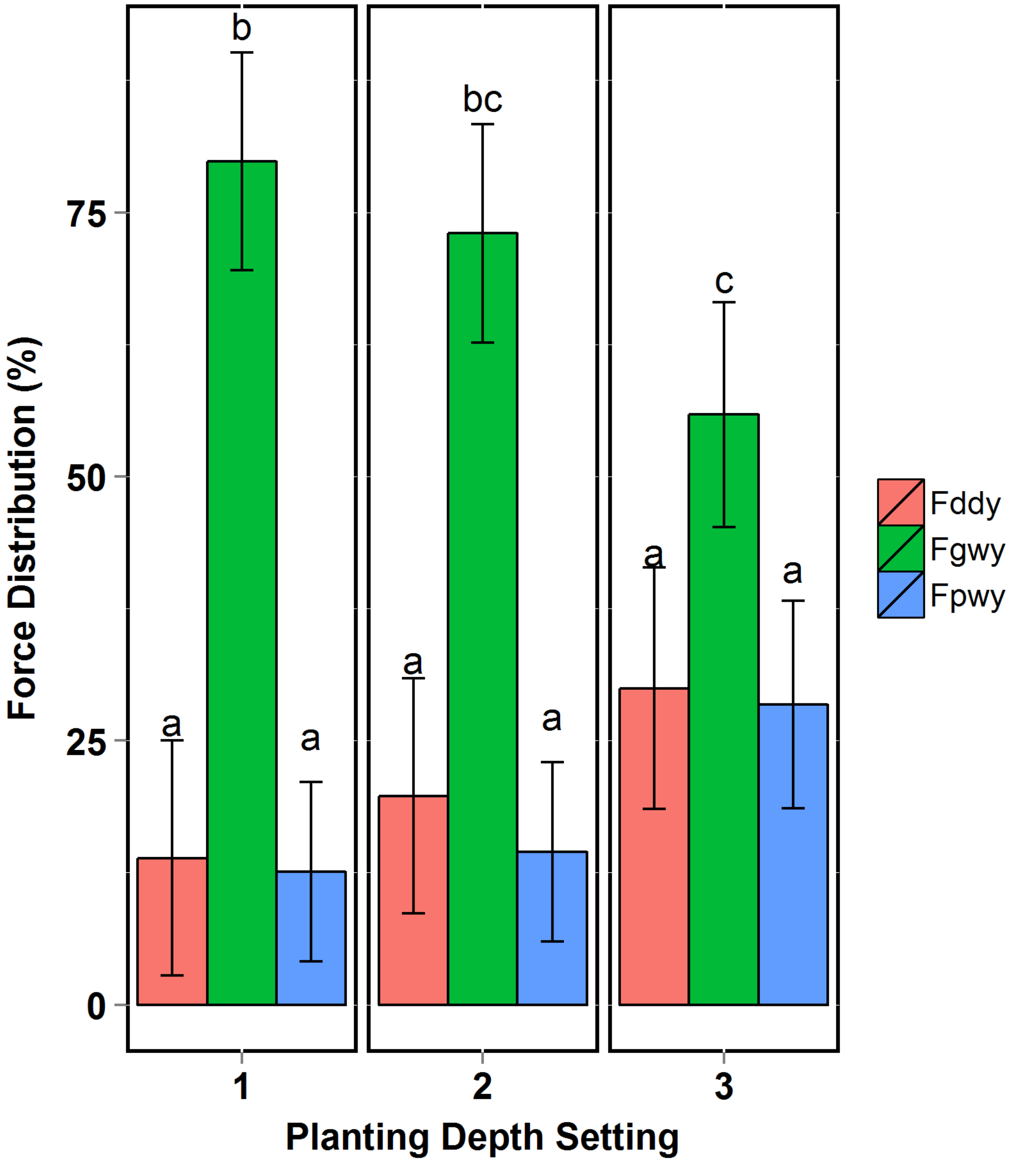

Figure 5.14: Vertical force distribution on planter components contacting the soil for configuration 2 treatments.

Error bars represent 95% confidence intervals. Standard deviations denoted by the same letter are not significantly different, based on 95% confidence intervals.

5.4.4 Planting Furrow Depth Prediction

In section 5.3.3, planting furrow depth was estimated using GWAS and PRD_{ref}. This model is not optimal for real-time planting depth control during field operations because press wheel rut depth is not easily measured during normal planting operations. A more desirable model would utilize planter row unit settings, configuration, and measurable forces acting on the planter row unit. A linear regression model was produced to predict planting furrow depth from planter settings, configuration, and the forces produced on the planter that have been discussed in this section. Several models showed linear relationships between planting furrow depth and the variables considered; however, all of the models reveal potential weaknesses. The first model, equation 5.7, utilized planting depth setting and configuration and produced the best adjusted R^2 and P-value of 0.81 and <0.001 respectively.

$$PD_{ref_1} = 2.09 * X_{PD_2} + 3.74 * X_{PD_3} + 0.06 * X_{Config_2} + 0.63 * X_{Congig_3} - 1.82 * X_{Config_4} + 3.97 \tag{5.7}$$

Where:

X_{PD_2} and X_{PD_3} are dummy variables representing planting depth settings 2 and 3 respectively.

X_{Config_2}, X_{Congig_3}, and X_{Config_4} are dummy variables representing planter configurations 2, 3, and 4 respectively.

Planting depth setting is not a continuous variable and does not account for situations when the gauge wheel arm is not contacting the planting depth setting rocker. With a total of 17 independent planting depth settings, a continuous and measurable variable such as GWAS would be more suitable to real-time planting depth setting control. Also, planter configurations 3 and 4 would not be used in actual field operations, and because of this a second model was fit (eq. 5.8). This model does not describe planting furrow depth as well with an adjusted R^2 and P-value of 0.76 and <0.001 respectively, but removes the unrealistic configuration 3 and 4 terms. Similar to the planting depth prediction models from section 5.3.3 that included press wheel rut depth (PRD_{ref}) (eq. 5.2 and 5.3), vertical press wheel force (Fpw_Y) was found to be significant in this model. As was previously stated, vertical press wheel force is directly related to the rotation of the press wheel assembly in relation to the planter row unit frame. Due to the uniform soil and operating conditions, Fpw_Y was a good indicator of planter row unit frame position relative to the soil surface and therefore planting furrow depth.

$$PD_{ref_2} = 2.27 * X_{PD_2} + 4.50 * X_{PD_3} - 7.0 * Fpw_Y + 6.14 \tag{5.8}$$

A third model for planting furrow depth was fit replacing planting depth setting with the continuous variable with GWAS (eq. 5.9). This model better predicts PD_{ref} than equation 5.8 but not as well as equation 5.7, with an adjusted R^2 and P-value of 0.78 and <0.001 respectively. Obviously, this model also has limitations. It can be reasonably expected that GWAS alone will not be capable of accurately describing planting furrow depth in field planting operations. This suggests that planter settings and soil conditions during the experiment were too uniform to describe the range of conditions that will be present in the field. Greater variation to system inputs such as: soil moisture, soil compaction, four-bar link angle, and applied down force, may have produced planting furrow prediction models including other planter operating conditions and force distribution.

$$PD_{ref_3} = -0.30 * GWAS + 11.95 \tag{5.9}$$

While vertical gauge wheel force is significant when predicting gauge wheel rut depth and total draft force, it was not a factor in planting furrow depth for the conditions present during the course of this experiment. Other variables such as: GWAS, FLAS, PRD_{ref}, and Fpw_Y appeared to be greater indicators of actual planting furrow depth.

Chapter 6

CONCLUSION

6.1 Review of Objectives

Research has shown that planting depth and soil loading due to vertical force on planter gauge wheels has a significant effect on emergence, early plant growth, and in some cases crop yield. To maximize crop yield potential, spatial variability present during the planting operation must be accounted for, and planter settings should be adjusted to match said variation. If variations in gauge wheel force input to the soil surface change conditions around the seed and potentially impact germination, as suggested by Hanna *et al.* (2010), press wheel force settings should also be adjusted as planting conditions vary. For these reasons, real-time control of planter settings for down force, depth setting, and press wheel force provide potential for improved performance in planting depth and soil surface inputs. Soil-implement interaction forces are very complex and have been extensively studied at the component level. However, in order to develop effective feedback control for planter adjustments, their effect on the distribution of forces acting on the planter row unit must be more clearly understood.

While operating a John Deere MaxEmerge™ Plus agricultural row planter in a soil bin with uniformly prepared Norfolk Sandy Loam soil, significant differences in planting furrow depth (PD_{ref}), gauge wheel rut depth (GRD), and press wheel rut depth (PRD_{ref}) were observed as planting depth setting was varied. A change in target planting depth of 2.54 cm (depth setting 1) to 7.62 cm (depth setting 3) produced a 112% decrease in gauge wheel rut depth, resulting in a negative mean rut depth for planting depth setting 3. For this setting there was not enough down force supported by the gauge wheels to re-consolidate the soil that was displaced by the double disc opener. This clearly demonstrates the effects of force redistribution that occur as planting furrow depth changes.

Across the same range of planting depth settings, press wheel rut depths, referencing the undisturbed soil surface (PRD_{ref}) and the gauge wheel rut (PRD_{grd}), produced an increase of 80% and 273% respectively with increased planting depth setting. For the conditions present at the time of the experiment, GRD could be estimated with an adjusted R^2=0.64 using gauge wheel arm angle (GWAS) and vertical force acting on the gauge wheels (Fgw_Y). Planting furrow depth, referencing the undisturbed soil surface (PD_{ref}), was successfully estimated using GWAS and PRD_{ref} at an adjusted R^2=0.82 (eq. 5.3). While GRD was not included in the final models for predicting planting furrow depth, it was included in models at a lower significance level.

Vertical force on the double disc opener did not change over the range of planting depth settings and conditions present during the soil bin experiment. However, a trend of increasing force with planting furrow depth was observed. This trend was consistent with the findings of Cochran *et al.* (1974) and Schaaf *et al.* (1981). Vertical force on the gauge wheels decreased by 48% as planting depth setting was increased, with significant changes occurring between planting depth settings 1 and 3 as well as depth settings 2 and 3. An increase in vertical force on the press wheels (Fpw_Y) of 55% was observed as planting depth setting was increased from setting 1 to 3, with significant changes present between all pairings.

Total draft force (F_d) produced on the planter increased by 64% from planting depth setting 1 to 3. Significant differences were observed for all planting depth settings and planter configurations. Interestingly, F_d increased as planter components contacting the soil were removed from configuration 1 to 3. This indicated that gauge wheel interaction with the soil contributed to draft force more so than coulter or press wheel inputs. As these components were removed the vertical force carried by them was partially transferred to the gauge wheels. This is supported by the presence of Fgw_Y in the model produced to predict Fd (eq. 5.6). While the increase in total draft force due to the removal of the coulter assembly is not likely to affect planting operation performance for a four or six row planter, farmers using large, multi-row planters should be aware of the potential impact of this configuration change.

The change in distribution of soil interaction forces acting on the planter, while not significant for every component across the settings and conditions tested, was as expected and does not conflict with previous research conducted on individual components. The only significant change observed in force distribution was that supported by the gauge wheels, which decreased from 80% to 56% of the total vertical force produced on the planter row unit.

Finally, a planting furrow depth estimation model was developed using planter settings, configuration, and soil interaction force distribution. Variables were eliminated through a stepwise method resulting in a model that included only GWAS (eq. 5.9). The model predicted planting furrow depth with the soil conditions in the experiment and yielded an R^2=0.78. Given the spatial variability in soil conditions and crop residues present during in-field planting operations it is not expected that gauge wheel arm angle alone will accurately predict planting furrow depth.

The soil bin experiment did not produce the expected change in force distribution on all components of the planter interacting with the soil. However, significant changes in rut depth and forces acting on the planter were observed. For components that did not produce significant changes in force, trends that were expected from previous research were observed. The changes in observed forces and actual planting furrow depth resulting from planting depth setting adjustments indicate that the relationship between planter adjustments and actual planting furrow depth are not one-to-one. A change made to any planter setting adjustment or planter configuration will affect not only that particular component, but also the balance of forces acting on the planter row unit as a whole. For this reason, actual planting furrow depth is a function of planting depth setting and the force distribution acting on the planter. Gauge wheel force monitoring, while valuable for ensuring proper wheel to soil contact and understanding gauge wheel soil loading, does not provide all of the information needed to describe the operation of the row unit in real-time. Planter control systems capable of producing optimal planting furrow depth and soil conditions for germination will also require systems to monitor applied down force, press wheel vertical force, and possibly double disc opener vertical force.

The results produced in the experiment indicate there is potential for improved planting depth performance through real-time planter down force, depth setting, and press wheel force control systems. However, further research into force distribution on planter row unit components is required.

6.2 Future Work

Future research is needed to expand the range of planter settings and operational conditions tested. To increase the number of planting furrow or seeding depth measurements that can be collected per treatment, a study should be conducted in-field or in an outdoor soil bin and seeding should occur. Seeding depth can then be measured within the plot after the stand is established. The experimental design should be a randomized split plot including four replications of the following factors: three planting depths, three down force settings, two press wheel force settings, and two field effect settings (moisture level, soil type, compaction, or field location). The field effect factor will be dependent upon experiment location and whether the study is conducted in-field or in an outdoor soil bin. As stated the experiment will include 144 experimental units. The following data should be collected at the time of planting: planter position within the field or bin, gauge wheel vertical force, four-bar link angle, gauge wheel arm angle, press wheel assembly angle or spring tension, force on the four-bar linkage, soil moisture, bulk density, and rut depths. Seeding depth should be measured after stand establishment, and finally yield data should be collected.

Conducting the experiment as described will provide data from an increased range of planter settings as well as operational conditions and forces that are not represented in indoor soil bin experiments. If the study is conducted in-field, load pins will need to be installed in the four-bar link attachment points and calibrated. Press wheel assembly rotational position can be measured at the hinge point with a rotational encoder as was done for the four-bar link and gauge wheel arm. Vertical press wheel force can be calculated from this angular measurement, or measured directly from a load pin installed at the spring attachment point.

Bibliography

[1] Ag Leader. (2015). ISOBUS 8 section hydraulic down force quick reference guide. Available at: https://dealer.agleader.com/kbp/index.php?View=entry&EntryID=1393. Accessed 2 January 2016.

[2] Agridry Rimik Pty Ltd. (2007). Rimik CP 20 cone penetrometer hardware instruction manual. Available at: http://rimik.com/file/software/cp20_manual.pdf. Accessed 2 January 2016.

[3] Batchelor, J. A., Jr. (1984). Properties of bin soils at the national tillage machinery laboratory. Auburn, Ala.: USDA National Tillage Machinery Laboratory.

[4] Cam2 Measure. 2015. 3D measurement software. Lake Mary, Fla.: FARO.

[5] Cochran, B. J., Porterfied, J. G., & Batchelder, D. G. (1974). Vertical forces on furrow openers and depth control devices. *Trans. ASAE*, 17(3),443-446.

[6] Deere & Company. (2016). Planting equipment product catalog. 15: Available at: http://www.deere.com/en_US/docs/html/brochures/publication.html?id=27109929#14. Accessed 2 January 2016.

[7] Erbach, D. C. (1982). Tillage for continuous corn and corn-soybean rotation. *Trans. ASAE*, 25(4): 906-911, 918.

[8] Erbach, D. E., Melvin, S. W., & Cruse, R. M. (1991). Low groundpressure equipment fleets for corn production. ASAE Paper No. 911517. St. Joseph, Mich.: ASAE.

[9] Erbach, D. C., Morrision, J. E., & Wilkins, D. E. (1983). Equipment modification and innovation for conservation tillage. *J. Soil Water Cons.*, 38(3),182-185.

[10] Hanna, H. M., Steward, B. L., & Aldinger, L. (2010). Soil loading effects of planter depth-gauge wheels on early corn growth. *Appl. Eng. in Agric.*, 26(4),551-556.

[11] Inventor. 2015. 3D CAD. Ver. 2015. 2015. San Francisco, Cal.: Autodesk Inc.

[12] Johnson, C. E., & Burt, E. C. (1990). A method of predicting soil stress state under tires. *Trans. ASAE*, 33(3),713-717.

[13] Knappenberger, T., & Köller, K. (2006). The dynamic variation of seeding depth of corn. *Proc. 8th Annual Intl. Conf. Precision Agric. Precision Res. Mgmt.*,CDROM. Minneapolis, Minn.

[14] Knappenberger, T., & Köller, K. (2012). Spatial assessment of the correlation of seeding depth with emergence and yield of corn. *Precision Agric.*, 13(2),163-180.

[15] LabVIEW. 2015. System design software. Ver. 14.0f1. 2015 . Austin, Texas.: National Instruments Corporation.

[16] Marghitu, D. B., & Dupac, M. (2011). *Dynamics: Advanced Analytical and Numerical Calculations with MATLAB®*. Auburn, Ala.: Springer.

[17] Morrison, J. E., Jr. (1988a). Hydraulic downpressure system performance for conservation planting machines. *Trans. ASAE*, 31(1),19-23.

[18] Morrison, J. E., Jr. (1988b). Interactive planter depth control and pneumatic downpressure system. *Trans. ASAE* 31(1),14-18.

[19] Morrision, J. E., Hendrick, J. G., III., & Schafer, R. L. (1996). Soil forces on coulter and disc-opener combinations. *Trans ASAE*, 39(2),369-376.

[20] Piepho, H. P., Büchse, A., & Emrich, K. (2003). A Hitchhiker's Guide to Mixed Models for Randomized Experiments. *J. Agron. & Crop Sci.*, (189),310-322.

[21] Precision Planting LLC. (2011). 20/20 AirForce® owners manual. Available at: https://cloud.precisionplanting.com/pubs/?file=0Bx7V2J-P2yNZaHJhaW9jNW00N2M. Accessed 2 January 2016.

[22] R. 2015. *R Project for Statistical Computing*. Ver. 3.2.2: The R Foundation®.

[23] Schaaf, D.E., Hann, S. A., & Lindwall, C.W. (1981). Performance evaluation on furrow openers cutting coulters and press wheels for seed drills. *Crop Production with Conservation in the 80's*. St. Joseph, Mich.: ASAE.

[24] Siemens, M. C., Darnell, T. J., & Hulick, D. E. (2007). Performance of two hoe-type air drills sowing green peas in a conservation tillage system. *Appl. Eng. Agric.*, 23(1),23-29.

[25] Soil Survey Staff. (2014). *Soil Survey Field and Laboratory Methods Manual*. Soil Survey Investigations Report No. 51 (Version 2.0 R. Burt & Soil Survey Staff (ed.)). Lincoln, Neb.: U.S. Department of Agriculture, Natural Resources Conservation Service.

[26] Spectrum Technologies, Inc. (2011). TDR 300 soil moisture meter product manual. Available at: http://www.specmeters.com/assets/1/22/6430TDR3001.pdf. Accessed 2 January 2016.

[27] Thomason, W. E., Phillips, S. B., Alley, M. M., Davis, P. H., Lewis, M. A., & Johnson, S. M. (2008). In-row subsoil tillage and planting depth influence on corn plant population and yield on sandy-textured mid-atlantic coastal plain soils. *Crop Mgmt.*, 7(1). doi: 10.1094/CM-2008-0519-01-RS.

[28] Tice, E. M., & Hendrick, J. G. (1991). Disc coulter forces: evaluation of mathematical models. *Trans. ASAE*, 34(6),2291-2298.

Appendices

Appendix A

John Deere Spring Down Force System Calibrations

A.1 Low Down Force

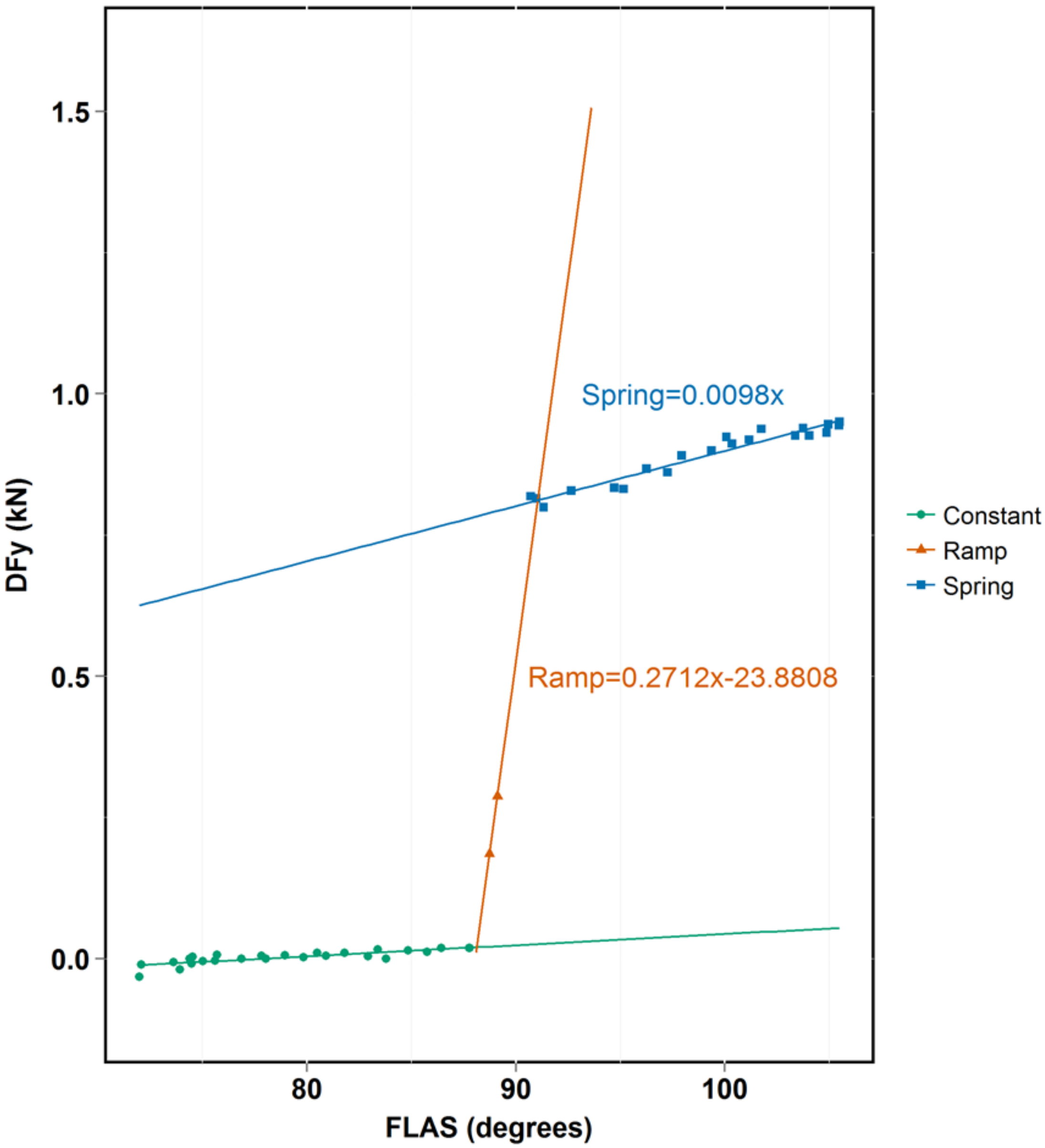

Figure A.1: Low spring down force calibration.

Applied spring down force measured in kN at the upper four-bar link attachment point on the row unit frame.

Table A.1: Linear regressions for "low" setting on the spring down force system.

Section	**Model**	**Adjusted R^2**	**P-value**
Constant	$DF_{Y_{const}} = 0$	NA	NA
Ramp	$DF_{Y_{ramp}} = 0.2712x - 23.8808$	NA	NA
Spring	$DF_{Y_{spring}} = 0.0098x$	0.94	<0.001

Where DF_Y is in kN, and x is the four-bar link angle, $FLAS$.

$$\begin{aligned} FLAS \leq 88.06^\circ \quad & DF_Y = 0 \\ 88.06^\circ < FLAS < 91.35^\circ \quad & DF_Y = 0.2712 * FLAS - 23.8808 \\ FLAS \geq 91.35^\circ \quad & DF_Y = 0.0098 * FLAS \end{aligned} \tag{A.1}$$

A.2 High Down Force

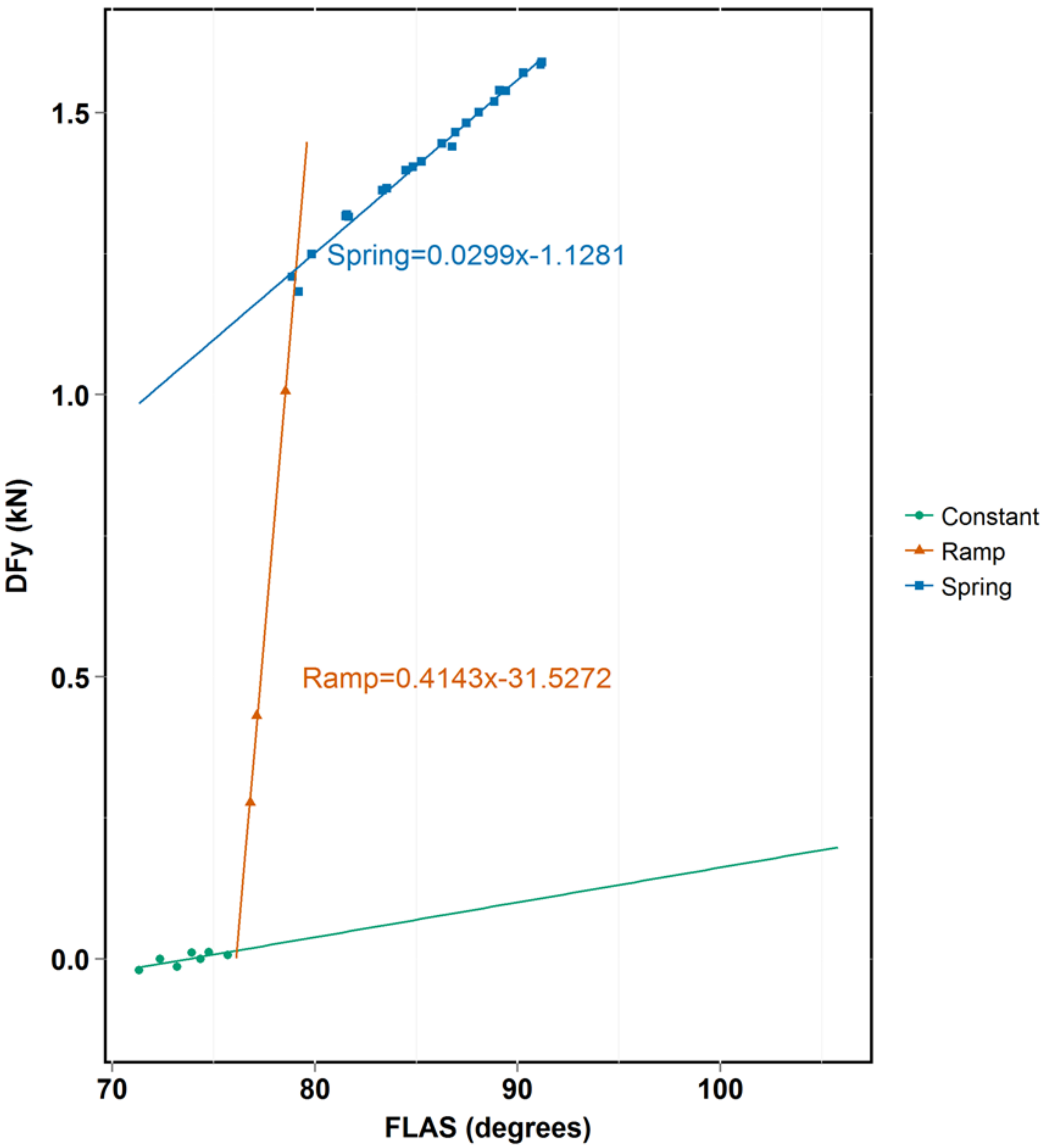

Figure A.2: High spring down force calibration.

Applied spring down force measured in kN at the upper four-bar link attachment point on the row unit frame.

Table A.2: Linear regressions for "high" setting on the spring down force system.

Section	**Model**	**Adjusted R^2**	**P-value**
Constant	$DF_{Y_{const}} = 0$	NA	NA
Ramp	$DF_{Y_{ramp}} = 0.4143x - 31.5272$	1.0	<0.05
Spring	$DF_{Y_{spring}} = 0.0299x - 1.1281$	0.99	<0.001

Where DF_Y is in kN, and x is the four-bar link angle, $FLAS$.

$$\begin{aligned}
FLAS \leq 76.1^\circ \quad & DF_Y = 0 \\
76.1^\circ < FLAS < 79.08^\circ \quad & DF_Y = 0.4143 * FLAS - 31.5272 \\
FLAS \geq 79.08^\circ \quad & DF_Y = 0.0299 * FLAS - 1.1281
\end{aligned} \tag{A.2}$$

Appendix B

Data Collection Programs

B.1 Planter Data Data Collection Program

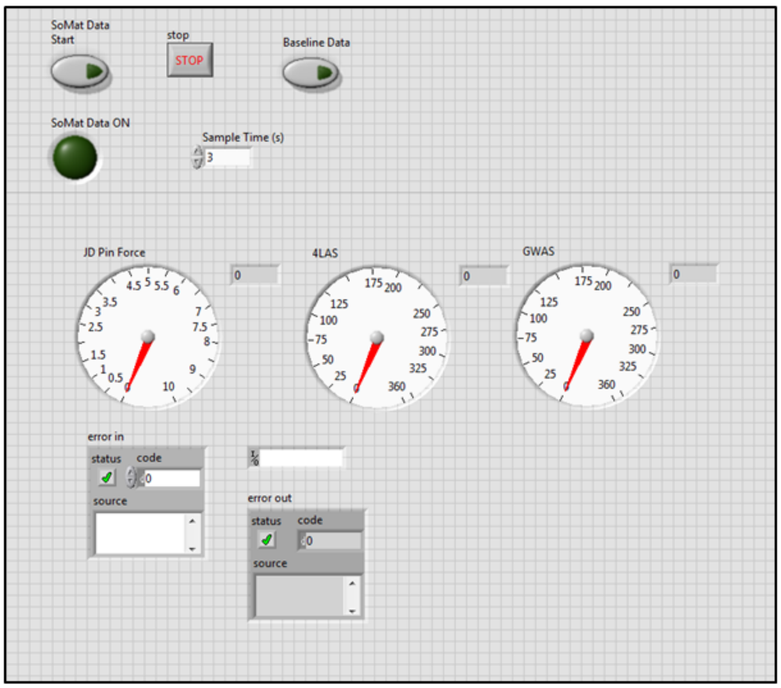

Figure B.1: Planter data collection front panel.

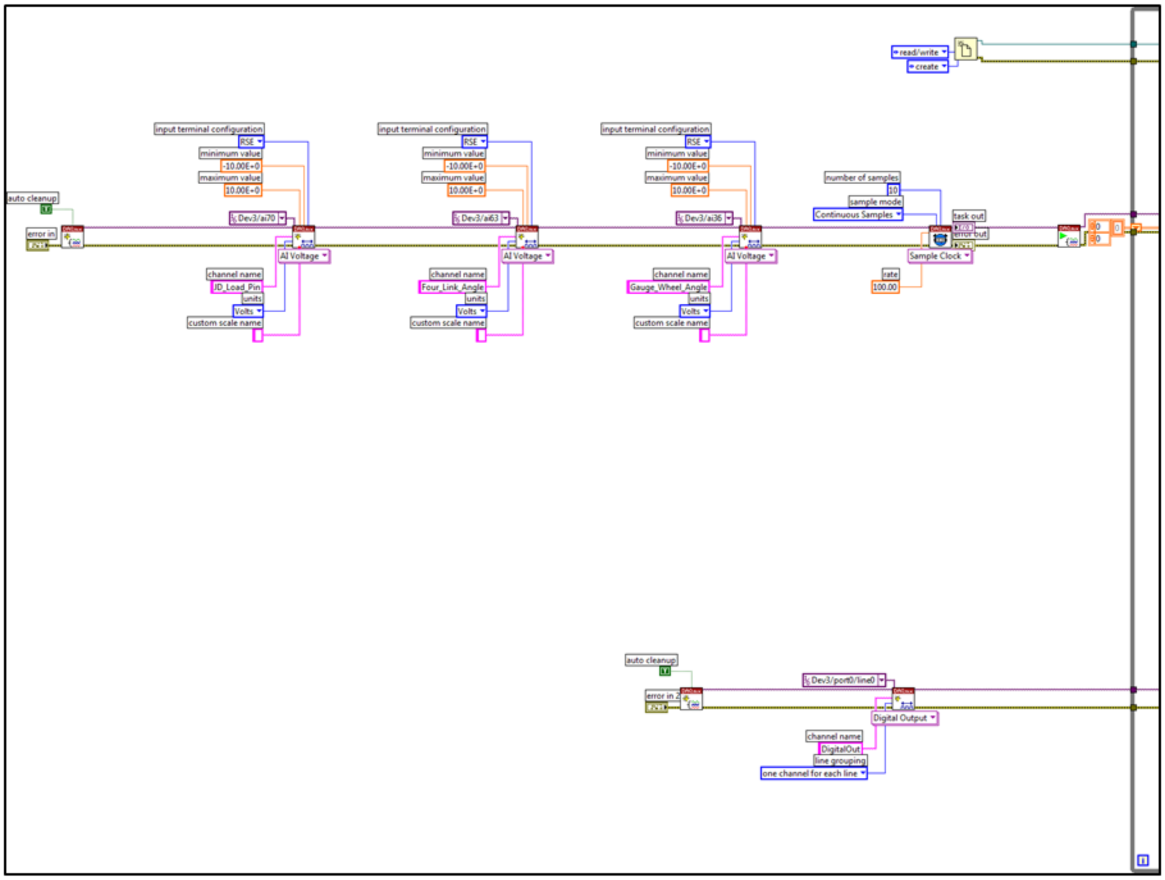

Figure B.2: Left hand side of planter data collection block diagram.

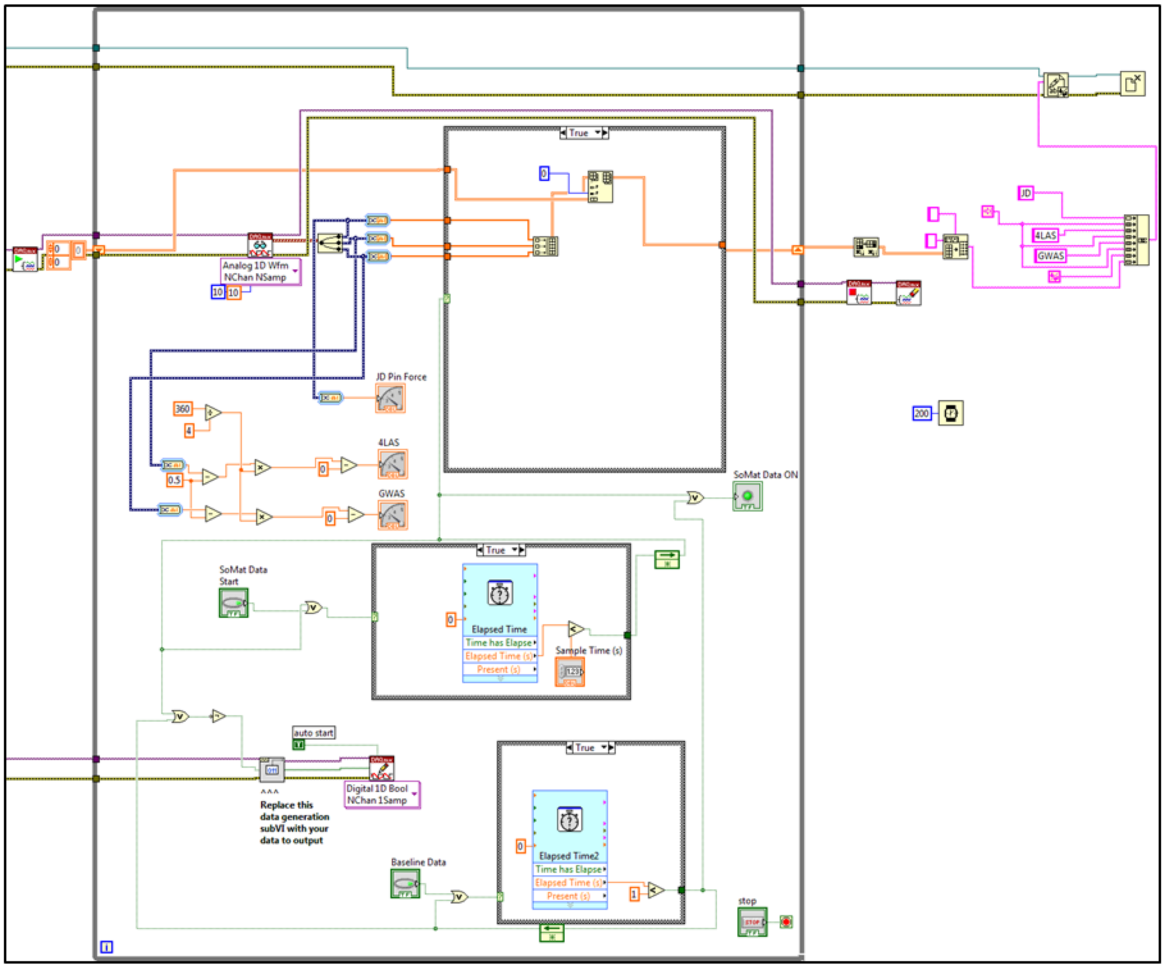

Figure B.3: Right hand side of planter data collection block diagram.

B.2 Component Calibration Data Collection Program

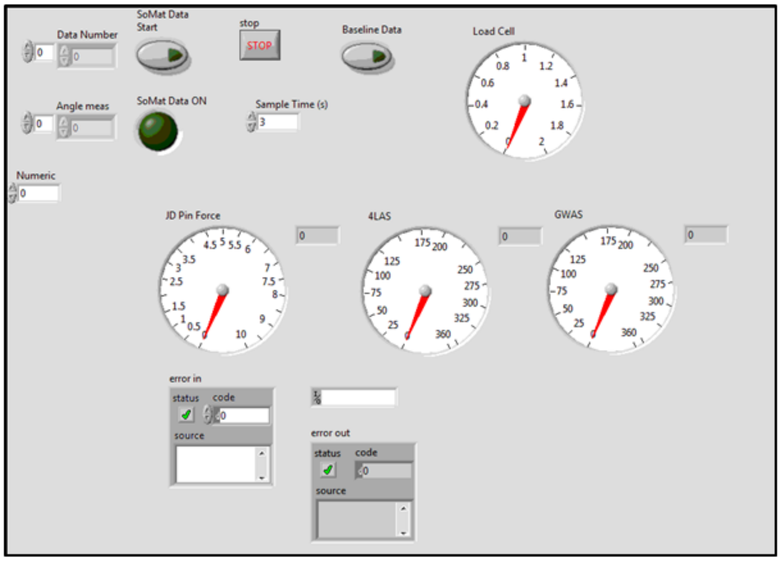

Figure B.4: Sensor and component calibration data collection front panel.

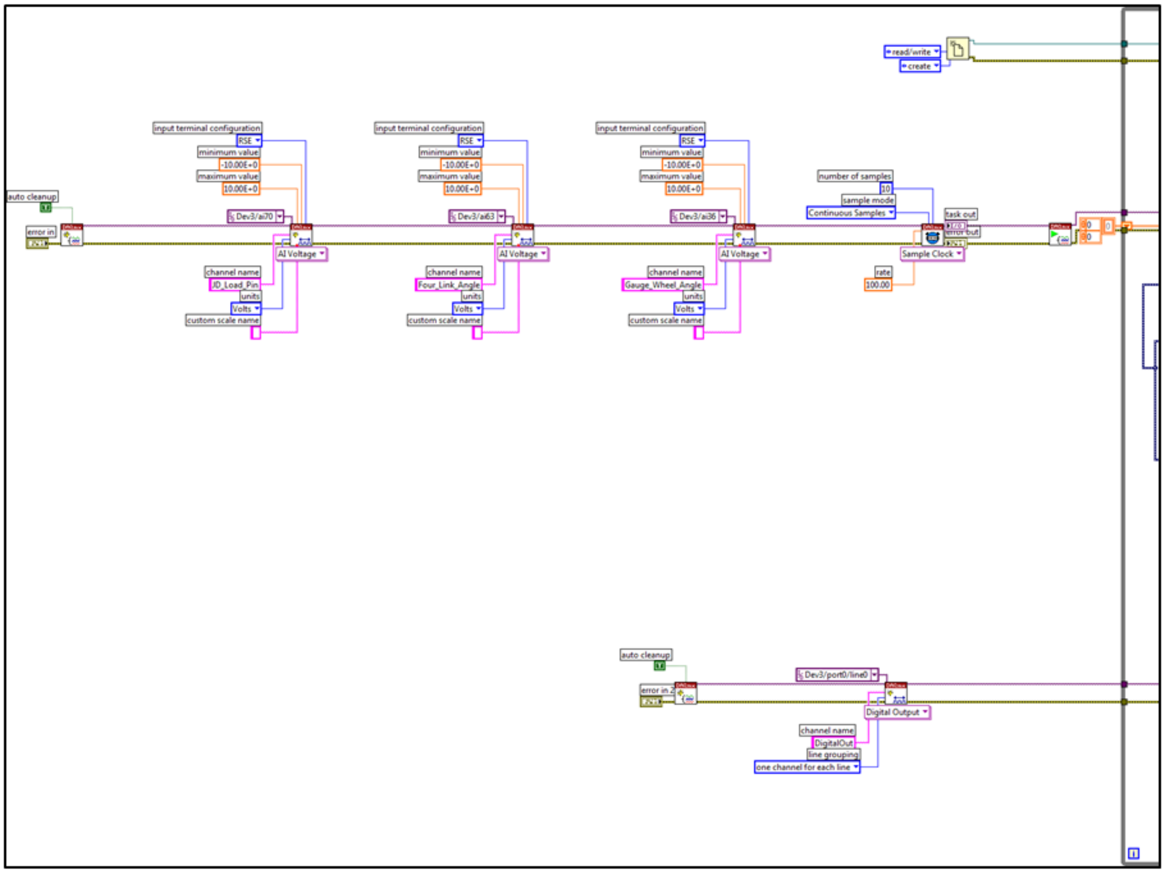

Figure B.5: Left hand side of calibration data collection block diagram.

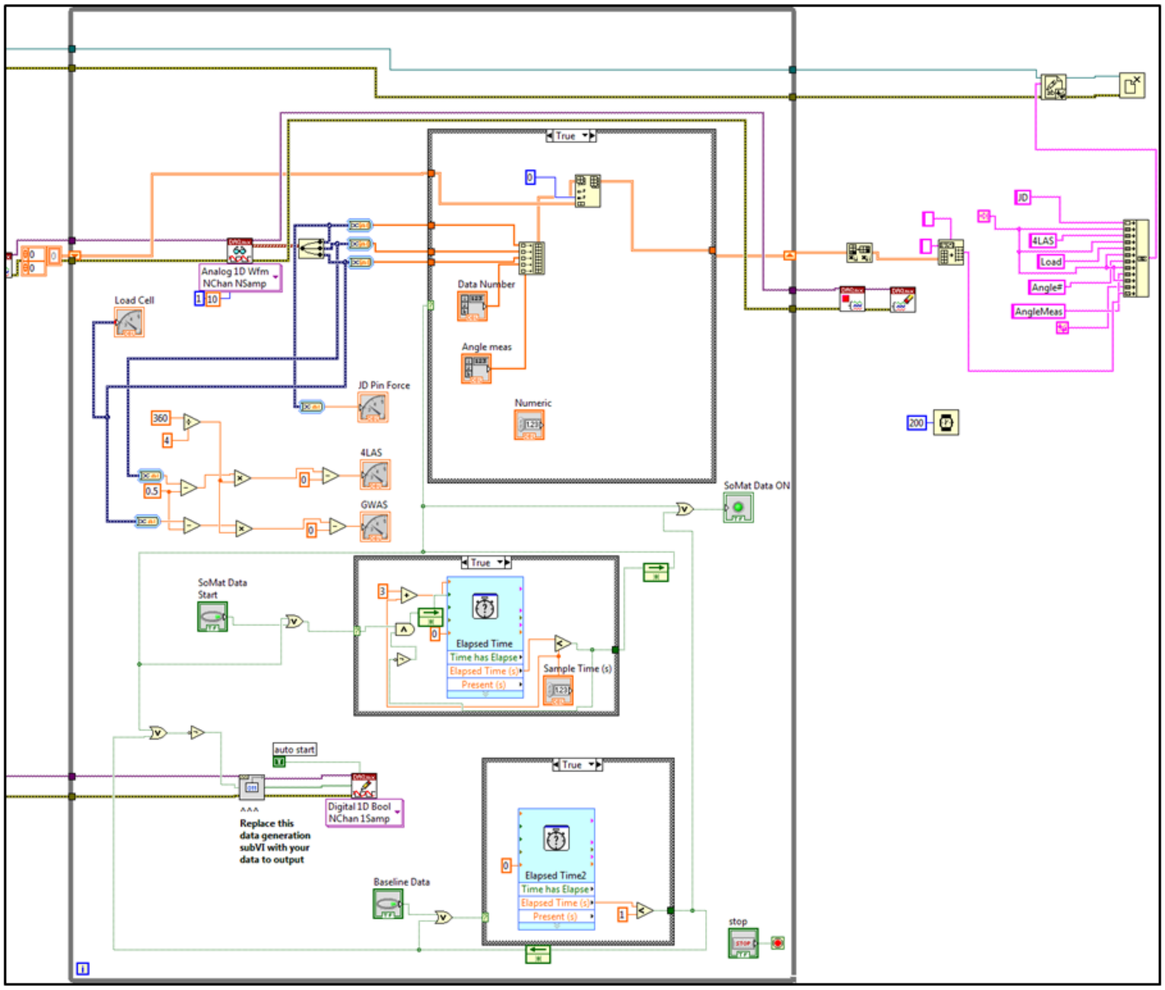

Figure B.6: Right hand side of calibration data collection block diagram.

Appendix C

USDA National Soil Dynamics Laboratory Indoor Soil Bin

C.1 Norfolk Sandy Loam Soil Properties

Table C.1: General Norfolk Sandy Loam Soil Information.

Norfolk Sandy Loam	
Item	Description
U.S.C.S.	SP-SM
Origin	Agricultural Engineering Farm, Auburn University, Marvyn, Ala.
1984 soil series name	Norfolk Sandy Loam
1984 soil sub-group name	Typic Paleudults
1984 soil family name	Fine loamy, siliceous, thermic
1966 soil series name	Norfolk Sandy Loam
1972 sub-group name	Tpyic Paleudults

* Norfolk Sandy Loam soil data referenced from Batchelor (1984).

Table C.2: Mechanical analysis of Norfolk Sandy Loam in the soil bin.

Particle Size Distribution									
Total					**Sand**			**Silt**	
Sand 2 - 0.05	Silt 0.05 - 0.002	Clay <0.002	Very Coarse 2-1	Coarse 1-0.5	Med. 0.5-0.25	Fine 0.25 - 0.01	Very Fine 0.01 - 0.05	0.05 - 0.02	0.02 - 0.002
Percent <2 mm									
71.6	17.4	11.0	6.8	25.5	16.6	17.4	5.3	5.0	12.4

* Norfolk Sandy Loam soil data referenced from Batchelor (1984).

Table C.3: Gravel content and specific gravity of Norfolk Sandy Loam in the soil bin.

Gravel Content <2 mm % Total	**Specific Gravity (g cc^{-1})**
0.0	2.65

* Norfolk Sandy Loam soil data referenced from Batchelor (1984).

Table C.4: Chemical properties of Norfolk Sandy Loam in the soil bin.

Cation Exchange Capacity (ma. 100g^{-1})	Organic Matter Dry Weight Basis (%)	pH
3	0.0	4.9

* Norfolk Sandy Loam soil data referenced from Batchelor (1984).

Table C.5: Mineralogical analysis of Norfolk Sandy Loam in soil bin.

Mineral Content of Clay Fraction							
Mont.[1]	Chlorite	Vermiculite	Mica	Int.[2]	Qtz	Kaolinite (%)	Gibbsite (%)
X-Ray Diffraction Determinations						Differential Thermal Analysis Determinations	
–	–	xxx	–	–	–	42	5

* Norfolk Sandy Loam soil data referenced from Batchelor (1984).
[1]Montmorillonite
[2]Interstratified layer silicates
– not detected, xxx abundant

Table C.6: Soil moisture retention of Norfolk Sandy Loam in soil bin.

Soil Moisture Suction			
1/3 ATM	1 ATM	3 ATM	15 ATM
Percent Moisture, Dry Weight Basis			
7.1	6.6	5.1	3.9

* Norfolk Sandy Loam soil data referenced from Batchelor (1984).

Table C.7: Rheological properties of Norfolk Sandy Loam in soil bin.

Lower Plastic Limit	**Lower Liquid Limit**	**Plasticity Index**	**Stickey Point**
Percent Moisture, Dry Weight Basis		**Number**	**Percent Moisture Dry Weight Basis**
17.6	20.5	2.9	17.9

* Norfolk Sandy Loam soil data referenced from Batchelor (1984).

Appendix D

R Code

D.1 Formatting Raw SoMat Data

```
""" R Script used to format somat data files for data analysis"""

#____________________________ Preliminary coding ___________________

# Import required library
library(xlsx) # deals with excel files
library( lme4)
library(lmerTest)

# set work directory - where files will be found and data exported
setwd("C:\\Users\\amp0028\\Desktop\\Rees\\somatdata")


# ------------------------- Step1: Import the Data and Split in 2 Files --------------
# Import data
file.name <- c("1508.txt","1507.txt","1202.txt","1309.txt","1501.txt")  # list of the file
    names to be formatted

plot.order <- c(1508,
                1507,1406,1106,1104,1101,1403,1505,1301,
                1202,1203,1404,1504,1305,1306,1307,1408,1310,1210,1110,
                1309,1409,1208,1207,1407,1206,1405,1503,1103,1204,1201,1401,
                1501,1502,1402,1302,1303,1304,1205,1105,1506,1107,1308,1109,1509)

# creation of global variables

# final dataset storing the experimental values
data.trt <- data.frame(Plot=numeric(), Time=numeric(), DC1=numeric(), DL2=numeric(),
                      DR3=numeric(), SU4=numeric(), SL5=numeric(), VC6=numeric(), Total_DR=
                          numeric(),
                      Total_Side=numeric(), Calc_MPH=numeric())
```

```r

# final dataset storing the baseline values
data.baseline <- data.trt


#nb.file <- c(1,8,11,12,13)
index.file <- 1 # indicate plot number

data.baseline.temp <- data.baseline[0,] # temporary data frame to store current section of baseline
data.trt.temp <- data.trt[0,]  # temporary data frame to store current section of experimental data


for (file in seq(1,length(file.name))){   # iterate over txt files

  # import data
  data.i <- read.table(file.name[file],header=T,sep="\t") # import data
  location <- "baseline"  # start file with baseline

  for (row in seq(1,length(data.i[,1])-1)) {  # iterate over observations within a file

   time.step <- data.i$Time[row+1] - data.i$Time[row]  # compare time with successive time

    if (time.step < 0.05) {  # if time is below threshold

      if(location == "baseline") {  # and we are looking at baseline data

        temp <- as.data.frame(c(plot.order[index.file]))  # then look for the plot number we are working on
        temp <- cbind(temp,data.i[row,])  # attach it to data from the observation we are considering
        data.baseline.temp <- rbind(data.baseline.temp,temp) # and store the data in the temporary data set for baseline data
      } # close smallest if

     else if(location == "treatments") {  # if we are looking at experimental data

        temp <- as.data.frame(c(plot.order[index.file])) # look at the plot number
        temp <- cbind(temp,data.i[row,]) # attach it to the observation considered
```

```
        data.trt.temp <- rbind(data.trt.temp,temp)  # and store in the temporary data set for experimental data
       } # close smallest if

    } # close middle if

     else if (time.step >= 0.05) {  # if time is above threshold

        if (location == "baseline") { # and we are considering the baseline data

          print(row)

          location <- "treatments" # after this observation we will move to experimental data
          temp <- as.data.frame(c(plot.order[index.file])) # attribute observation to plot
          temp <- cbind(temp,data.i[row,]) # attach plot data to the line data
          data.baseline.temp <- rbind(data.baseline.temp,temp)  # save last baseline line into the baseline temporary file

          data.baseline <- rbind(data.baseline, data.baseline.temp) # save data from the temporary file to the final file
          data.baseline.temp <- data.baseline[0,]  # empty the temporary file for baseline data
          } #close smaller if

      else if (location == "treatments") { # if we are considering the experimental data

          print(row)

          location <-"baseline" # after this observation we will move to another baseline data
          temp <- as.data.frame(c(plot.order[index.file])) # attribute observation data to plot
          temp <- cbind(temp,data.i[row,]) # attach plot to the line data
          data.trt.temp <- rbind(data.trt.temp,temp)  # save last experimental observation to the temporary file

          data.trt <- rbind(data.trt, data.trt.temp) # save data from the temporary data set to the final data set for experimental data
          data.trt.temp <- data.trt[0,] # empty the temporary file for experimental data
          index.file <- index.file + 1 # moving to next plot....
```

```
          print(index.file) # print to console for control

          } #close smaller if

        } # close medium if

  } # second loop - over observations within a file

      temp <- as.data.frame(c(plot.order[index.file])) # attribute observation data to plot
      temp <- cbind(temp,data.i[length(data.i[,1]),]) # attach plot to the line data
      data.trt.temp <- rbind(data.trt.temp,temp)  # save last experimental observation to the temporary file

      data.trt <- rbind(data.trt, data.trt.temp) # save data from the temporary data set to the final data set for experimental data
      data.trt.temp <- data.trt[0,] # empty the temporary file for experimental data
      index.file <- index.file + 1 # moving to next plot....
      print(index.file) # print to console for control



}  # main loop - over file

rm(data.i); rm(data.baseline.temp); rm(data.trt.temp); rm(temp)
rm(file); rm(file.name); rm(index.file); rm(location); rm(plot.order); rm(row); rm(time.step)

# ------------------------ Step2: Reshape and Export the data  --------------

# export baseline data
write.table(data.baseline,file="Baseline_Data_July_9-10_15.txt")
write.xlsx(data.baseline, file="Baseline_Data_July_9-10_15.xlsx")


# export treatment data
write.table(data.trt, file="Experimental_Data_July_9-10_15.txt")
write.xlsx(data.trt, file="Experimental_Data_July_9-10_15.xlsx")

# import data
data.baseline <- read.table("Baseline_Data_July_9-10_15.txt", header=T)

```

```
colnames(data.baseline) <- c("Plot","Time","DC1","DL2","DR3","SU4","SL5","VC6","Total_DR","
    Total_Side","Calc_MPH")

# Compute mean values
data.baseline.agg <- aggregate(list(data.baseline$DC1,data.baseline$DL2,data.baseline$DR3,
                                    data.baseline$SU4,data.baseline$SL5,data.baseline$VC6,
                                    data.baseline$Total_DR,data.baseline$Total_Side,data.
                                        baseline$Calc_MPH),
                               list(data.baseline$Plot),mean,na.rm=T)

#provide header to matrix
colnames(data.baseline.agg) <- c("Plot","DC1","DL2","DR3","SU4","SL5","VC6","Total_DR","
    Total_Side","Calc_MPH")


# export mean data for baseline
write.table(data.baseline.agg,file="Baseline_Data_Average_July_9-10_15.txt")
write.xlsx(data.baseline.agg, file="Baseline_Data_Average_July_9-10_5.xlsx")

rm(data.baseline); rm(data.baseline.agg); rm(data.trt)

# ------------------------- Step 3: Analysis on Baseline data ---------

data.b <- read.table("Baseline_Data_Average_July_9-10_15.txt")
data.trt <- read.table("configurations.txt",header=T,sep="\t")


data.bm <- merge(data.trt, data.b, by.x="Plot", by.y = "Plot", all.x=F)


# change class of data for anova

data.bm <- within(data.bm, Config <- factor(Config))
data.bm <- within(data.bm, Plant_Depth <- factor(Plant_Depth))
data.bm <- within(data.bm, Rep <- factor(Rep))


anova.1 <- lmer(VC6 ~ Config*Plant_Depth + (1|Rep), data = data.bm)
results.1 <- anova(anova.1)
lsmeans.1 <- lsmeans(anova.1)
lsmeans.1.df <- as.data.frame(lsmeans.1[1])
```

```
write.xlsx(lsmeans.1.df,"Anova_Baseline_VC6_lsmeans.xlsx")
```

Appendix/Format_Somat_Data.R

D.2 Formatting Raw LabVIEW Data

```
  # Set working directory
setwd("C:/Users/bridgrw/Documents/JD Planter Simulation/Soil Model/R Data/Labview_7_9_15")

# create a list of treatments
treatment<-c(1101,1102,1103,1104,1105,1106,1107,1108,1109,1110,1201,1202,
             1203,1204,1205,1206,1207,1208,1209,1210,1301,1302,1303,1304,
             1305,1306,1307,1308,1309,1310,1401,1402,1403,1404,1405,1406,
             1407,1408,1409,1410,1501,1502,1503,1504,1505,1507,1508,1509)
#Create empty data frame
PlanterData<-data.frame(JD_V=numeric(), X4LAS_V=numeric(), GWAS_V=numeric(),  JD=numeric(),
                        X4LAS=numeric(),   GWAS=numeric(), plot=character(),ID=numeric(),
                            Merge=numeric())

#  For Loop to import and combine test files
k<-1:48

for(file in k) {
  filename<-paste(treatment[file],".txt",sep = "")
  #Import data
  temp1<-read.table(filename,header = T,sep = "\t")

  # Add plot column to temp1 file
  temp1<-within(temp1,plot<-as.character(treatment[file]))

  temp1<-within(temp1,ID<-1)
  for(line in seq(2,length(temp1[,1]))){
    temp1[line,8] <-  temp1[line-1,8] + 1
  }

  #Create merge column with "treatment-ID"
  for(line in seq(1,length(temp1[,1]))){
    temp1[line,9] <-  paste(temp1[line,7],temp1[line,8],sep="")
  }

```

```
  # Row bind to planterdata
  PlanterData<-rbind(PlanterData,temp1)
}

#Remove temp1
rm(temp1)

## Remove incorrect calibration columns
PlanterData<-PlanterData[,c(1,2,3,5,6,7,8,9)]

setwd("C:/Users/bridgrw/Documents/JD Planter Simulation/Soil Model/R Data")

#Import data
config.table<-read.table("treatment_config.txt",header = T,sep = "\t")
#Import data
calibration.table<-read.table("JD_DF_calibration_Table.txt",header = T,sep = "\t")
# remove two uneeded columns (X and X.1)
config.table<-config.table[,1:4]
#Merging tables by planting depth
config.table <- merge(calibration.table, config.table,by="plant_depth",all=T)
#Merging tables by plot
PlanterData <- merge(PlanterData, config.table,by="plot",all=T)

# Reorder PlanterData table
PlanterData <- PlanterData[,c(1,12,9,13,7,8,10,11,2,3,4,5,6)]

#Calculate JD pin calibrated values
PlanterData <- within(PlanterData,JD <- a*JD_V+b)

sapply(PlanterData,class)

k<-1:length(PlanterData[,1])
for(line in k){
  if(PlanterData[line,2]==4){
    PlanterData[line,14]<-"."
  }
}
PlanterData <- within(PlanterData,JD <- as.numeric(JD))
PlanterData <- within(PlanterData,GWAS <- as.numeric(GWAS))

# Rename colums that started with "4"
```

```
colnames(PlanterData)[10]<-"FLAS_V"
colnames(PlanterData)[12]<-"FLAS"
# Rename merge column name
colnames(PlanterData)[6]<-"Merge"

#Set working directory
setwd("C:/Users/bridgrw/Documents/JD Planter Simulation/Soil Model/R Data/Labview_7_9_15")

#Write file to csv
write.csv(PlanterData,"PlanterData_Labview_7_9_15.csv")
```

Appendix/Format_Labview_Data.R

D.3 Combine LabVIEW and SoMat Data Sets

```
#  Combine Labview and Somat data files

setwd("C:/Users/bridgrw/Documents/JD Planter Simulation/Soil Model/R Data")

#Import somat data
somat.data <- read.csv("SomatData_7_9_15.csv",header = T,sep = ",")

#Import Laview data
labview.data <- read.csv("PlanterData_Labview_7_9_15.csv",header = T,sep = ",")

#List of labview plot numbers
labview.plot.num<-unique(labview.data$plot)

#Create Complete.data
Complete.data <- data.frame(ID=numeric(),plot.x=numeric(),config=integer(),
                            plant_depth=integer(),rep=integer(),
                            Merge.x=numeric(),a=numeric(),b=numeric(),
                            JD_V=numeric(),FLAS_V=numeric(),GWAS_V=numeric(),
                            FLAS=numeric(),GWAS=numeric(),JD=numeric(),
                            plot.y=numeric(),Merge.y=numeric(),time=numeric(),
                            DC1=numeric(),DL2=numeric(),DR3=numeric(),
                            SU4=numeric(),SL5=numeric(),VC6=numeric(),
                            Total_DR=numeric(),Total_Side=numeric(),
                            Calc_MPH=numeric())

```

```
# Loop to create subset of somat.data and labview.data by treatment
# Subsets will then be merged, and recombined at Complete.data
k <- 1:length(labview.plot.num)
for (treatment in k){
  temp.labview <- subset(labview.data,labview.data$plot==labview.plot.num[treatment])
  temp.somat <- subset(somat.data,somat.data$plot==labview.plot.num[treatment])
  #temp.labview <- subset(labview.data,labview.data$plot==labview.plot.num[1])
  #temp.somat <- subset(somat.data,somat.data$plot==labview.plot.num[1])
  #Merging files
  temp.merge <- merge(temp.labview,temp.somat,by="ID",all=T)
  #Row bind temp.merge to Complete.data
  Complete.data <- rbind(Complete.data,temp.merge)
}
#Remove temp files
rm(temp.labview)
rm(temp.somat)
rm(temp.merge)

# Loop to put Plot numbers in plot.x from plot.y where missing
i <- 1:length(Complete.data[,1])
for (line in i){
  if(is.na(Complete.data[line,2])==T){
    Complete.data[line,2] <- Complete.data[line,15]
  }
}

#Remove Merge and extra plot columns (plot.x, config,plant_depth, rep, Merge.x, plot.y,
    Merge.y)
Complete.data <- Complete.data[,c(-3,-4,-5,-6,-15,-16)]

#Rename plot.x to plot
colnames(Complete.data)[2]<-"plot"

#Import treatment configuration data
config.table<-read.table("treatment_config.txt",header = T,sep = "\t")
config.table<-config.table[,1:4]

#Merge with config table
Complete.data <- merge(Complete.data, config.table,by="plot",all=T)

#Reorder table to bring config data to left side
```

```
Complete.data <- Complete.data[,c
    (1,2,21,22,23,3,4,5,6,7,8,9,10,11,12,13,14,15,16,17,18,19,20)]

#Write file to csv
write.csv(Complete.data,"Complete_SensorData_7_9_15.csv")
```

Appendix/Combine_Labview_Somat_Data.R

D.4 Data Analysis

```
# Rees Bridges
# 10/1/15
# Soil Model Data Analysis


# ----------------Working Directory and Data Import--------------------

#setwd("C:/Users/bridgrw/Documents/JD Planter Simulation/Soil Model/R Data")
setwd("C:/Users/Bridges/Documents/Soil Model/R Data")
## Import files
Sensor.data<-read.table("Complete_SensorData_7_9_15.csv",header = T,sep = ",")
Hand.data<-read.table("Complete_HandData_7_9_15.csv",header = T,sep = ",")
Config.table<-read.table("treatment_config.txt",header = T,sep = "\t")
Baseline.data<-read.table("Baseline_Data_Average_7_9_15.txt",header = T,sep = "\t")

# ----------------Import packages--------------------
require(ggplot2)
require(lme4)
require(lmerTest)



#-----------------Data Frame Configuration and Clean Up-------------------

# Rename Baseline columns
colnames(Baseline.data)<-c("plot","Base_DC1","Base_DL2","Base_DR3","Base_SU4","Base_SL5","
    Base_VC6","Base_Total_DR", "Base_Total_Side","Calc_MPH")

# Remove a,b, FLAS_V, GWAS_V, and JD_V columns that were used to calculate FLAS, GWAS, and
    JD value
Sensor.data<-Sensor.data[,c(-6:-10)]
```

```

# ***Conversions***
for (line in 1:length(Sensor.data[,1])) {
  Sensor.data$JD[line]<-Sensor.data$JD[line]*.00444822 # Convert JD Downforce pin values from lbf to Kn
  #Sensor.data$FLAS[line]<-Sensor.data$FLAS[line]*pi/180 # Convert FLAS to radians
}

# ----------------Calculate Averages for Hand Data by Treatment and Remove 1102-----------------
Hand.data <- within(Hand.data, PDavg <- NA)
Hand.data <- within(Hand.data, PRDavg <- NA)
Hand.data <- within(Hand.data, GRDavg <- NA)
# Correct treatment 1110 planting depth value
Hand.data[10,5]<-7
Hand.data[10,6]<-8.3


for (line in 1:length(Hand.data[,1])) {
  Hand.data$PDavg[line] <- mean(c(Hand.data$PD1[line], Hand.data$PD2[line],Hand.data$PD3[line],
                                  Hand.data$PD4[line], Hand.data$PD5[line]),na.rm=T)

  Hand.data$PRDavg[line] <- mean(c(Hand.data$PRD1[line], Hand.data$PRD2[line],Hand.data$PRD3[line],
                                  Hand.data$PRD4[line], Hand.data$PRD5[line]),na.rm=T)

  Hand.data$GRDavg[line] <- mean(c(Hand.data$GRD1[line], Hand.data$GRD2[line],Hand.data$GRD3[line],
                                   Hand.data$GRD4[line], Hand.data$GRD5[line]),na.rm=T)
}


#-----------------Create new variables------------------------

# Force values
Sensor.data<-within(Sensor.data,DFy<-as.numeric(NA)) # Force on planter from the down force system in Global Y
Sensor.data<-within(Sensor.data,Fddy<-as.numeric(NA)) # Force on Double disc opener in Y
Sensor.data<-within(Sensor.data,Fddx<-as.numeric(NA)) # Force on Double disc opener in X
Sensor.data<-within(Sensor.data,Fgwy<-as.numeric(NA)) # Force on Gauge wheels in Y
```

```
Sensor.data<-within(Sensor.data,Fgwx<-as.numeric(NA)) # Force on Gauge wheels in X
Sensor.data<-within(Sensor.data,Fpwy<-as.numeric(NA)) # Force on Press wheels in Y
Sensor.data<-within(Sensor.data,Fpwx<-as.numeric(NA)) # Force on Press wheels in X
Sensor.data<-within(Sensor.data,Fcty<-as.numeric(NA)) # Force on Coulter in Y
Sensor.data<-within(Sensor.data,Fctx<-as.numeric(NA)) # Force on Coulter in X
WtPlt<-as.numeric(262.3333)*.00444822 # Weight of planter + component of the links
  # links that are supported by the planter (kn)
Sensor.data<-within(Sensor.data,Fpws<-as.numeric(NA)) # Press wheel spring force
Sensor.data<-within(Sensor.data,Fpwsy<-as.numeric(NA)) # Press wheel spring force in Global Y
Sensor.data<-within(Sensor.data,Fpwsx<-as.numeric(NA)) # Press wheel spring force in Global X
Sensor.data<-within(Sensor.data,FpwHy<-as.numeric(NA)) # Press wheel spring force in the Global Y
Sensor.data<-within(Sensor.data,FpwHx<-as.numeric(NA)) # Press wheel spring force in the Global X
Sensor.data<-within(Sensor.data,Ftl1<-as.numeric(NA)) # Force in Upper toolbar link
Sensor.data<-within(Sensor.data,Ftl2<-as.numeric(NA)) # Force in Lower toolbar link
Sensor.data<-within(Sensor.data,F2<-as.numeric(NA))  # Force upward on Downforce spring system arm from upper link
Sensor.data<-within(Sensor.data,F1<-as.numeric(NA))  # Force downward on toolbar mount from upper link, due to downforce spring system


# Coordinates
Sensor.data<-within(Sensor.data,GWx<-as.numeric(NA)) # Gauge wheel hub in Global X
Sensor.data<-within(Sensor.data,GWy<-as.numeric(NA)) # Gauge wheel hub in Global Y
Sensor.data<-within(Sensor.data,GWz<-as.numeric(NA)) # Gauge wheel hub in Global Z
Sensor.data<-within(Sensor.data,PWx<-as.numeric(NA)) # Press wheel hub in Global X
Sensor.data<-within(Sensor.data,PWy<-as.numeric(NA)) # Press wheel hub in Global Y
#Sensor.data<-within(Sensor.data,PWz<-as.numeric(NA)) # Press wheel hub in Global Z

# Distances
Sensor.data<-within(Sensor.data,D1<-as.numeric(NA)) # Vertical Dist along Global XYZ
  # from origin to ground surface in gauge wheel rut (includes gauge wheel rut)
Sensor.data<-within(Sensor.data,D2<-as.numeric(NA)) # Vertical Dist along Global XYZ
  # from origin to ground surface in press wheel rut (includes gauge wheel and press wheel ruts)
D3<-as.numeric(16.906) # Vertical Dist along Global XYZ
  # from origin to hinge axis of press wheel assembly
Sensor.data<-within(Sensor.data,D4<-as.numeric(NA)) # Vertical Dist along Global XYZ
```

```
  # from the hinge axis of the press wheel assembly to the ground surface
  # in the press wheel rut (includes the gauge wheel and press wheel ruts)
D5<-as.numeric(19.025) # Horizontal dist along Global XYZ from the origin
  # to the hinge axis of the press wheel assembly
R1y<-as.numeric(7.817) # Gauge wheel radius in the Global Y direction
R2y<-as.numeric(6.007) # Press wheel radius in the Global Y direction
D6<-as.numeric(9.02) # Distance from press wheel assembly hinge axis to
  # the press wheel hub axis
D7<-as.numeric(4.161) # Distance from press wheel assembly hinge axis to
  # the forward (fixed) spring attachment point
D8<-as.numeric(10.088) # Distance from press wheel assembly hinge axis to
  # the rear (adjustment) spring attachement point
Sensor.data<-within(Sensor.data,D9<-as.numeric(NA)) # Press wheel spring length

# Angles  **Angles are in radians unless denoted otherwise
Gamma1<-as.numeric(57.26*pi/180) # Angle of the forward (fixed) press
  # wheel spring attachement point to the horizontal axis, through the
  # press wheel hinge axis
Gamma2<-as.numeric(23.8*pi/180) # Angle from the press wheel hub to the
  # rear (adjustable) press wheel  spring attachement point, through
  # the press wheel hinge axis
Sensor.data<-within(Sensor.data,GammaPW<-as.numeric(NA)) # Angle of
  # press wheel position to the horizontal, through the hinge axis
Sensor.data<-within(Sensor.data,GammaPWSpg<-as.numeric(NA)) # Angle
  # about press wheel assembly hinge axis that corresponds to the
  # spring length by law of cosines

# Rotation Matrices and required variables
Rglb<-matrix(c(0.9967159764143170000,0,0.0809769248641521000 0,
               -0.0059963313674615900 0,0.9973897841210730000 0,0.0719559764095365000 0,
               -0.0800152043333741000 0,-0.0720136839000342000 0,0.9941889138421500000 0),
             nrow = 3, ncol = 3,byrow = T)
RTglb<-t(Rglb)  #Transpose of Rglb
AB<-matrix(c(17.509,-13.724,1.042),nrow = 3,ncol=1) #AB vector - vector from global coordinate system to body coordinate system
BC<-matrix(c(-9.5,0,2.5),nrow=3,ncol=1) #BC vector - vector from body coordinate system origin to hub point in body system----------------


# ----------------Calculate Key Component Postions ----------------

```

```
# LH Gauge Wheel Hub Position in Global XYZ
  # Variables GWx, GWy, and GWz
for (line in 1:length(Sensor.data[,1])){
  if(Sensor.data$config[line]!=4){
c1<-cos(Sensor.data$GWAS[line]*-pi/180)
s1<-sin(Sensor.data$GWAS[line]*-pi/180)
Rz<-matrix(c(c1,s1,0, -s1,c1,0, 0,0,1),nrow = 3,ncol=3,byrow=T)
GWhub<-AB+(RTglb %*% (Rz %*% BC))
Sensor.data$GWx[line]<-GWhub[1]
Sensor.data$GWy[line]<-GWhub[2]
Sensor.data$GWz[line]<-GWhub[3]
  }
}
# Remove variables c1, s1, Rz, and GWhub
rm(c1); rm(s1); rm(Rz); rm(GWhub)

#-------------------Toolbar Link Forces-------------------------------------
for (line in 1:length(Sensor.data[,1])) {
  temp.table<-subset(Baseline.data,plot==Sensor.data[line,1]) # creates temporary table to
      pull baseline data
  if(is.na(Sensor.data$time[line])==T){
    Sensor.data$Ftl1[line]<-NA
    Sensor.data$Ftl2[line]<-NA
  }
  else{
  # Upper toolbar link force
  temp.D1<-3.21875
  temp.D2<-4.78125
  temp.D3<-10.0625
  temp.D4<-10
  temp.D5<-14.25
  temp.D6<-6.47
  run.DC1<-Sensor.data$DC1[line]-temp.table$Base_DC1
  run.DL2<-Sensor.data$DL2[line]-temp.table$Base_DL2
  run.DR3<-Sensor.data$DR3[line]-temp.table$Base_DR3
  run.VC6<-Sensor.data$VC6[line]-temp.table$Base_VC6
  run.DL<-run.DL2+run.DR3
  # Calculating force F2
  Sensor.data$F2[line]<-Sensor.data$DFy[line]*(13.75*sin(Sensor.data$FLAS[line]*pi/180))/
                        6.47
  # Caluculating force F1
```

```
  Sensor.data$F1[line]<-Sensor.data$F2[line]-Sensor.data$DFy[line]
  # Calculation for lower 4-link force
  Sensor.data$Ftl2[line]<-(-run.DC1*(temp.D3-temp.D1)+run.DL*(temp.D4+temp.D1)-
                             run.VC6*temp.D5+Sensor.data$F2[line]*temp.D6)/
                          (-8*sin(Sensor.data$FLAS[line]*pi/180))
  # Calculation for upper 4-link forces (combined)
  Sensor.data$Ftl1[line]<-(-run.DC1-run.DL-Sensor.data$Ftl2[line]*sin(Sensor.data$FLAS[line]
      *pi/180))/
                          sin(Sensor.data$FLAS[line]*pi/180)

  }
}
# Remove temp variables
rm(temp.table); rm(temp.D1); rm(temp.D2); rm(temp.D3)
rm(temp.D4); rm(temp.D5); rm(temp.D6);rm(run.DC1); rm(run.DL2); rm(run.DR3)
rm(run.DL); rm(run.VC6)


# ------------------Press Wheel Assembly Position and Force------------------
# LH Press Wheel Hub Position (in Global XYZ) and forces
# Calculate D2, D4, PWy, PWx, GammaPW, GammaPWSpg, D9, Fpws, Fpwy, FpwHy, and FpwHx
temp.table<-data.frame("plot"=numeric(), "PRDavg"=numeric()) # Temp table to pull Hand.data
    PRD average value
for (line in 1:length(Sensor.data[,1])) {
  if(Sensor.data$config[line]==1||Sensor.data$config[line]==2) {
    temp.table[1,1]<-Sensor.data$plot[line]
    temp.table[1,2]<-Hand.data$PRDavg[match(temp.table$plot,Hand.data$plot)]
    Sensor.data$D2[line]<--Sensor.data$GWy[line]+R1y+temp.table$PRDavg
    Sensor.data$PWy[line]<- Sensor.data$GWy[line]-R1y-temp.table$PRDavg+R2y
    Sensor.data$D4[line]<--Sensor.data$PWy[line]-D3+R2y
    Sensor.data$GammaPW[line]<-asin((Sensor.data$D4[line]-R2y)/D6)
    Sensor.data$GammaPWSpg[line]<- Gamma1-(Sensor.data$GammaPW[line]-Gamma2)
    Sensor.data$PWx[line]<-D5+D6*cos(Sensor.data$GammaPW[line])
    #Press wheel spring length D9
    Sensor.data$D9[line]<-(D8^2+D7^2-(2*D8*D7)*cos(Sensor.data$GammaPWSpg[line]))^0.5
    Sensor.data$Fpws[line]<-(Sensor.data$D9[line]-6.75)*79.433*.00444822  # Spring force (
        tension) in Kn
    # Temp calculation of internal angle to calculate force component angle
    Gamma3<-acos((-(D8^2)+D7^2+Sensor.data$D9[line]^2)/(2*D7*Sensor.data$D9[line]))
    Gamma4<-pi-Gamma1-Gamma3
```

```
    Sensor.data$Fpwsy[line]<-Sensor.data$Fpws[line]*sin(Gamma4) # Press wheel spring force in Global Y
    Sensor.data$Fpwsx[line]<-Sensor.data$Fpws[line]*cos(Gamma4) # Press wheel spring force in Global X

    # Press wheel resultant force in Global Y (Kg)
    Sensor.data$Fpwy[line]<-(-Sensor.data$Fpwsy[line]*(D8*cos(Sensor.data$GammaPW[line]-Gamma2))-
                              Sensor.data$Fpwsx[line]*(D8*sin(abs(Sensor.data$GammaPW[line]-Gamma2))))/
                             -(D6*cos(Sensor.data$GammaPW[line]))

    # Press wheel component forces at press wheel assembly hinge axis
    Sensor.data$FpwHy[line]<--Sensor.data$Fpwsy[line]+Sensor.data$Fpwy[line] # Force from press wheel FBD in Global Y
    Sensor.data$FpwHx[line]<-Sensor.data$Fpwsx[line] # Force from press wheel FBD in Global X

  }
}
# Remove temp.table
rm(temp.table); rm(Gamma3); rm(Gamma4)


#---------------Calculate Configuration 4 Forces -----------------------------

# Configuration 4 will only have forces on the Double Disk Opener
# Calculate Drag and vertical force on opening disk from config 4
  # readings VC6 and Total_DR
# Variables Fddy and Fddx
for (line in 1:length(Sensor.data[,1])){
  temp.table<-subset(Baseline.data,plot==Sensor.data[line,1]) # creates temporary table to pull baseline data
  if(Sensor.data$config[line]==4){
    Sensor.data$Fddy[line]<-temp.table$Base_VC6-Sensor.data$VC6[line]
    Sensor.data$Fddx[line]<--(Sensor.data$Total_DR[line]-temp.table$Base_Total_DR)

  }
}
# Remove temp.table
rm(temp.table)
```

```
#---------------Calculate Configuration 3 Forces -----------------------------

# Calculate Drag and vertical force on opening disk and Gauge wheels
  # from config 3 readings VC6, JD, and Total_Dr
# Variables Fddy and Fddx
for (line in 1:length(Sensor.data[,1])){
  #temp.table<-subset(Baseline.data,plot==Sensor.data[line,1]) # creates temporary table to
      pull baseline data
  if(is.na(Sensor.data$time[line])==T){
    Sensor.data$Fddy[line]<-NA
  }
  else if(Sensor.data$config[line]==3){
    Sensor.data$Fddy[line]<--Sensor.data$Ftl1[line]*cos(Sensor.data$FLAS[line]*pi/180)-
                            Sensor.data$Ftl2[line]*cos(Sensor.data$FLAS[line]*pi/180)+
                            Sensor.data$DFy[line]+WtPlt-Sensor.data$JD[line]

  }
}
# Remove temp.table
#rm(temp.table)"

#---------------Calculate Configuration 2 Forces -----------------------------

# Calculate vertical forces on opening disk, gauge wheels and
#   press wheels
for (line in 1:length(Sensor.data[,1])){
  if(is.na(Sensor.data$time[line])==T){
    Sensor.data$Fddy[line]<-NA
  }
  else if(Sensor.data$config[line]==2){
    Sensor.data$Fddy[line]<--Sensor.data$Ftl1[line]*cos(Sensor.data$FLAS[line]*pi/180)-
                            Sensor.data$Ftl2[line]*cos(Sensor.data$FLAS[line]*pi/180)+
                            Sensor.data$DFy[line]+WtPlt-Sensor.data$JD[line]-
                            Sensor.data$Fpwy[line]
  }
}


#---------------Calculate Configuration 1 Forces -----------------------------
```

```
for (line in 1:length(Sensor.data[,1])){
  temp.table<-subset(Baseline.data,plot==Sensor.data[line,1]) # creates temporary table to
      pull baseline data
  if(is.na(Sensor.data$time[line])==T){
  Sensor.data$Fddy[line]<-NA
  Sensor.data$Fcty[line]<-NA
}
  else if(Sensor.data$config[line]==1){
  ang<-Sensor.data$FLAS[line]*pi/180
  Sensor.data$Fddy[line]<-(Sensor.data$Ftl1[line]*(20.16*sin(ang)+
                          14.31*cos(ang))+Sensor.data$Ftl2[line]*
                          (12.16*sin(ang)+14.31*cos(ang))-
                          Sensor.data$DFy[line]*14.31-WtPlt*(14.31+5.89)+
                          Sensor.data$JD[line]*(14.31+Sensor.data$GWx[line])+
                          Sensor.data$Fpwy[line]*(14.31+Sensor.data$PWx[line])+
                          abs(Sensor.data$Total_DR[line]-temp.table$Base_Total_DR)*
                          (abs(Sensor.data$GWy[line])+R1y-20.16))/-(14.31+5.31)

  Sensor.data$Fcty[line]<--Sensor.data$Ftl1[line]*cos(ang)-
                          Sensor.data$Ftl2[line]*cos(ang)+
                          Sensor.data$DFy[line]+WtPlt-Sensor.data$Fddy[line]-
                          Sensor.data$JD[line]-Sensor.data$Fpwy[line]
  }
}

# Remove temporary variables
rm(temp.table); rm(ang)

# ----------------Soil Table---------------------------------------
#
# Create Fd data (Running - baseline of Total_DR)
Sensor.data<-within(Sensor.data,Fd<-as.numeric(NA))
for (line in 1:length(Sensor.data[,1])){
  Baseline.DR<-subset(Baseline.data,Baseline.data$plot==Sensor.data$plot[line])

  if (is.na(Sensor.data$time[line])==T){
    Sensor.data$Fd[line]<-NA
  }
  else {
    Sensor.data$Fd[line]<--(Sensor.data$Total_DR[line]-Baseline.DR$Base_Total_DR)
  }
```

```
}

# Remove Baseline.DR
rm(Baseline.DR)

# Aggretate fundtion of Sensor.data to produce Soil.Table
colnames(Sensor.data)
Soil.Table<-aggregate(list(Sensor.data$FLAS,Sensor.data$GWAS,Sensor.data$DFy,Sensor.data$Fd,
                      Sensor.data$JD),list(Sensor.data$plot),
                      mean,na.rm=T)
# Asign column names
colnames(Soil.Table)<-c("plot", "FLAS","GWAS", "DFy", "Fd", "JD")

# Merge Soil.Table with Config Table
Soil.Table<-merge(Soil.Table,Config.table,by="plot",all=T)
# Reorder Soil.Table and remove 2 unneeded columns
Soil.Table<-Soil.Table[,c(1,7:9,2:6)]

# Merge Soil.Table and averages from Hand.data
# Add columns to Soil.Table
Soil.Table<-merge(Soil.Table,Hand.data[,c(1,35:37)],by="plot",all = T)

# Reset colunm names
colnames(Soil.Table)[10:12]<-c("PD.ref","PRD.ref","GRD")
# Add colunms for PD referencing GW rut and PRD referencing GW rut
Soil.Table<-within(Soil.Table,PD.GRD<-as.numeric(NA)) # Planting depth referencing GW rut depth
Soil.Table<-within(Soil.Table,PRD.GRD<-as.numeric(NA)) # Pres wheel rut depth referncing GW rut depth

# Calculate PD.GRD and PRD.GRD
for (line in 1:length(Soil.Table[,1])){
  Soil.Table$PD.GRD[line]<-Soil.Table$PD.ref[line]-Soil.Table$GRD[line]
  Soil.Table$PRD.GRD[line]<-Soil.Table$PRD.ref[line]-Soil.Table$GRD[line]
}

# Remove treatment 1506 from Soil.Table
Soil.Table<-Soil.Table[-46,]
# Renumber rows in Soil.Table
rownames(Soil.Table)<-1:length(Soil.Table[,1])
```

```r
# Remove treatment 1506 from Hand.data
Hand.data<-Hand.data[-46,]
# Renumber rows in Hand.data
rownames(Hand.data)<-1:length(Hand.data[,1])


# list of plots run on 7/9/15
SM.list1<-c(1410,1209,1108,1508,1507,1406,1106,1104,1101,1403,
            1505,1301,1102,1202,1203,1404,1504,1305,1306,1307,
            1408,1310,1210,1110)
# list of plots run on 7/10/15
SM.list2<-c(1309,1409,1208,1207,1407,1206,1405,1503,1103,1204,
            1201,1401,1501,1502,1402,1302,1303,1304,1205,1105,
            1107,1308,1109,1509)

# Pulls Soil Moisture value for the day that the plot was run for Soil.Table
for (line in 1:length(Soil.Table[,1])){
  temp.table<-subset(Hand.data,Hand.data$plot==Soil.Table$plot[line])
  if((Soil.Table$plot[line] %in% SM.list1)==T){
    Soil.Table$SM[line]<-temp.table$SM_7_9_15
  }
  else if((Soil.Table$plot[line] %in% SM.list2)==T){
    Soil.Table$SM[line]<-temp.table$SM_7_10_15
  }
  else {
    Soil.Table$SM[line]<-NA
  }
}

# Remove temp.table, and SM list
rm(temp.table); rm(SM.list1); rm(SM.list2)

## Create Std. Dev. soil table
# Aggretate fundtion of Sensor.data to produce Soil.Table.sd
colnames(Sensor.data)
Soil.Table.sd<-aggregate(list(Sensor.data$FLAS,Sensor.data$DFy,Sensor.data$Fd,
                              Sensor.data$JD),list(Sensor.data$plot),
                         sd,na.rm=T)
# Asign column names
colnames(Soil.Table.sd)<-c("plot", "FLAS.sd", "DFy.sd", "Fd.sd", "JD.sd")
```

```
# Calculate the Std. Dev. of PD, PRD, and GRD for Soil.Table.sd
for (line in 1:length(Soil.Table.sd[,1])){
    Soil.Table.sd$PD.ref.sd[line]<-sd(Hand.data[Hand.data$plot==Soil.Table.sd$plot[line],5:9],na.rm = T)
    Soil.Table.sd$PRD.ref.sd[line]<-sd(Hand.data[Hand.data$plot==Soil.Table.sd$plot[line],10:14],na.rm = T)
    Soil.Table.sd$GRD.sd[line]<-sd(Hand.data[Hand.data$plot==Soil.Table.sd$plot[line],15:19],na.rm = T)
}
# Merge meads and std. dev. tables
Soil.Table<-merge(Soil.Table,Soil.Table.sd,by="plot",all = T)

# Export Soil.Table to csv
#write.csv(Soil.Table,"Soil.Table.csv")

# Remove Soil.Table.sd
rm(Soil.Table.sd)

# Replace values in every column of plot 1102 with NA
Soil.Table[2,c(5:22)]<-NA

# Change Config, Plant_depth, and Rep to factors
Soil.Table<-within(Soil.Table,config<-factor(config))
Soil.Table<-within(Soil.Table,plant_depth<-factor(plant_depth))
Soil.Table<-within(Soil.Table,rep<-factor(rep))

#-------------- Mixed model anaylsis of Soil.Table-------------------
# Blank data frame that will be used for comparison later
blank<-data.frame("n1"=as.numeric(),"n2"=as.numeric(),"n3"=as.numeric(),
                  "n4"=as.numeric(),"n5"=as.numeric(),"n6"=as.numeric(),
                  "n7"=as.numeric(),"n8"=as.numeric(),"n9"=as.numeric(),
                  "n10"=as.numeric(),"n11"=as.numeric(),"n12"=as.numeric(),
                  "n13"=as.numeric(),"n14"=as.numeric(),"n15"=as.numeric(),
                  "n16"=as.numeric(),"n17"=as.numeric(),"n18"=as.numeric(),
                  "n19"=as.numeric())

## Model Fd
Model.Fd<-lmer(Fd~config*plant_depth+(1|rep),data = Soil.Table)
anova(Model.Fd)
# Calculate lsmeans table
```

```
lsmeans.Fd <- lsmeans(Model.Fd)
# Produce data frame from first table of lsmeans
lsmeans.Fd <- as.data.frame(lsmeans.Fd[1])
# Rename columns
colnames(lsmeans.Fd)<-c("config","plant_depth","Estimate","SE","DF","t.val",
                         "LCI","UCI","p.val")
# Merge Lsmeans with Blank data frame
lsmeans.Fd<-merge(lsmeans.Fd,blank,by = 0,all = T)
# Order data frame by decending UCI
#lsmeans.Fd<-lsmeans.Fd[order(-lsmeans.Fd$UCI),]
# Renumber row names
#rownames(lsmeans.Fd)<-1:length(lsmeans.Fd[,1])

# Treatemnt comparisons loop
for (k in 1:length(lsmeans.Fd[,1])){
  for (i in 1:length(lsmeans.Fd[,1])){
    if ((lsmeans.Fd[i,8]>=lsmeans.Fd[k,8] & lsmeans.Fd[i,8]<=lsmeans.Fd[k,9])||
        (lsmeans.Fd[i,9]>=lsmeans.Fd[k,8] & lsmeans.Fd[i,9]<=lsmeans.Fd[k,9])) {
      lsmeans.Fd[i,(k+10)]<-k
    } else{
      lsmeans.Fd[i,(k+10)]<-999
    }
  }
}
# Export lsmeans csv
#write.csv(lsmeans.Fd,"lsmeans.Fd.csv")

## Model JD
Model.JD<-lmer(JD~config*plant_depth+(1|rep),data = Soil.Table)
anova(Model.JD)
# Calculate lsmeans table
lsmeans.JD <- lsmeans(Model.JD)
# Produce data frame from first table of lsmeans
lsmeans.JD <- as.data.frame(lsmeans.JD[1])
# Rename columns
colnames(lsmeans.JD)<-c("config","plant_depth","Estimate","SE","DF","t.val",
                        "LCI","UCI","p.val")
# Merge Lsmeans with Blank data frame
lsmeans.JD<-merge(lsmeans.JD,blank,by = 0,all = T)
# Order data frame by decending UCI
#lsmeans.JD<-lsmeans.JD[order(-lsmeans.JD$UCI),]
```

```
# Renumber row names
#rownames(lsmeans.JD)<-1:length(lsmeans.JD[,1])

# Treatemnt comparisons loop
for (k in 1:length(lsmeans.JD[,1])){
  for (i in 1:length(lsmeans.JD[,1])){
    if ((lsmeans.JD[i,8]>=lsmeans.JD[k,8] & lsmeans.JD[i,8]<=lsmeans.JD[k,9])||
        (lsmeans.JD[i,9]>=lsmeans.JD[k,8] & lsmeans.JD[i,9]<=lsmeans.JD[k,9])) {
      lsmeans.JD[i,(k+10)]<-k
    } else{
      lsmeans.JD[i,(k+10)]<-999
    }
  }
}
# Export lsmeans csv
#write.csv(lsmeans.JD,"lsmeans.JD.csv")

## Model PD.ref
Model.PD.ref<-lmer(PD.ref~config*plant_depth+(1|rep),data = Soil.Table)
anova(Model.PD.ref)
# Calculate lsmeans table
lsmeans.PD.ref <- lsmeans(Model.PD.ref)
# Produce data frame from first table of lsmeans
lsmeans.PD.ref <- as.data.frame(lsmeans.PD.ref[1])
# Rename columns
colnames(lsmeans.PD.ref)<-c("config","plant_depth","Estimate","SE","DF","t.val",
                        "LCI","UCI","p.val")
# Merge Lsmeans with Blank data frame
lsmeans.PD.ref<-merge(lsmeans.PD.ref,blank,by = 0,all = T)
# Order data frame by decending UCI
#lsmeans.PD.ref<-lsmeans.PD.ref[order(-lsmeans.PD.ref$UCI),]
# Renumber row names
#rownames(lsmeans.PD.ref)<-1:length(lsmeans.PD.ref[,1])

# Treatemnt comparisons loop
for (k in 1:length(lsmeans.PD.ref[,1])){
  for (i in 1:length(lsmeans.PD.ref[,1])){
    if ((lsmeans.PD.ref[i,8]>=lsmeans.PD.ref[k,8] & lsmeans.PD.ref[i,8]<=lsmeans.PD.ref[k
        ,9])||
        (lsmeans.PD.ref[i,9]>=lsmeans.PD.ref[k,8] & lsmeans.PD.ref[i,9]<=lsmeans.PD.ref[k
            ,9])) {
```

```
      lsmeans.PD.ref[i,(k+10)]<-k
    } else{
      lsmeans.PD.ref[i,(k+10)]<-999
    }
  }
}
# Export lsmeans csv
#write.csv(lsmeans.PD.ref,"lsmeans.PD.ref.csv")

## Model PD.GRD
Model.PD.GRD<-lmer(PD.GRD~config*plant_depth+(1|rep),data = Soil.Table)
anova(Model.PD.GRD)
# Calculate lsmeans table
lsmeans.PD.GRD <- lsmeans(Model.PD.GRD)
# Produce data frame from first table of lsmeans
lsmeans.PD.GRD <- as.data.frame(lsmeans.PD.GRD[1])
# Rename columns
colnames(lsmeans.PD.GRD)<-c("config","plant_depth","Estimate","SE","DF","t.val",
                            "LCI","UCI","p.val")
# Merge Lsmeans with Blank data frame
lsmeans.PD.GRD<-merge(lsmeans.PD.GRD,blank,by = 0,all = T)

# Treatemnt comparisons loop
for (k in 1:length(lsmeans.PD.GRD[,1])){
  for (i in 1:length(lsmeans.PD.GRD[,1])){
    if ((lsmeans.PD.GRD[i,8]>=lsmeans.PD.GRD[k,8] & lsmeans.PD.GRD[i,8]<=lsmeans.PD.GRD[k
        ,9])||
        (lsmeans.PD.GRD[i,9]>=lsmeans.PD.GRD[k,8] & lsmeans.PD.GRD[i,9]<=lsmeans.PD.GRD[k
            ,9])) {
      lsmeans.PD.GRD[i,(k+10)]<-k
    } else{
      lsmeans.PD.GRD[i,(k+10)]<-999
    }
  }
}
# Export lsmeans csv
write.csv(lsmeans.PD.GRD,"lsmeans.PD.GRD.csv")

# Model GRD
Model.GRD<-lmer(GRD~config*plant_depth+(1|rep),data = Soil.Table)
anova(Model.GRD)
```

```
# Calculate lsmeans table
lsmeans.GRD <- lsmeans(Model.GRD)
# Produce data frame from first table of lsmeans
lsmeans.GRD <- as.data.frame(lsmeans.GRD[1])
# Rename columns
colnames(lsmeans.GRD)<-c("config","plant_depth","Estimate","SE","DF","t.val",
                        "LCI","UCI","p.val")
# Merge Lsmeans with Blank data frame
lsmeans.GRD<-merge(lsmeans.GRD,blank,by = 0,all = T)
# Order data frame by decending UCI
#lsmeans.GRD<-lsmeans.GRD[order(-lsmeans.GRD$UCI),]
# Renumber row names
#rownames(lsmeans.GRD)<-1:length(lsmeans.GRD[,1])

# Treatemnt comparisons loop
for (k in 1:length(lsmeans.GRD[,1])){
  for (i in 1:length(lsmeans.GRD[,1])){
    if ((lsmeans.GRD[i,8]>=lsmeans.GRD[k,8] & lsmeans.GRD[i,8]<=lsmeans.GRD[k,9])||
        (lsmeans.GRD[i,9]>=lsmeans.GRD[k,8] & lsmeans.GRD[i,9]<=lsmeans.GRD[k,9])) {
      lsmeans.GRD[i,(k+10)]<-k
    } else{
      lsmeans.GRD[i,(k+10)]<-999
    }
  }
}
# Export lsmeans csv
#write.csv(lsmeans.GRD,"lsmeans.GRD.csv")

## Model PRD.ref
Model.PRD.ref<-lmer(PRD.ref~config*plant_depth+(1|rep),data = Soil.Table)
anova(Model.PRD.ref)
# Calculate lsmeans table
lsmeans.PRD.ref <- lsmeans(Model.PRD.ref)
# Produce data frame from first table of lsmeans
lsmeans.PRD.ref <- as.data.frame(lsmeans.PRD.ref[1])
# Rename columns
colnames(lsmeans.PRD.ref)<-c("config","plant_depth","Estimate","SE","DF","t.val",
                        "LCI","UCI","p.val")
# Merge Lsmeans with Blank data frame
lsmeans.PRD.ref<-merge(lsmeans.PRD.ref,blank,by = 0,all = T)
# Order data frame by decending UCI
```

```
#lsmeans.PRD.ref<-lsmeans.PRD.ref[order(-lsmeans.PRD.ref$UCI),]
# Renumber row names
#rownames(lsmeans.PRD.ref)<-1:length(lsmeans.PRD.ref[,1])

# Treatemnt comparisons loop
for (k in 1:length(lsmeans.PRD.ref[,1])){
  for (i in 1:length(lsmeans.PRD.ref[,1])){
    if ((lsmeans.PRD.ref[i,8]>=lsmeans.PRD.ref[k,8] & lsmeans.PRD.ref[i,8]<=lsmeans.PRD.ref[
        k,9])||
        (lsmeans.PRD.ref[i,9]>=lsmeans.PRD.ref[k,8] & lsmeans.PRD.ref[i,9]<=lsmeans.PRD.ref[
            k,9])) {
      lsmeans.PRD.ref[i,(k+10)]<-k
    } else{
      lsmeans.PRD.ref[i,(k+10)]<-999
    }
  }
}
# Export lsmeans csv
#write.csv(lsmeans.PRD.ref,"lsmeans.PRD.ref.csv")

## Model PRD.GRD
Model.PRD.GRD<-lmer(PRD.GRD~config*plant_depth+(1|rep),data = Soil.Table)
anova(Model.PRD.GRD)
# Calculate lsmeans table
lsmeans.PRD.GRD <- lsmeans(Model.PRD.GRD)
# Produce data frame from first table of lsmeans
lsmeans.PRD.GRD <- as.data.frame(lsmeans.PRD.GRD[1])
# Rename columns
colnames(lsmeans.PRD.GRD)<-c("config","plant_depth","Estimate","SE","DF","t.val",
                              "LCI","UCI","p.val")
# Merge Lsmeans with Blank data frame
lsmeans.PRD.GRD<-merge(lsmeans.PRD.GRD,blank,by = 0,all = T)

# Treatemnt comparisons loop
for (k in 1:length(lsmeans.PRD.GRD[,1])){
  for (i in 1:length(lsmeans.PRD.GRD[,1])){
    if ((lsmeans.PRD.GRD[i,8]>=lsmeans.PRD.GRD[k,8] & lsmeans.PRD.GRD[i,8]<=lsmeans.PRD.GRD[
        k,9])||
        (lsmeans.PRD.GRD[i,9]>=lsmeans.PRD.GRD[k,8] & lsmeans.PRD.GRD[i,9]<=lsmeans.PRD.GRD[
            k,9])) {
      lsmeans.PRD.GRD[i,(k+10)]<-k
```

```
    } else{
      lsmeans.PRD.GRD[i,(k+10)]<-999
    }
  }
}
# Export lsmeans csv
#write.csv(lsmeans.PRD.GRD,"lsmeans.PRD.GRD.csv")

## Model FLAS
Model.FLAS<-lmer(FLAS~config*plant_depth+(1|rep),data = Soil.Table)
anova(Model.FLAS)
# Calculate lsmeans table
lsmeans.FLAS <- lsmeans(Model.FLAS)
# Produce data frame from first table of lsmeans
lsmeans.FLAS <- as.data.frame(lsmeans.FLAS[1])
# Rename columns
colnames(lsmeans.FLAS)<-c("config","plant_depth","Estimate","SE","DF","t.val",
                        "LCI","UCI","p.val")
# Merge Lsmeans with Blank data frame
lsmeans.FLAS<-merge(lsmeans.FLAS,blank,by = 0,all = T)
# Order data frame by decending UCI
#lsmeans.FLAS<-lsmeans.FLAS[order(-lsmeans.FLAS$UCI),]
# Renumber row names
#rownames(lsmeans.FLAS)<-1:length(lsmeans.FLAS[,1])

# Treatemnt comparisons loop
for (k in 1:length(lsmeans.FLAS[,1])){
  for (i in 1:length(lsmeans.FLAS[,1])){
    if ((lsmeans.FLAS[i,8]>=lsmeans.FLAS[k,8] & lsmeans.FLAS[i,8]<=lsmeans.FLAS[k,9])||
        (lsmeans.FLAS[i,9]>=lsmeans.FLAS[k,8] & lsmeans.FLAS[i,9]<=lsmeans.FLAS[k,9])) {
      lsmeans.FLAS[i,(k+10)]<-k
    } else{
      lsmeans.FLAS[i,(k+10)]<-999
    }
  }
}
# Export lsmeans csv
#write.csv(lsmeans.FLAS,"lsmeans.FLAS.csv")

## Model SM
Model.SM<-lmer(SM~config*plant_depth+(1|rep),data = Soil.Table)
```

```
anova(Model.SM)
# Calculate lsmeans table
lsmeans.SM <- lsmeans(Model.SM)
# Produce data frame from first table of lsmeans
lsmeans.SM <- as.data.frame(lsmeans.SM[1])
# Rename columns
colnames(lsmeans.SM)<-c("config","plant_depth","Estimate","SE","DF","t.val",
                        "LCI","UCI","p.val")
# Merge Lsmeans with Blank data frame
lsmeans.SM<-merge(lsmeans.SM,blank,by = 0,all = T)
# Order data frame by decending UCI
#lsmeans.SM<-lsmeans.SM[order(-lsmeans.SM$UCI),]
# Renumber row names
#rownames(lsmeans.SM)<-1:length(lsmeans.SM[,1])

# Treatemnt comparisons loop
for (k in 1:length(lsmeans.SM[,1])){
  for (i in 1:length(lsmeans.SM[,1])){
    if ((lsmeans.SM[i,8]>=lsmeans.SM[k,8] & lsmeans.SM[i,8]<=lsmeans.SM[k,9])||
        (lsmeans.SM[i,9]>=lsmeans.SM[k,8] & lsmeans.SM[i,9]<=lsmeans.SM[k,9])) {
      lsmeans.SM[i,(k+10)]<-k
    } else{
      lsmeans.SM[i,(k+10)]<-999
    }
  }
}
# Export lsmeans csv
#write.csv(lsmeans.SM,"lsmeans.SM.csv")

## Model DFy
Model.DFy<-lmer(DFy~config*plant_depth+(1|rep),data = Soil.Table)
anova(Model.DFy)
# Calculate lsmeans table
lsmeans.DFy <- lsmeans(Model.DFy)
# Produce data frame from first table of lsmeans
lsmeans.DFy <- as.data.frame(lsmeans.DFy[1])
# Rename columns
colnames(lsmeans.DFy)<-c("config","plant_depth","Estimate","SE","DF","t.val",
                         "LCI","UCI","p.val")
# Merge Lsmeans with Blank data frame
lsmeans.DFy<-merge(lsmeans.DFy,blank,by = 0,all = T)
```

```r
# Order data frame by decending UCI
#lsmeans.DFy<-lsmeans.DFy[order(-lsmeans.DFy$UCI),]
# Renumber row names
#rownames(lsmeans.DFy)<-1:length(lsmeans.DFy[,1])

# Treatemnt comparisons loop
for (k in 1:length(lsmeans.DFy[,1])){
  for (i in 1:length(lsmeans.DFy[,1])){
    if ((lsmeans.DFy[i,8]>=lsmeans.DFy[k,8] & lsmeans.DFy[i,8]<=lsmeans.DFy[k,9])||
        (lsmeans.DFy[i,9]>=lsmeans.DFy[k,8] & lsmeans.DFy[i,9]<=lsmeans.DFy[k,9])) {
      lsmeans.DFy[i,(k+10)]<-k
    } else{
      lsmeans.DFy[i,(k+10)]<-999
    }
  }
}
# Export lsmeans csv
#write.csv(lsmeans.DFy,"lsmeans.DFy.csv")


## --------Mixed effect models of Standard Deviation of variables-----

## Model Fd.sd
Model.Fd.sd<-lmer(Fd.sd~config*plant_depth+(1|rep),data = Soil.Table)
anova(Model.Fd.sd)
# Calculate lsmeans table
lsmeans.Fd.sd <- lsmeans(Model.Fd.sd)
# Produce data frame from first table of lsmeans
lsmeans.Fd.sd <- as.data.frame(lsmeans.Fd.sd[1])
# Rename columns
colnames(lsmeans.Fd.sd)<-c("config","plant_depth","Estimate","SE","DF","t.val",
                        "LCI","UCI","p.val")
# Merge Lsmeans with Blank data frame
lsmeans.Fd.sd<-merge(lsmeans.Fd.sd,blank,by = 0,all = T)

# Treatemnt comparisons loop
for (k in 1:length(lsmeans.Fd.sd[,1])){
  for (i in 1:length(lsmeans.Fd.sd[,1])){
    if ((lsmeans.Fd.sd[i,8]>=lsmeans.Fd.sd[k,8] & lsmeans.Fd.sd[i,8]<=lsmeans.Fd.sd[k,9])||
        (lsmeans.Fd.sd[i,9]>=lsmeans.Fd.sd[k,8] & lsmeans.Fd.sd[i,9]<=lsmeans.Fd.sd[k,9])) {
      lsmeans.Fd.sd[i,(k+10)]<-k
```

```
    } else{
      lsmeans.Fd.sd[i,(k+10)]<-999
    }
  }
}
# Export lsmeans csv
#write.csv(lsmeans.Fd.sd,"lsmeans.Fd.sd.csv")

## Model JD.sd
Model.JD.sd<-lmer(JD.sd~config*plant_depth+(1|rep),data = Soil.Table)
anova(Model.JD.sd)
# Calculate lsmeans table
lsmeans.JD.sd <- lsmeans(Model.JD.sd)
# Produce data frame from first table of lsmeans
lsmeans.JD.sd <- as.data.frame(lsmeans.JD.sd[1])
# Rename columns
colnames(lsmeans.JD.sd)<-c("config","plant_depth","Estimate","SE","DF","t.val",
                        "LCI","UCI","p.val")
# Merge Lsmeans with Blank data frame
lsmeans.JD.sd<-merge(lsmeans.JD.sd,blank,by = 0,all = T)

# Treatemnt comparisons loop
for (k in 1:length(lsmeans.JD.sd[,1])){
  for (i in 1:length(lsmeans.JD.sd[,1])){
    if ((lsmeans.JD.sd[i,8]>=lsmeans.JD.sd[k,8] & lsmeans.JD.sd[i,8]<=lsmeans.JD.sd[k,9])||
        (lsmeans.JD.sd[i,9]>=lsmeans.JD.sd[k,8] & lsmeans.JD.sd[i,9]<=lsmeans.JD.sd[k,9])) {
      lsmeans.JD.sd[i,(k+10)]<-k
    } else{
      lsmeans.JD.sd[i,(k+10)]<-999
    }
  }
}
# Export lsmeans csv
#write.csv(lsmeans.JD.sd,"lsmeans.JD.sd.csv")

## Model PD.ref.sd
Model.PD.ref.sd<-lmer(PD.ref.sd~config*plant_depth+(1|rep),data = Soil.Table)
anova(Model.PD.ref.sd)
# Calculate lsmeans table
lsmeans.PD.ref.sd <- lsmeans(Model.PD.ref.sd)
# Produce data frame from first table of lsmeans
```

```
lsmeans.PD.ref.sd <- as.data.frame(lsmeans.PD.ref.sd[1])
# Rename columns
colnames(lsmeans.PD.ref.sd)<-c("config","plant_depth","Estimate","SE","DF","t.val",
                            "LCI","UCI","p.val")
# Merge Lsmeans with Blank data frame
lsmeans.PD.ref.sd<-merge(lsmeans.PD.ref.sd,blank,by = 0,all = T)

# Treatemnt comparisons loop
for (k in 1:length(lsmeans.PD.ref.sd[,1])){
  for (i in 1:length(lsmeans.PD.ref.sd[,1])){
    if ((lsmeans.PD.ref.sd[i,8]>=lsmeans.PD.ref.sd[k,8] & lsmeans.PD.ref.sd[i,8]<=lsmeans.PD
        .ref.sd[k,9])||
        (lsmeans.PD.ref.sd[i,9]>=lsmeans.PD.ref.sd[k,8] & lsmeans.PD.ref.sd[i,9]<=lsmeans.PD
            .ref.sd[k,9])) {
      lsmeans.PD.ref.sd[i,(k+10)]<-k
    } else{
      lsmeans.PD.ref.sd[i,(k+10)]<-999
    }
  }
}
# Export lsmeans csv
#write.csv(lsmeans.PD.ref.sd,"lsmeans.PD.ref.sd.csv")

# Model GRD.sd
Model.GRD.sd<-lmer(GRD.sd~config*plant_depth+(1|rep),data = Soil.Table)
anova(Model.GRD.sd)
# Calculate lsmeans table
lsmeans.GRD.sd <- lsmeans(Model.GRD.sd)
# Produce data frame from first table of lsmeans
lsmeans.GRD.sd <- as.data.frame(lsmeans.GRD.sd[1])
# Rename columns
colnames(lsmeans.GRD.sd)<-c("config","plant_depth","Estimate","SE","DF","t.val",
                         "LCI","UCI","p.val")
# Merge Lsmeans with Blank data frame
lsmeans.GRD.sd<-merge(lsmeans.GRD.sd,blank,by = 0,all = T)

# Treatemnt comparisons loop
for (k in 1:length(lsmeans.GRD.sd[,1])){
  for (i in 1:length(lsmeans.GRD.sd[,1])){
    if ((lsmeans.GRD.sd[i,8]>=lsmeans.GRD.sd[k,8] & lsmeans.GRD.sd[i,8]<=lsmeans.GRD.sd[k
        ,9])||
```

```
        (lsmeans.GRD.sd[i,9]>=lsmeans.GRD.sd[k,8] & lsmeans.GRD.sd[i,9]<=lsmeans.GRD.sd[k
            ,9])) {
      lsmeans.GRD.sd[i,(k+10)]<-k
    } else{
      lsmeans.GRD.sd[i,(k+10)]<-999
    }
  }
}
# Export lsmeans csv
#write.csv(lsmeans.GRD.sd,"lsmeans.GRD.sd.csv")

## Model PRD.ref.sd
Model.PRD.ref.sd<-lmer(PRD.ref.sd~config*plant_depth+(1|rep),data = Soil.Table)
anova(Model.PRD.ref.sd)
# Calculate lsmeans table
lsmeans.PRD.ref.sd <- lsmeans(Model.PRD.ref.sd)
# Produce data frame from first table of lsmeans
lsmeans.PRD.ref.sd <- as.data.frame(lsmeans.PRD.ref.sd[1])
# Rename columns
colnames(lsmeans.PRD.ref.sd)<-c("config","plant_depth","Estimate","SE","DF","t.val",
                             "LCI","UCI","p.val")
# Merge Lsmeans with Blank data frame
lsmeans.PRD.ref.sd<-merge(lsmeans.PRD.ref.sd,blank,by = 0,all = T)

# Treatemnt comparisons loop
for (k in 1:length(lsmeans.PRD.ref.sd[,1])){
  for (i in 1:length(lsmeans.PRD.ref.sd[,1])){
    if ((lsmeans.PRD.ref.sd[i,8]>=lsmeans.PRD.ref.sd[k,8] & lsmeans.PRD.ref.sd[i,8]<=lsmeans
        .PRD.ref.sd[k,9])||
        (lsmeans.PRD.ref.sd[i,9]>=lsmeans.PRD.ref.sd[k,8] & lsmeans.PRD.ref.sd[i,9]<=lsmeans
            .PRD.ref.sd[k,9])) {
      lsmeans.PRD.ref.sd[i,(k+10)]<-k
    } else{
      lsmeans.PRD.ref.sd[i,(k+10)]<-999
    }
  }
}
# Export lsmeans csv
#write.csv(lsmeans.PRD.ref.sd,"lsmeans.PRD.ref.sd.csv")

## Model FLAS.sd
```

```
Model.FLAS.sd<-lmer(FLAS.sd~config*plant_depth+(1|rep),data = Soil.Table)
anova(Model.FLAS.sd)
# Calculate lsmeans table
lsmeans.FLAS.sd <- lsmeans(Model.FLAS.sd)
# Produce data frame from first table of lsmeans
lsmeans.FLAS.sd <- as.data.frame(lsmeans.FLAS.sd[1])
# Rename columns
colnames(lsmeans.FLAS.sd)<-c("config","plant_depth","Estimate","SE","DF","t.val",
                          "LCI","UCI","p.val")
# Merge Lsmeans with Blank data frame
lsmeans.FLAS.sd<-merge(lsmeans.FLAS.sd,blank,by = 0,all = T)

# Treatemnt comparisons loop
for (k in 1:length(lsmeans.FLAS.sd[,1])){
  for (i in 1:length(lsmeans.FLAS.sd[,1])){
    if ((lsmeans.FLAS.sd[i,8]>=lsmeans.FLAS.sd[k,8] & lsmeans.FLAS.sd[i,8]<=lsmeans.FLAS.sd[
        k,9])||
        (lsmeans.FLAS.sd[i,9]>=lsmeans.FLAS.sd[k,8] & lsmeans.FLAS.sd[i,9]<=lsmeans.FLAS.sd[
            k,9])) {
      lsmeans.FLAS.sd[i,(k+10)]<-k
    } else{
      lsmeans.FLAS.sd[i,(k+10)]<-999
    }
  }
}
# Export lsmeans csv
#write.csv(lsmeans.FLAS.sd,"lsmeans.FLAS.sd.csv")

## Model DFy.sd
Model.DFy.sd<-lmer(DFy.sd~config*plant_depth+(1|rep),data = Soil.Table)
anova(Model.DFy.sd)
# Calculate lsmeans table
lsmeans.DFy.sd <- lsmeans(Model.DFy.sd)
# Produce data frame from first table of lsmeans
lsmeans.DFy.sd <- as.data.frame(lsmeans.DFy.sd[1])
# Rename columns
colnames(lsmeans.DFy.sd)<-c("config","plant_depth","Estimate","SE","DF","t.val",
                         "LCI","UCI","p.val")
# Merge Lsmeans with Blank data frame
lsmeans.DFy.sd<-merge(lsmeans.DFy.sd,blank,by = 0,all = T)

```

```
# Treatemnt comparisons loop
for (k in 1:length(lsmeans.DFy.sd[,1])){
  for (i in 1:length(lsmeans.DFy.sd[,1])){
    if ((lsmeans.DFy.sd[i,8]>=lsmeans.DFy.sd[k,8] & lsmeans.DFy.sd[i,8]<=lsmeans.DFy.sd[k
        ,9])||
        (lsmeans.DFy.sd[i,9]>=lsmeans.DFy.sd[k,8] & lsmeans.DFy.sd[i,9]<=lsmeans.DFy.sd[k
            ,9])) {
      lsmeans.DFy.sd[i,(k+10)]<-k
    } else{
      lsmeans.DFy.sd[i,(k+10)]<-999
    }
  }
}
# Export lsmeans csv
#write.csv(lsmeans.DFy.sd,"lsmeans.DFy.sd.csv")


## ---------Create Regression model for soil effects---------------
# Create subset of Soil.Table to include only config 1 & 2
Soil.Table2<-subset(Soil.Table,Soil.Table$config==1 | Soil.Table$config==2)
#Soil.Table2<-subset(Soil.Table,Soil.Table$config==1)

# Change Plot, Config, and Plant_Depth to factors
Soil.Table2<-within(Soil.Table2,plot<-factor(plot))
Soil.Table2<-within(Soil.Table2,config<-factor(config))
Soil.Table2<-within(Soil.Table2,plant_depth<-factor(plant_depth))

## Linear regression for configurations 1 & 2
# PD.ref regression
PD.ref.Reg<-lm( PD.ref~GWAS+PRD.ref,
         data=Soil.Table2)

summary(PD.ref.Reg)
plot(PD.ref.Reg)
anova(PD.ref.Reg)

# Fd regression
Fd.Reg<-lm(Fd~GWAS+JD,
           data = Soil.Table2)

summary(Fd.Reg)
```

```r
anova(Fd.Reg)
plot(Fd.Reg)

# JD regression
JD.Reg<-lm(JD~GWAS+config+FLAS+Fd,
           data = Soil.Table2)

summary(JD.Reg)
anova(JD.Reg)
plot(JD.Reg)

# GRD regression
GRD.Reg<-lm(GRD~GWAS+JD,
           data = Soil.Table2)

summary(GRD.Reg)
anova(GRD.Reg)
plot(GRD.Reg)


# PDgrd regression
PDgrd.Reg<-lm(PD.GRD~GWAS+PRD.GRD,
              data=Soil.Table2)

summary(PDgrd.Reg)
anaova(PDgrd.Reg)
plot(PDgrd.Reg)


#-------------Force Table--------------------------------------
# Aggregrate function for forces on planter
Force.Table<-aggregate(list(Sensor.data$FLAS,Sensor.data$GWAS,Sensor.data$DFy,Sensor.data$Fd
    ,
                           Sensor.data$JD, Sensor.data$Fpwy, Sensor.data$Fddy,
                           Sensor.data$Fcty),
                       list(Sensor.data$plot),mean,na.rm=T)
# Asign column names
colnames(Force.Table)<-c("plot", "FLAS","GWAS", "DFy", "Fd", "JD", "Fpwy", "Fddy", "Fcty")
# Merge Force.Table with config.table
Force.Table<-merge(Force.Table,Config.table, by="plot", all = T)
# Reorder Force.Table and remove empty variables x & x.1
```

```r
Force.Table<-Force.Table[,c(1,10:12,2:9)]
# Replace values in every column of plot 1102 with NA
Force.Table[2,c(5:12)]<-NA

# Aggregrate function for Std. Deviation of forces on planter
Force.Table.SD <- aggregate(list(Sensor.data$Fpwy,Sensor.data$Fddy,
                                 Sensor.data$Fcty),
                            list(Sensor.data$plot),sd,na.rm=T)
# Asign colum names
colnames(Force.Table.SD) <- c("plot","Fpwy.sd","Fddy.sd","Fcty.sd")

# Merge Force.Table.SD with Force.Table
Force.Table <- merge(Force.Table,Force.Table.SD, by="plot", all = T)
# Remove Force.Table.SD
rm(Force.Table.SD)

## Loop to place NA in Fcty and Fddy of Config.1 treatments
for (line in 1:length(Force.Table[,1])){
  if (Force.Table$config[line]==1){
    Force.Table[line,c(11:12,14:15)]<-NA
  }
}

# Change Config, Plant_depth, and Rep to factors
Force.Table<-within(Force.Table,config<-factor(config))
Force.Table<-within(Force.Table,plant_depth<-factor(plant_depth))
Force.Table<-within(Force.Table,rep<-factor(rep))

# Create Force.Table3 containing configs 2 and 3
Force.Table3 <- subset(Force.Table,Force.Table$config==2 | Force.Table$config==3)
# Loop to calculate force distribution values
for (i in 1:length(Force.Table3[,1])){
  # total vertical force on components in contact with soil
  total.force <- sum(Force.Table3$Fddy[i],Force.Table3$JD[i],Force.Table3$Fpwy[i], na.rm = T)
  # New force percentage of total values
  Force.Table3$Fddy.dist[i] <- Force.Table3$Fddy[i]/total.force
  Force.Table3$JD.dist[i] <- Force.Table3$JD[i]/total.force
  Force.Table3$Fpwy.dist[i] <- Force.Table3$Fpwy[i]/total.force
}

```

```
#------------Mixed Model Analysis of Force Data----------------

## Model Fddy
Model.Fddy<-lmer(Fddy~config*plant_depth+(1|rep),data = Force.Table)
anova(Model.Fddy)
# Calculate lsmeans table
lsmeans.Fddy <- lsmeans(Model.Fddy)
# Produce data frame from first table of lsmeans
lsmeans.Fddy <- as.data.frame(lsmeans.Fddy[1])
# Rename columns
colnames(lsmeans.Fddy)<-c("config","plant_depth","Estimate","SE","DF","t.val",
                          "LCI","UCI","p.val")
# Merge Lsmeans with Blank data frame
lsmeans.Fddy<-merge(lsmeans.Fddy,blank,by = 0,all = T)

# Treatemnt comparisons loop
for (k in 1:length(lsmeans.Fddy[,1])){
  for (i in 1:length(lsmeans.Fddy[,1])){
    if ((lsmeans.Fddy[i,8]>=lsmeans.Fddy[k,8] & lsmeans.Fddy[i,8]<=lsmeans.Fddy[k,9])||
        (lsmeans.Fddy[i,9]>=lsmeans.Fddy[k,8] & lsmeans.Fddy[i,9]<=lsmeans.Fddy[k,9])) {
      lsmeans.Fddy[i,(k+10)]<-k
    } else{
      lsmeans.Fddy[i,(k+10)]<-999
    }
  }
}

## Model Fpwy
Model.Fpwy<-lmer(Fpwy~config*plant_depth+(1|rep),data = Force.Table)
anova(Model.Fpwy)
# Calculate lsmeans table
lsmeans.Fpwy <- lsmeans(Model.Fpwy)
# Produce data frame from first table of lsmeans
lsmeans.Fpwy <- as.data.frame(lsmeans.Fpwy[1])
# Rename columns
colnames(lsmeans.Fpwy)<-c("config","plant_depth","Estimate","SE","DF","t.val",
                          "LCI","UCI","p.val")
# Merge Lsmeans with Blank data frame
lsmeans.Fpwy<-merge(lsmeans.Fpwy,blank,by = 0,all = T)

```

```
# Treatemnt comparisons loop
for (k in 1:length(lsmeans.Fpwy[,1])){
  for (i in 1:length(lsmeans.Fpwy[,1])){
    if ((lsmeans.Fpwy[i,8]>=lsmeans.Fpwy[k,8] & lsmeans.Fpwy[i,8]<=lsmeans.Fpwy[k,9])||
        (lsmeans.Fpwy[i,9]>=lsmeans.Fpwy[k,8] & lsmeans.Fpwy[i,9]<=lsmeans.Fpwy[k,9])) {
      lsmeans.Fpwy[i,(k+10)]<-k
    } else{
      lsmeans.Fpwy[i,(k+10)]<-999
    }
  }
}

## Model Fddy.dist
Model.Fddy.dist<-lmer(Fddy.dist~config*plant_depth+(1|rep),data = Force.Table3)
anova(Model.Fddy.dist)
# Calculate lsmeans table
lsmeans.Fddy.dist <- lsmeans(Model.Fddy.dist)
# Produce data frame from first table of lsmeans
lsmeans.Fddy.dist <- as.data.frame(lsmeans.Fddy.dist[1])
# Rename columns
colnames(lsmeans.Fddy.dist)<-c("config","plant_depth","Estimate","SE","DF","t.val",
                          "LCI","UCI","p.val")
# Merge Lsmeans with Blank data frame
lsmeans.Fddy.dist<-merge(lsmeans.Fddy.dist,blank,by = 0,all = T)

# Treatemnt comparisons loop
for (k in 1:length(lsmeans.Fddy.dist[,1])){
  for (i in 1:length(lsmeans.Fddy.dist[,1])){
    if ((lsmeans.Fddy.dist[i,8]>=lsmeans.Fddy.dist[k,8] & lsmeans.Fddy.dist[i,8]<=lsmeans.
        Fddy.dist[k,9])||
        (lsmeans.Fddy.dist[i,9]>=lsmeans.Fddy.dist[k,8] & lsmeans.Fddy.dist[i,9]<=lsmeans.
            Fddy.dist[k,9])) {
      lsmeans.Fddy.dist[i,(k+10)]<-k
    } else{
      lsmeans.Fddy.dist[i,(k+10)]<-999
    }
  }
}

## Model JD.dist
Model.JD.dist<-lmer(JD.dist~config*plant_depth+(1|rep),data = Force.Table3)
```

```r
anova(Model.JD.dist)
# Calculate lsmeans table
lsmeans.JD.dist <- lsmeans(Model.JD.dist)
# Produce data frame from first table of lsmeans
lsmeans.JD.dist <- as.data.frame(lsmeans.JD.dist[1])
# Rename columns
colnames(lsmeans.JD.dist)<-c("config","plant_depth","Estimate","SE","DF","t.val",
                              "LCI","UCI","p.val")
# Merge Lsmeans with Blank data frame
lsmeans.JD.dist<-merge(lsmeans.JD.dist,blank,by = 0,all = T)

# Treatemnt comparisons loop
for (k in 1:length(lsmeans.JD.dist[,1])){
  for (i in 1:length(lsmeans.JD.dist[,1])){
    if ((lsmeans.JD.dist[i,8]>=lsmeans.JD.dist[k,8] & lsmeans.JD.dist[i,8]<=lsmeans.JD.dist[
        k,9])||
        (lsmeans.JD.dist[i,9]>=lsmeans.JD.dist[k,8] & lsmeans.JD.dist[i,9]<=lsmeans.JD.dist[
            k,9])) {
      lsmeans.JD.dist[i,(k+10)]<-k
    } else{
      lsmeans.JD.dist[i,(k+10)]<-999
    }
  }
}

## Model Fpwy.dist
Model.Fpwy.dist<-lmer(Fpwy.dist~plant_depth+(1|rep),data = Force.Table3)
anova(Model.Fpwy.dist)
# Calculate lsmeans table
lsmeans.Fpwy.dist <- lsmeans(Model.Fpwy.dist)
# Produce data frame from first table of lsmeans
lsmeans.Fpwy.dist <- as.data.frame(lsmeans.Fpwy.dist[1])
# Rename columns
colnames(lsmeans.Fpwy.dist)<-c("plant_depth","Estimate","SE","DF","t.val",
                              "LCI","UCI","p.val")
# Merge Lsmeans with Blank data frame
lsmeans.Fpwy.dist<-merge(lsmeans.Fpwy.dist,blank,by = 0,all = T)

# Treatemnt comparisons loop
for (k in 1:length(lsmeans.Fpwy.dist[,1])){
  for (i in 1:length(lsmeans.Fpwy.dist[,1])){
```

```
    if ((lsmeans.Fpwy.dist[i,8]>=lsmeans.Fpwy.dist[k,8] & lsmeans.Fpwy.dist[i,8]<=lsmeans.Fpwy.dist[k,9])||
        (lsmeans.Fpwy.dist[i,9]>=lsmeans.Fpwy.dist[k,8] & lsmeans.Fpwy.dist[i,9]<=lsmeans.Fpwy.dist[k,9])) {
      lsmeans.Fpwy.dist[i,(k+10)]<-k
    } else{
      lsmeans.Fpwy.dist[i,(k+10)]<-999
    }
  }
}


## ------------Mixed model analysis for Force Std. Deviation Values-----

## Model Fddy.sd
Model.Fddy.sd<-lmer(Fddy.sd~config*plant_depth+(1|rep),data = Force.Table)
anova(Model.Fddy.sd)
# Calculate lsmeans table
lsmeans.Fddy.sd <- lsmeans(Model.Fddy.sd)
# Produce data frame from first table of lsmeans
lsmeans.Fddy.sd <- as.data.frame(lsmeans.Fddy.sd[1])
# Rename columns
colnames(lsmeans.Fddy.sd)<-c("config","plant_depth","Estimate","SE","DF","t.val",
                          "LCI","UCI","p.val")
# Merge Lsmeans with Blank data frame
lsmeans.Fddy.sd<-merge(lsmeans.Fddy.sd,blank,by = 0,all = T)

# Treatemnt comparisons loop
for (k in 1:length(lsmeans.Fddy.sd[,1])){
  for (i in 1:length(lsmeans.Fddy.sd[,1])){
    if ((lsmeans.Fddy.sd[i,8]>=lsmeans.Fddy.sd[k,8] & lsmeans.Fddy.sd[i,8]<=lsmeans.Fddy.sd[k,9])||
        (lsmeans.Fddy.sd[i,9]>=lsmeans.Fddy.sd[k,8] & lsmeans.Fddy.sd[i,9]<=lsmeans.Fddy.sd[k,9])) {
      lsmeans.Fddy.sd[i,(k+10)]<-k
    } else{
      lsmeans.Fddy.sd[i,(k+10)]<-999
    }
  }
}
# Export lsmeans csv
```

```
write.csv(lsmeans.Fddy.sd,"lsmeans.Fddy.sd.csv")

## Model Fpwy.sd
Model.Fpwy.sd<-lmer(Fpwy.sd~config*plant_depth+(1|rep),data = Force.Table)
anova(Model.Fpwy.sd)
# Calculate lsmeans table
lsmeans.Fpwy.sd <- lsmeans(Model.Fpwy.sd)
# Produce data frame from first table of lsmeans
lsmeans.Fpwy.sd <- as.data.frame(lsmeans.Fpwy.sd[1])
# Rename columns
colnames(lsmeans.Fpwy.sd)<-c("config","plant_depth","Estimate","SE","DF","t.val",
                             "LCI","UCI","p.val")
# Merge Lsmeans with Blank data frame
lsmeans.Fpwy.sd<-merge(lsmeans.Fpwy.sd,blank,by = 0,all = T)

# Treatemnt comparisons loop
for (k in 1:length(lsmeans.Fpwy.sd[,1])){
  for (i in 1:length(lsmeans.Fpwy.sd[,1])){
    if ((lsmeans.Fpwy.sd[i,8]>=lsmeans.Fpwy.sd[k,8] & lsmeans.Fpwy.sd[i,8]<=lsmeans.Fpwy.sd[
        k,9])||
        (lsmeans.Fpwy.sd[i,9]>=lsmeans.Fpwy.sd[k,8] & lsmeans.Fpwy.sd[i,9]<=lsmeans.Fpwy.sd[
            k,9])) {
      lsmeans.Fpwy.sd[i,(k+10)]<-k
    } else{
      lsmeans.Fpwy.sd[i,(k+10)]<-999
    }
  }
}

## Regression Models
# Add Soil.Table values to Force.Table
Force.Table<-merge(Force.Table,Soil.Table[,c(1,10:15)],by="plot",all = T)

# Create subset of Force.Table to include only config 1 & 2
Force.Table2<-subset(Force.Table,Force.Table$config==1 | Force.Table$config==2)

# Fddy Regression Model
Fddy.Reg <- lm(Fddy~GWAS:JD+DFy+Fd,
               data = Force.Table)

summary(Fddy.Reg)
```

```r
anova(Fddy.Reg)
plot(Fddy.Reg)

# Pd.ref REgression Model
PD.ref.Reg <- lm(PD.ref~GWAS,
               data = Force.Table)

summary(PD.ref.Reg)
anova(PD.ref.Reg)
plot(PD.ref.Reg)

# Fpwy Regression Model
Fpwy.Reg <- lm(Fpwy~GWAS,
                 data = Force.Table)

summary(Fpwy.Reg)
anova(Fpwy.Reg)
plot(Fpwy.Reg)

# PDgrd REgression Model
PDgrd.Reg <- lm(PD.GRD~GWAS+Fpwy+Fddy+JD,
                 data = Force.Table)

summary(PDgrd.Reg)
anova(PD.ref.Reg)
plot(PD.ref.Reg)

#-------------------Aggregate Function-------------------------
# Aggregate Means
colnames(Sensor.data)
agg.means <- aggregate(list(Sensor.data$Fcty,Sensor.data$Fddy,
                            Sensor.data$JD,Sensor.data$Total_DR,
                            Sensor.data$Fpwy),
                       list(Sensor.data$config,Sensor.data$plant_depth),
                       mean,na.rm=T)
# colnames(agg.means) <- c("Plot","Config","Rep","Plant_Depth","Fcty","Fddy","JD","Total_DR","Fpwy")
colnames(agg.means)<-c("Config","Plant_Depth","Fcty","Fddy","JD","Total_DR","Fpwy")

# write CSV file
write.csv(agg.means,"agg.means.csv")
```

```
# Aggregate Std. Deviation
colnames(Sensor.data)
agg.std.dev <- aggregate(list(Sensor.data$Fcty,Sensor.data$Fddy,
                              Sensor.data$JD,Sensor.data$Total_DR,
                              Sensor.data$Fpwy),
                         list(Sensor.data$config,Sensor.data$plant_depth),
                         sd,na.rm=T)
colnames(agg.std.dev) <- c("Config","Plant_Depth","Fcty","Fddy","JD","Total_DR","Fpwy")

# write CSV file
write.csv(agg.std.dev,"agg.std.dev.csv")

#---------------------Force Means--------------------------------
# Aggregate means of forces and postions to calculate loads on planter
Force.means<-aggregate(list(Sensor.data$FLAS,Sensor.data$JD,Sensor.data$DC1,
                            Sensor.data$DL2,Sensor.data$DR3,Sensor.data$VC6,
                            Sensor.data$Total_DR,Sensor.data$DFy,
                            Sensor.data$Fpwy,Sensor.data$F1,Sensor.data$F2,
                            Sensor.data$GWx,Sensor.data$GWy,Sensor.data$PWx,
                            Sensor.data$PWy,Sensor.data$Fd),
                       list(Sensor.data$plot),mean,na.rm=T)

# Reset column names for Force.means
colnames(Force.means)<-c("plot","FLAS","JD","DC1","DL2","DR3","VC6","Total_DR",
                         "DFy","Fpwy","F1","F2","GWx","GWy","PWx","PWy","Fd")
# Merge config table with Force.means
Force.means<-merge(Force.means,Config.table,by="plot",all = T)
# Reorder columns
Force.means<-Force.means[,c(1,18:20,2:17)]
```

Appendix/Data_Analysis.R